

2018

Design, Modeling, and Implementation of an Environmental Control Chamber

Aaron Matarese
University of Rhode Island, amatarese205@gmail.com

Follow this and additional works at: <https://digitalcommons.uri.edu/theses>

Recommended Citation

Matarese, Aaron, "Design, Modeling, and Implementation of an Environmental Control Chamber" (2018).
Open Access Master's Theses. Paper 1327.
<https://digitalcommons.uri.edu/theses/1327>

This Thesis is brought to you by the University of Rhode Island. It has been accepted for inclusion in Open Access Master's Theses by an authorized administrator of DigitalCommons@URI. For more information, please contact digitalcommons-group@uri.edu. For permission to reuse copyrighted content, contact the author directly.

DESIGN, MODELING, AND IMPLEMENTATION OF AN
ENVIRONMENTAL CONTROL CHAMBER

BY

AARON S. MATARESE

A THESIS SUBMITTED IN PARTIAL FULFILLMENT OF THE
REQUIREMENTS FOR THE DEGREE OF
MASTER OF SCIENCE
IN
MECHANICAL ENGINEERING AND APPLIED MECHANICS

UNIVERSITY OF RHODE ISLAND

2018

MASTER OF SCIENCE THESIS
OF
AARON S. MATARESE

APPROVED:

Thesis Committee:

Major Professor Musa Jouaneh

Chengzhi Yuan

Richard Vaccaro

Nasser H. Zawia

DEAN OF THE GRADUATE SCHOOL

UNIVERSITY OF RHODE ISLAND

2018

ABSTRACT

This thesis goes over the details of humidification and temperature modeling for an enclosed, non-hermetically sealed space. Review of common methods of thermal and humidification design was performed to detail which method is suitable for any given application. For the application of designing an enclosure for the preparation of Cryo-TEM sample grids, it was determined that system design via lumped capacitance methods was the best option. A detailed and practical analysis of the application of the lumped capacitance method is described.

A detailed overview of how to apply control of relative humidity and temperature in an enclosed space is also included. It was required to build the entire system from the ground up to implement a control scheme for the preparation of Cryo-TEM grids. This includes the design of heaters, a humidifier, an enclosure, electronics, and programming. Heating of the enclosure was accomplished through the utilization of cartridge heaters in an application to take advantage of the benefits of forced convection. Humidification was accomplished with a closed loop design where moist air is fed to the enclosure and the dry air of the enclosure is returned to the humidifier. Water vapour was produced through an ultrasonic piezoelectric transducer. Control of these elements was established via PC and electronic control.

Work has shown the effectiveness of the lumped methods for developing accurate higher order models for thermal systems. Experiments had to be performed to determine the thermodynamic parameters associated with convection required to develop the state space equations to represent the system. This is due to the many unknowns present without the use of CFD simulations. For portions of the system relying on thermal conduction, the predictive model calculated shows excellent agreement with real world data. Once the thermal model for the overall system

was developed, experimentation of various inputs and changes in thermodynamics were used to verify the effectiveness of the model.

There was also a need to develop a model for humidification based on direct measurements of relative humidity. The model is based on pressure driven mass flow in terms of partial pressures and conservation of mass. This leads to a system where the active input is water vapour and the passive input being the ambient water vapour partial pressure. Since relative humidity is based off of dry bulb temperature, there was a need to develop a model to take temperature into consideration. A model was developed to consider all of these factors in a first-order system.

ACKNOWLEDGMENTS

I would like to thank all of the staff in the University of Rhode Island's Department of Mechanical, Industrial and Systems Engineering for their unwavering support throughout my time here at the University of Rhode Island. I want to specifically thank my advisor, Professor Musa Jouaneh, for supporting my education and providing great advice and wisdom throughout my research. In addition, I would like to acknowledge Jim Byrnes and Joe Gomez for their practical and technical expertise in their respective fields of electronics and manufacturing. Special thanks goes to the sponsor of my research, NanoSoft LLC., not only for their funding, but for their expertise and assistance in the project.

Last but not least, I would like to thank my family and friends for supporting me throughout my undergraduate and graduate career at the University of Rhode Island. Between their personal and academic support, I was able to persevere and succeed in graduate school.

TABLE OF CONTENTS

ABSTRACT	ii
ACKNOWLEDGMENTS	iv
TABLE OF CONTENTS	v
LIST OF FIGURES	viii
LIST OF TABLES	xi
CHAPTER	
1 Introduction	1
1.1 Electron Microscopy Technologies	1
1.2 Cryo-TEM Sample Grid Preparation	2
1.3 Objective	7
List of References	8
2 Literature Review	10
2.1 Temperature Control	10
2.1.1 Heat Transfer Mechanics	10
2.1.2 System analysis and design	13
2.2 Humidity Control	23
2.2.1 Mechanics of Humidification	23
2.2.2 Humidification Methods	28
List of References	29
3 Methodology	33

	Page
3.1 Electronics and Software Design	33
3.1.1 Firmware	33
3.1.2 Software	34
3.1.3 Electronics	36
3.2 Prototype Enclosure Design	41
3.3 Temperature Control	42
3.3.1 Heater Design	42
3.3.2 Thermal State Space Representation	49
3.4 Humidity Control	52
3.4.1 Humidifier Design	52
3.4.2 Humidifier Characterization	54
List of References	56
4 Findings	58
4.1 System Performance	58
4.1.1 Thermal Performance	58
4.1.2 Humidity Performance	66
List of References	75
5 Conclusion	76
5.1 Conclusions	76
5.2 Future Work	77
 APPENDIX	
Programs	79
A.1 Arduino Code	79

	Page
A.2 Visual Basic Code	83
Technical Drawings	91
B.1 Electronic Schematics	91
B.2 Enclosure	94
B.3 Heater Assembly	112
B.4 Humidifier	120
Matlab Scripts	124
C.1 Heater Model Function	124
C.2 Enclosure Model Function	126
C.3 Enclosure Model Function With Humidifier Attached	128
C.4 Humidification Model	130
Manufacturer Datasheets	132
D.1 Heat Sink	132
D.2 Heater Fan	134
BIBLIOGRAPHY	136

LIST OF FIGURES

Figure		Page
1.1	Graphic of EM grid with a carbon film overlaid on a copper grid [9]. Grids are typically 3 mm in diameter.	3
1.2	Picture of a FEI Vitrobot machine, a commonly found Cryo-TEM grid preparation system. A dewar is filled with liquid ethane for sample vitrification (A) located below the temperature and humidity controlled chamber (B). A pair of tweezers with a Cryo-TEM grid (C) is mounted onto the machine's plunger inside the environmental control chamber [11].	4
1.3	Graphic of EM grid after preparation. Starting from the left, a macro-view of the EM grid, a close up of the porous carbon film within one grid square, top view of specimen suspended in the carbon film, cross-sectional view of specimen suspended in carbon film [12].	4
1.4	Pictures of ice under a TEM. Vitreous ice (A), hexagonal ice formations (B), ice formation (C), ethane contamination (D) [8].	6
2.1	Eighth-order polynomial fit for saturation vapour pressure of water vapour in air versus dry bulb temperature based off of the Hyland-Wexler formulation.	27
3.1	Graphical user interface for control of temperature and humidity.	35
3.2	3-D CAD model of enclosure assembly without heaters or humidifier.	42
3.3	Cross section of heater sub-assembly showing the cavities for cartridge heaters and RTD temperature sensor. 1. cartridge heaters, 2. RTD, 3. fan, 4. heat sink fins, 5. copper blocks. . . .	44
3.4	A 3-D CAD image of the heater assembly which consists of two heater sub-assemblies capable of delivering 240 Watts of heat via forced convection.	45
3.5	Electrical analog for heater thermal dynamics.	47

Figure		Page
3.6	Heater model simulation for $v=7.05$ m/s air stream and three cartridge heaters in heater block with a 116.2 Watt step input. Heater temperature is relative to ambient temperature.	48
3.7	Electrical analog for a fourth-order thermal system.	49
3.8	Humidifier assembly. 1. intake nozzle, 2. exhaust nozzle, 3. fan, 4. water reservoir.	53
3.9	Cross section of humidifier. 1. ultrasonic humidifier 2. water reservoir.	54
4.1	Comparison of heater model with actual test data for $v=7.05$ m/s air stream, and 116 Watt step input of heat in each heater block with heater assembly in open air. Values are relative to room temperature at time of test.	59
4.2	Plots for the four state variables associated with the thermal system with a heat rate input of 153 Watts and humidifier not connected. Plots compare the model (dashed line) and the actual results (solid line).	61
4.3	Plots for the four state variables associated with the thermal system with a heat rate input of 153 Watts and only humidifier fan on. Plots compare the model (dashed line) and the actual results (solid line).	61
4.4	Plots of the thermal system state variables with heat rate input of 153 Watts and no humidifier attached in terms of percentage of model's steady state value. Plots compare the model (dashed line) and the actual results (solid line).	62
4.5	Plots for the thermal system with a heat rate input of 153 Watts and only humidifier fan on in terms of percentage of model's final steady state value. Plots compare the model (dashed line) and the actual results (solid line).	62
4.6	Plots for the thermal system with a heat rate input of 78.3 Watts and only the humidifier fan turned on. Plots compare the model (dashed) and the actual results (solid).	64

Figure	Page
4.7	Plots for the thermal system with a heat rate input of 78.3 Watts and only humidifier fan turned on in terms of percentage of model's final steady state value. Plots compare the model (dashed) and the actual results (solid). 65
4.8	Enclosure air temperature change comparison between original model and differing the thermodynamics via adding a stainless steel cylinder. All tests have the humidifier attached and only the humidifier fan turned on. 66
4.9	Plots for relative humidity performance. Data collection started after 4000 seconds from applying 153 Watt heat rate input. . . 68
4.10	Plots for relative humidity performance. Data collection started after 4000 seconds from applying 116 Watt heat rate input. . . 68
4.11	Plots for relative humidity performance. Data collection started after 4000 seconds from applying 78.3 Watt heat rate input. . . 69
4.12	Percent difference of relative humidity model to experimental data. 69
4.13	Plots of relative humidity versus dry bulb temperature for various heat rate inputs. 71
4.14	Plots of relative humidity versus dry bulb temperature for various heat rate inputs, includes model of relative humidity for comparison. 72
4.15	Plots of relative humidity versus dry bulb temperature for constant water vapour mass flow rate with 153 Watts of heat rate input for a portion of the test. 74

LIST OF TABLES

Table		Page
4.1	Model values for enclosure without humidifier attached.	63
4.2	Model values for enclosure with humidifier attached with the humidification element turned off.	63
4.3	Model values for the enclosure's humidity response. Used for predicting response of water vapour partial pressure for a given input.	67
4.4	Inputs for relative humidity model resulting in the plots found in Figure 4.14.	72

CHAPTER 1

Introduction

Environmental control is an important aspect of many industrial and scientific applications. Such applications require the accurate control of temperature and relative humidity in a confined space and allows for processes that need such control. Examples of where temperature and humidity control are implemented are in incubators for bacteria as well as Cryogenic Electron Microscopy (Cryo-EM) along with a myriad of other applications [1] [2]. The reason for why temperature and humidity control are needed varies upon the application and parameters needed for certain processes. Temperature control for biological applications are important in order to preserve proteins as too high of a temperature can cause proteins to denature [3]. Humidity regulates processes where there is a system comprising of water. Anything that is water-based and exposed to air can lead to water evaporation dependent upon the humidity of the surrounding air [4]. Control of humidity allows for the control of evaporation or condensation in an enclosed environment [5]. The objective of this thesis is to study the mechanics of temperature and humidity control and implement a control system for a Cryo-EM sample preparation system.

1.1 Electron Microscopy Technologies

There are two distinct EM technologies that are widely used today; the Scanning Electron Microscope (SEM) and the Transmission Electron Microscope (TEM) [6]. The TEM is analogous to a light microscope where the electrons are transmitted from the electron gun through a thin specimen and the electrons that are able to pass through the specimen are detected on an imaging plate. SEM on the other hand relies on the reflection of electrons off of a surface which is great

for three-dimensional specimens but at a resolution that is one order of magnitude less than TEM [7].

A subset of electron microscopy is the use of cryogens to prepare EM samples. Cryogenically frozen specimens can be used in both TEM and SEM systems which are respectively named Cryo-TEM and Cryo-SEM or Cryo-EM for general cryogenic electron microscopy. One of the main reasons that Cryo-EM is utilized in the scientific world is that Cryo-EM allows for the imaging of a specimen in its native aqueous environment as opposed to negative staining where the specimen is subjected to heavy metal salts and dehydration [8]. The freezing of an aqueous specimen allows for the specimen to be subjected to the vacuum present in the electron microscope where the specimen would otherwise be damaged due to water or other liquids evaporating out of the sample.

1.2 Cryo-TEM Sample Grid Preparation

Careful preparation of EM specimens is required for high quality imaging. TEM requires the specimen to be thin enough for electrons to pass through without the appearance of visual aberrations on the image or where the signal to noise ratio is satisfactory [8]. For the scope of this research, the system being implemented will focus on the preparation of samples that are suspended in carbon on an EM grid. An example of an EM grid is depicted in Figure 1.1.

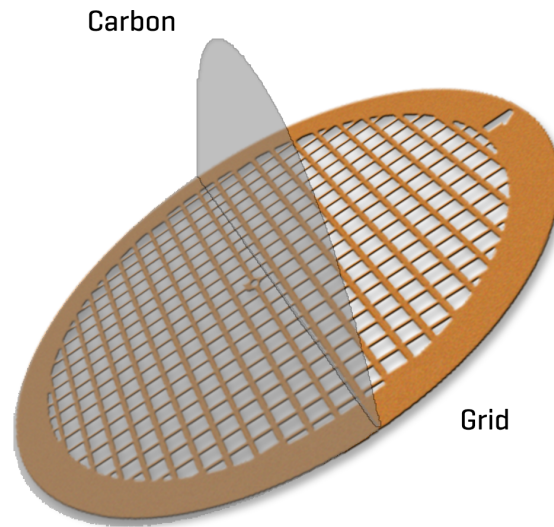


Figure 1.1. Graphic of EM grid with a carbon film overlaid on a copper grid [9]. Grids are typically 3 mm in diameter.

The preparation of Cryo-TEM grids is a highly involved process. In short, the process can be summarized into a few steps. The selection of the proper sample grid is the first step and is dependent upon the desired application of the grid. There are various carbon pore sizes as well as grid mesh sizes to consider. Grid mesh material can be a limiting factor depending on how the user wants to prepare their specimen. Copper is the most common material but it is not recommended if the user wants to grow a biological specimen on the grid itself since copper is a known biocide [8]. Once the grid type is known, the user mounts the grid onto a pair of tweezers mounted on a plunger located in an environmentally controlled chamber as shown in Figure 1.2. Next, about 5 μL of aqueous sample is pipetted onto the grid. Then, the loaded EM grid is blotted with filter paper to remove excess liquid and to achieve a uniformly thin sample. The EM grid is then plunged into a dewar, located outside of the environmentally controlled chamber, filled with liquid ethane where the specimen is vitrified. The specimen must be carefully maintained at a temperature below $-137\text{ }^{\circ}\text{C}$ at all times until the specimen is imaged in the electron

microscope per the satisfaction of the user. If the specimen reaches a temperature above $-137\text{ }^{\circ}\text{C}$, then it will become devitrified and the image of the specimen will contain aberrations due to ice crystal formation. For a more detailed step by step procedure in preparing EM grids, refer to [10]. A graphical representation of the specimen in the prepared EM grid is shown in Figure 1.3.

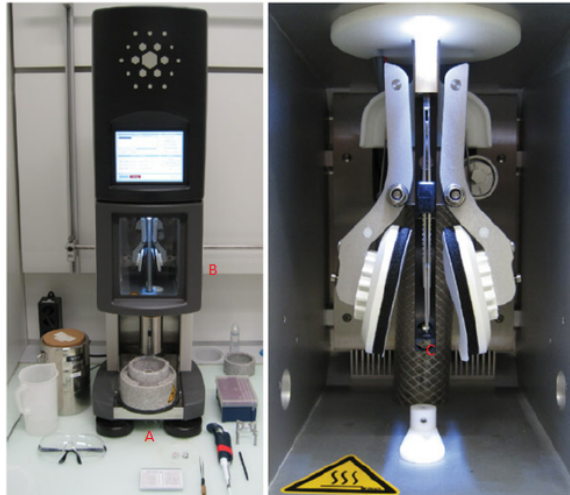


Figure 1.2. Picture of a FEI Vitrobot machine, a commonly found Cryo-TEM grid preparation system. A dewar is filled with liquid ethane for sample vitrification (A) located below the temperature and humidity controlled chamber (B). A pair of tweezers with a Cryo-TEM grid (C) is mounted onto the machine's plunger inside the environmental control chamber [11].

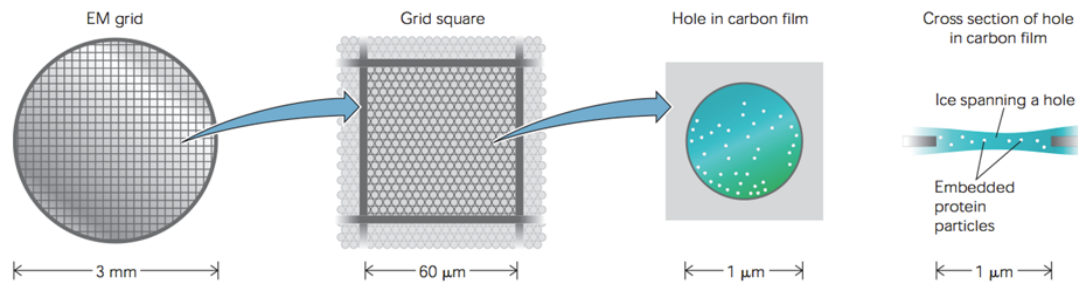


Figure 1.3. Graphic of EM grid after preparation. Starting from the left, a macro-view of the EM grid, a close up of the porous carbon film within one grid square, top view of specimen suspended in the carbon film, cross-sectional view of specimen suspended in carbon film [12].

All of the preceding steps need to be followed for proper vitrification of the specimen. Any deviations can lead to non-uniformities in the specimen, non-vitreous ice, or other complications when the specimen is ultimately imaged with an electron microscope. Some visual examples of how poor vitrification can adversely affect image quality is shown in Figure 1.4. For the scope of this research, the temperature and humidity control of the system is the most important aspect being addressed. Improper temperature and/or humidity control can adversely affect the specimen being prepared. Improper humidity control, as discussed earlier, will cause an increase in evaporation in the specimen causing it to be dehydrated prior to vitrification [13]. Temperature control will affect the humidity in the enclosure as well since the saturation pressure or density of air is dependent upon the temperature of air [14]. Therefore, to ensure that there is not excessive evaporation in the specimen, the temperature needs to be held at a steady state so that the relative humidity in air is not affected and can maintain a desired set point.

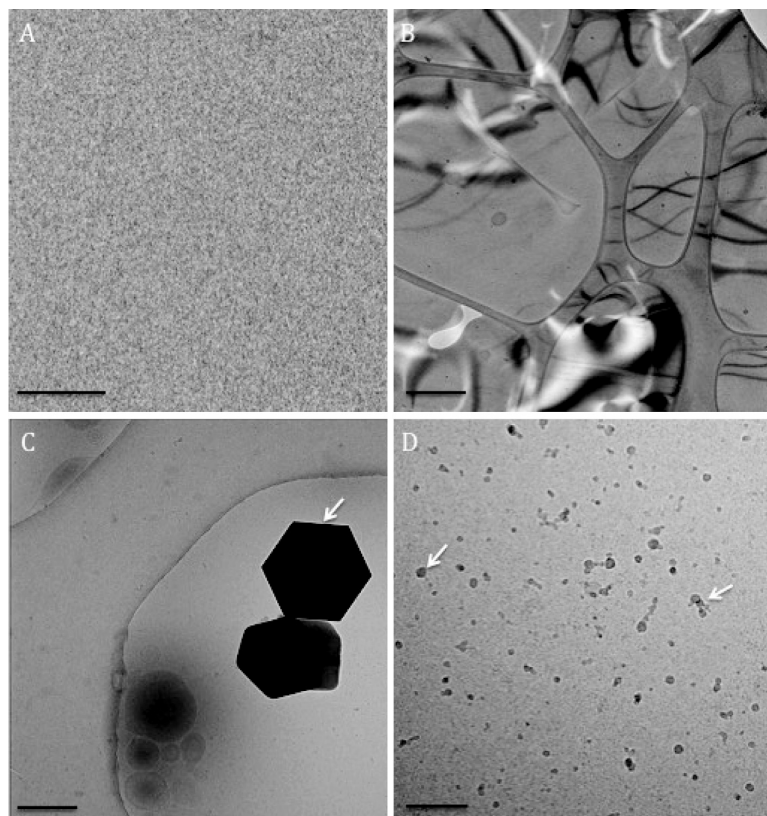


Figure 1.4. Pictures of ice under a TEM. Vitreous ice (A), hexagonal ice formations (B), ice formation (C), ethane contamination (D) [8].

In addition to the environment encountered by the specimen, the blotting process itself has been known to cause specimens to be poorly imaged or imaged in a non-native state. Conventionally, the use of blotting paper or filter paper is used to wick excess specimen solution off of the EM grid to ensure a uniform thin thickness of sample on the grid. This can cause shear rates in the specimen that are approximately 10^3 to 10^5 s^{-1} where shear rates as low as 600 s^{-1} can cause worm-like micelles [15] [16]. A new method presented by [15] utilizes capillary tubes replacing blotting paper. Results have shown that capillary tubes are able to reduce the shear rates in the specimen by one to three order of magnitude on average when compared to blotting. This allows for the wider application of Cryo-TEM to produce specimen images of nano-scale objects in its native morphology

that may not have been feasible with conventional blotting.

1.3 Objective

The primary objective in this research is to develop an environmental control chamber that is able to perform the processes needed for a proper Cryo-TEM sample preparation system similar to the process developed in [15]. The chamber must be able to control the temperature and humidity to conform to the user's specified settings and to enable the proper preparation of EM sample grids. The control of the operation is governed by a PC program with a graphical user interface (GUI) which communicates with the sample preparation system via a custom control board. Temperature and humidity is controlled via two separate control loops and is implemented in software. Any auxiliary equipment needed for the process, such as actuators, are also controlled by the software along with supporting hardware with user specified inputs.

To accomplish this, modeling of the system is required to determine the design parameters for the system. Such modeling includes determining the temperature's transient response to a user specified desired temperature input and the input of the ambient air temperature. The humidity response of the system is based off of the dry bulb temperature of the enclosure's air and the mass flow rate of water vapour in the control volume. Knowing this, it is possible to model the humidity of the system as a function of the physical characteristics of the system, dry bulb temperature, and the mass flow rate of water vapor into the system. Therefore, to properly design the system, a model of the system's thermal properties needs to be developed to govern the thermal and humidity performance of the environment chamber.

In addition to the thermal and humidity design, the development of control hardware is necessary for the system to function. This will be accomplished by

designing a printed circuit board (PCB) that will effectively act as an intermediate piece of the system between the PC and the EM sample preparation instrument. The PCB has to be able to direct power to individual components in the system in concert with the digital commands given by the PC via a data acquisition card. The PCB is also responsible for connecting various sensors to the system. The sensors that are to be used in the system utilize an analog voltage signal that represents a state variable. These analog signals have to be processed before being read by the PC by using various analog signal processing hardware which includes op-amps, wheatstone bridges, and electrical filters. This is necessary to prevent any analog noise that may be present in the system to not reach the PC and cause inaccurate readings.

List of References

- [1] Rotronic. “Incubators and humidity.” June 2015. [Online]. Available: <https://www.rotronic.com/en-us/rotronic-cases-read?id=361/>
- [2] ThermoFisher Scientific. “Vitrobot for life sciences.” [Online]. Available: <https://www.fei.com/Vitrobot/>
- [3] Elmhurst College. “Denaturing of proteins.” 2003. [Online]. Available: <http://chemistry.elmhurst.edu/vchembook/568denaturation.html>
- [4] Lumen Learning. “Humidity, evaporation, and boiling.” [Online]. Available: <https://courses.lumenlearning.com/physics/chapter/13-6-humidity-evaporation-and-boiling/>
- [5] National Physical Laboratory. “Why is humidity important?” [Online]. Available: <http://www.npl.co.uk/publications/good-practice-online-modules/humidity/humidity-basics/why-is-humidity-important/>
- [6] Science Learning Hub. “Types of electron microscope.” Feb. 2012. [Online]. Available: <https://www.sciencelearn.org.nz/resources/502-types-of-electron-microscope>
- [7] Miami University. “What is resolution?” Nov. 2013. [Online]. Available: <https://www.cas.miamioh.edu/mbiws/microscopes/resolution.html>
- [8] R. F. Thompson, M. Walker, C. A. Siebert, S. P. Muench, and N. A. Ranson, “An introduction to sample preparation and imaging by cryo-electron

- microscopy for structural biology,” vol. 100, pp. 3–15, Feb. 2016. [Online]. Available: <https://doi.org/10.1016/j.ymeth.2016.02.017>
- [9] EM Resolutions. “Carbon film on copper 400 mesh.” [Online]. Available: https://emresolutions.com/wp-content/uploads/2015/12/Carbon_on_square_grid-57.png
- [10] R. A. Grassucci, D. J. Taylor, and J. Frank, “Preparation of macromolecular complexes for cryo-electron microscopy,” *Nature Protocols*, vol. 2, no. 12, pp. 3239–3246, 2007. [Online]. Available: <https://doi.org/10.1016/j.ymeth.2016.02.017>
- [11] K. N. Goldie, P. Abeyrathne, F. Kebbel, M. Chami, P. ringler, and H. Stahlberg. ResearchGate. “Cryo-electron microscopy of membrane proteins.” Jan. 2014. [Online]. Available: https://www.researchgate.net/The-plunge-freezing-device-FEI-Vitrobot-fitted-with-a-humidity-and-temperature_fig1_259395292
- [12] University of Washington. “What is cryo-EM?” [Online]. Available: <https://faculty.washington.edu/lw32/images/fig1.png>
- [13] V. Cabra and M. Sams, “Do’s and don’ts of cryo-electron microscopy: A primer on sample preparation and high quality data collection for macromolecular 3D reconstruction,” *Journal of Visualized Experiments*, vol. 95, Jan. 2015. [Online]. Available: <http://www.jove.com/video/52311>
- [14] Engineering ToolBox. “Relative humidity in air.” 2004. [Online]. Available: https://www.engineeringtoolbox.com/relative-humidity-air-d_687.html
- [15] D. Croote, M. P. Godfrin, A. Bose, A. Tripathi, and J. Lee, “A platform for retaining native morphology at sub-second time scales in cryogenic transmission electron microscopy,” *Review of Scientific Instruments*, vol. 84, 2013. [Online]. Available: <http://dx.doi.org/10.1063/1.4804648>
- [16] V. K. Jindal, J. Kalus, H. Pilsl, H. Hoffmann, and P. Linder, “Dynamic small-angle neutron scattering study of rodlike micelles in a surfactant solution,” *The Journal of Physical Chemistry*, vol. 94, no. 7, 1990. [Online]. Available: <https://doi.org/10.1021/j100370a070>

CHAPTER 2

Literature Review

2.1 Temperature Control

The control of temperature, as mentioned earlier, is an important factor during the design stage of this product. To accurately design a temperature control system, one must know the parameters and mechanics associated with the plant dynamics for the enclosure. Several methods of analyzing the thermodynamics of a system exist each with their own advantages and disadvantages. This includes the use of a priori methods such as analytical and numerical methods, as well as methods utilizing experimental data to determine the system dynamics. This section will go over the variety of methods that are most commonly used for thermal design.

2.1.1 Heat Transfer Mechanics

Temperature control is governed by the mechanics of heat transfer. Heat transfer can be broken down into three basic mechanisms; conduction, convection, and radiation [1]. These mechanisms can be used to determine the temperature values at different points in the system during the steady-state portion of its dynamics.

Thermal conduction is the most basic form of heat transfer mechanics but it is generally limited to heat transfer in solids. It is defined as the energy transfer between adjacent parts of a solid body [2]. This generally limits the use of thermal conduction calculations to solid-solid interfaces and is not applicable for fluids as heat transfer at solid-fluid interfaces are defined under convection. Thermal conduction can be mathematically defined in Equation 2.1 where q is heat rate, k is known as the thermal conductivity and is a constant dependent on the material used, A is the area associated with the heat transfer in question, T_i is

the temperature associated with a point in the solid body, and x_i is the position associated with the temperature T_i [3]. This equation is limited to heat transfer in one-dimension but it is extremely useful for design as there are various applications in which an assumption can be made to model a system as one-dimensional. For scenarios where heat transfer cannot be looked at with one-dimensional models, there exist theories for steady-state and transient analysis of thermal systems in [4].

$$q = \frac{kA(T_j - T_i)}{x_j - x_i} \quad (2.1)$$

For heat transfer boundary conditions where there is a solid-fluid interface, there exists the heat transfer mechanism of convection. The mathematics behind convection is similar to heat transfer through conduction and is stated in Equation 2.2 below. The convective heat transfer coefficient, h , is a parameter that is dependent upon the specific convection boundary conditions that is related to the Nusselt number of the fluid in the heat transfer problem. The Nusselt number of a fluid is a dimensionless term that characterizes the ratio between the convective and conductive heat transfer in a fluid and its formulation is dependent upon the geometry of the solid-fluid interface as well as the flow's thermodynamic conditions [5]. Therefore, the convective heat transfer coefficient will also depend upon these factors. Specifically, it is a function of the steam velocity U , body length L , wall roughness height γ , wall temperature T_w , freestream temperature T_∞ , density ρ_o , viscosity μ , fluid thermal conductivity k , fluid specific heat c_p , buoyant specific weight $g\Delta\rho$, and the overall shape or geometry of the object that is immersed in fluid [6]. This relationship is better expressed visually in the form of a function in Equation 2.3. Various scenarios of heat transfer with forced, free, and combined convection with laminar and turbulent fluid conditions are covered in [7]. Once

the Nusselt number of the boundary condition of a specific problem is known, the convective heat transfer coefficient can be calculated using Equation 2.4 where \overline{Nu} is the average Nusselt number and L is the length or effective length of the heat transfer boundary [8].

$$q = hAdT \quad (2.2)$$

$$h = f(U, L, \gamma, T_w, T_\infty, \rho_o, \mu, k, c_p, g\Delta\rho, \text{shape}) \quad (2.3)$$

$$\bar{h} = \frac{\overline{Nu}k}{L} \quad (2.4)$$

The other form of heat transfer is the mechanism of radiation. Radiation is a specialized case where thermal energy is emitted from an object via electromagnetic radiation and does not require a medium to travel through. J. Stefan and L. Boltzmann determined that the thermal power radiated from an object is proportional to the absolute temperature of the object to the fourth power. For real surfaces, this relation is scaled by the surface's emissivity, ϵ , which is a value ranging between zero and one [9]. This relationship is shown in Equation 2.5 where T is the surface temperature of the object in absolute units, σ is the Boltzmann constant, and A is the surface area associated with the origin of emitted radiation. Every object emits thermal radiation into space, but it can potentially be ignored in the overall thermal system performance calculations if the absolute temperature of the object and the application of the object deems that it is a small percentage of the overall heat transfer. There are numerous other factors at play when dealing with radiative heat transfer and it can get fairly complex when looking at the details. To learn more about the intricacies associated with radiative heat transfer, [10] goes over the details from a physics perspective and covers heat transfer from

a single body as well as heat transfer between two or more bodies within line of sight of each other.

$$q = \sigma\epsilon AT^4 \quad (2.5)$$

The previously discussed heat transfer mechanics covers the extent of steady-state analysis of thermal systems. If it is desired to understand the transient response of the system, then the thermal energy storage capabilities of materials needs to be taken into consideration. Otherwise known as thermal capacitance, the transient response of an object is dependent upon the mass of the object, m , and its specific heat, c_p . Using these parameters, the heat flow going into an object can be characterized into a lumped thermal capacitance formulation shown in Equation 2.6 as a first order ordinary differential equation. For systems with a fixed mass, the product of the mass and specific heat of the object can be represented as a thermal capacitance, C [11].

$$q = mc_p \frac{dT}{dt} = C \frac{dT}{dt} \quad (2.6)$$

2.1.2 System analysis and design

There exist a few methods for the design and analysis of physical thermal systems. For simple systems that consist of a few parts, or that have a simple geometry, it may be advantageous to utilize an analytical approach to modeling such a system as it will reduce the amount of computing time necessary during the design phase of a project [12]. All one would have to do if one wants to experiment with different design characteristics, is change the physical characteristics in their model and recalculate with a computer program such as Matlab. For design applications where it is difficult to determine the convective heat transfer coefficient due to a complex fluid flow problem or for applications that require greater

detail in the thermal system performance over time, then the use of a numerical simulation through the use of a Computational Fluid Dynamics (CFD) program such as the open-source C++ toolbox Open-FOAM or a commercially available finite element analysis software such as COMSOL Multiphysics may be of better use [13] [14]. This methodology could also be used for calculating variables over a plane or 3-D space. There is also a method that combines experimentally derived data with that of an analytical model to simulate the thermal response for certain inputs that is used for complex problems or for those with larger physical scale. All of these approaches are touched upon in the following sections.

Numerical methods

To solve problems that consist of complex geometries, many intricate factors, or boundary conditions that may be extremely difficult to generate a priori, numerical analysis can be performed. This is especially valuable for models that contain convective boundary conditions for geometries that are not covered by readily available resources on heat transfer. Cylinders, flat plates, spheres, and other simple geometries are covered by formulations in [15] or other available literature in the subject and the convective heat transfer coefficient can be determined using these formulations if the velocity, material properties of the fluid surrounding the object, and the object's geometry is known. However, this calculation is rarely used by itself in practical design of common devices due to the limitations of simplifying the design problem. Therefore, to practically design complex thermal systems without having to do many experiments in the early parts of the design phase, it is recommended to use numerical analysis. Unlike analytical methods, numerical analysis can only determine an approximation of variables where analytical can provide exact solutions to define the values of variables across a geometry. For practical design, it is usually not necessary to have perfect results as there will

most likely be error in variable values due to real-world implementation.

As described earlier, numerical methods provide an approximation to a flow property such as flow velocity, density, pressure, and temperature. To accomplish this calculation, the use of finite-difference methods (FDM) or finite-element methods (FEM) are utilized where each node or element represents a flow property. A finite-difference methodology explained by [16] goes into great detail of how flow properties can be determined by having defined the boundary conditions and initial conditions of the problem and then approximating the numerical quantity at adjacent nodes for a certain parameter. FEM is similar to FDM where a system is discretized but instead of having a mesh of discrete nodes and approximating solutions for neighboring nodes, FEM uses discrete elements where the flow problem is modeled between nodes. Determining an FEM solution will require more computing power than its FDM counterpart since there is greater detail to the data between nodes needed to be calculated [16].

In order to solve for a discretized system in an FEM or FDM application, the governing fluid flow equations need to be evaluated to get an accurate solution. There are three governing partial differential equations that fully model the properties of a Newtonian fluid with viscous, heat-conducting, compressible, transient flow and are detailed in Equations 2.7 through 2.10 for flow in a Cartesian coordinate system [17]. Equation 2.7 was derived from the conservation of mass and consists of mass flow terms for each axis as well as transient mass flow where u , v , and w are the flow velocities for the x , y , and z axes respectively. The momentum equations are shown in Equation 2.8 where g is the acceleration due gravity, p is pressure, and τ_{ij} are components of the fluid's stress tensor. Finally, Equation 2.9 models the temperature profile of the bulk fluid where Φ is represented by Equation 2.10 known as the viscous-dissipation function with μ being the fluid's

viscosity.

$$\frac{\partial \rho}{\partial t} + \frac{\partial(\rho u)}{\partial x} + \frac{\partial(\rho v)}{\partial y} + \frac{\partial(\rho w)}{\partial z} = 0 \quad (2.7)$$

$$\begin{aligned} \rho g_x - \frac{\partial p}{\partial x} + \frac{\partial \tau_{xx}}{\partial x} + \frac{\partial \tau_{yx}}{\partial y} + \frac{\partial \tau_{zx}}{\partial z} &= \rho \left(\frac{\partial u}{\partial t} + u \frac{\partial u}{\partial x} + v \frac{\partial u}{\partial y} + w \frac{\partial u}{\partial z} \right) \\ \rho g_y - \frac{\partial p}{\partial y} + \frac{\partial \tau_{xy}}{\partial x} + \frac{\partial \tau_{yy}}{\partial y} + \frac{\partial \tau_{zy}}{\partial z} &= \rho \left(\frac{\partial v}{\partial t} + u \frac{\partial v}{\partial x} + v \frac{\partial v}{\partial y} + w \frac{\partial v}{\partial z} \right) \\ \rho g_z - \frac{\partial p}{\partial z} + \frac{\partial \tau_{xz}}{\partial x} + \frac{\partial \tau_{yz}}{\partial y} + \frac{\partial \tau_{zz}}{\partial z} &= \rho \left(\frac{\partial w}{\partial t} + u \frac{\partial w}{\partial x} + v \frac{\partial w}{\partial y} + w \frac{\partial w}{\partial z} \right) \end{aligned} \quad (2.8)$$

$$\rho c_p \left(\frac{\partial T}{\partial t} + u \frac{\partial T}{\partial x} + v \frac{\partial T}{\partial y} + w \frac{\partial T}{\partial z} \right) = k \nabla^2 T + \Phi \quad (2.9)$$

$$\Phi = \mu \left[2 \left(\frac{\partial u}{\partial x} \right)^2 + 2 \left(\frac{\partial v}{\partial y} \right)^2 + 2 \left(\frac{\partial w}{\partial z} \right)^2 + \left(\frac{\partial v}{\partial x} + \frac{\partial u}{\partial y} \right)^2 + \left(\frac{\partial w}{\partial y} + \frac{\partial v}{\partial z} \right)^2 + \left(\frac{\partial u}{\partial z} + \frac{\partial w}{\partial x} \right)^2 \right] \quad (2.10)$$

There are countless examples of the application of CFD programs to design thermal and mass flow systems all with various degrees of CFD simulations and analytical design. The design of ovens is analogous to the thermal design portion of this project since ovens are a heated enclosure. An example of where CFD modeling was performed with an oven is explained by Mistry et. al. in [18] for a vented oven heated by natural convection and radiative heat transfer. Mistry notes that the dominant mode of heat transfer in an electric oven is radiation emitted from the coil at both unsteady and steady states as well as radiation emitted from the oven walls during steady-state conditions. This particular example demonstrates that while CFD modeling can be an effective tool, it can be misleading if not done with proper care. It is a common practice to use experimental results to validate a model generated numerically as well to use experiments to determine certain parameters needed for CFD simulation. With proper care, one can numerically

model the transient and steady-state performance of an oven with good accuracy. In the case of Mistry et. al., the average error of the numerical model for the bake cycle is only 4% and the broil cycle is 10%.

Lumped capacitance method

To analyze and design systems with the discussed steady state and transient response formulation, it is common to reorganize the equations to reflect that of components of an electrical circuit. The construction of such an electrical analog, known as the lumped capacitance method, can be used to simulate the response of a thermal system as done by [19] with the use of a resistor-capacitor network. This method has also been used by design engineers for analyzing a convection oven and comparing it to its real world thermal performance over time with temperature control with little error between the analytical model and real world data [12]. The use of such a method eliminates the need for complex partial differential equations for cases where the need for such detail is not required and is seen as a more practical approach to thermal system design. It replaces these partial differential equations with algebraic relationships which reduces the needed computational time and resources considerably. The heat transfer equations can be converted to resemble an electrical circuit by representing the steady state formulations with electrical resistors and the transient formulations can be treated as electrical capacitors.

The generation of the electrical analog relationships is quite simple. Steady state heat transfer can be modeled using a relationship identical to Ohm's law which is shown in Equation 2.11 where the voltage drop V is equivalent to the product of the resistance R and the current I through a resistive element. To convert this to the steady state representation of heat transfer, voltage drop, electrical current, and electric resistance are substituted by its heat transfer counterparts,

temperature drop, heat flow, and thermal resistance respectively and is shown in Equation 2.12 [20]. As you can see, steady state heat transfer is a direct analogy to steady-state electrical properties. The same can be said for transient properties in electrical and thermal systems where transient temperature response is analogous to the voltage across a capacitor. Both thermal and electrical capacitance is a measure of how much energy can be stored in a component. Equation 2.13 shows the mathematical model of a capacitor as a first-order ordinary differential equation. The thermal version of this was touched upon earlier in Equation 2.6 where thermal capacitance is dependent upon the mass and specific heat of the component. For solids and incompressible fluids, the specific heat is independent of the pressure exerted on the component in normal circumstances. Care must be taken with compressible fluids since the specific heat is dependent on whether the circumstance calls for constant volume or constant pressure values.

$$V = IR_{electric} \quad (2.11)$$

$$\Delta T = qR \quad (2.12)$$

$$I = C_{electric} \frac{dV}{dt} \quad (2.13)$$

Resistance is fairly simple to determine for practical applications in electronics, but the same simplicity does not transfer over to the heat conducting world. As described in Section 2.1.1, there are three modes of heat transfer; conduction, convection, and radiation. Electric resistance analogs can be determined for each mode with a simple understanding of the mathematics behind heat transfer.

Conduction in a single dimension can be determined with the geometry of the component as well as the component's material properties. More specifically, heat

flow via conduction is governed by the surface area the heat flux is traveling through A , the distance heat has to travel through the material (Δx), and is governed by a material property constant known as the coefficient of thermal conductivity, k . This relationship is shown in Equation 2.14 and results in a single resistance value R [21].

$$R_{conduction} = \frac{\Delta x}{kA} \quad (2.14)$$

The thermal resistance due to convection can be characterized if the average convective heat transfer coefficient (\bar{h}) and the surface area where heat flux is traveling through is known. The equivalent thermal resistance can then be expressed as the inverse of the product of these two characteristics as shown in Equation 2.15 [21]. Unlike the coefficient of thermal conductivity, the average heat transfer coefficient is not entirely based upon the properties of the materials involved in the heat transfer. As previously discussed in the heat transfer mechanics section, the coefficient is a function of flow properties, flow and object thermodynamics, and the overall geometry of the problem and is determined via the Nusselt number.

$$R_{convection} = \frac{1}{\bar{h}A} \quad (2.15)$$

To determine an electrical resistance analog for radiative heat transfer, it is solely based upon an intuitive derivation from Equation 2.5. The calculation of this resistance is performed by utilizing Equation 2.16 below. The one caveat with this thermal resistance is unlike conductive and convective heat transfer, the relationship between radiation's heat transfer properties and its heat dissipation rate is a non-linear one as shown in Equation 2.5. Therefore, it is important to note that when using this analog with Ohm's law, the temperature drop has to be expressed as the difference between the constituent temperatures to the fourth

power as shown in Equation 2.17.

$$R_{radiation} = \frac{1}{\epsilon\sigma A} \quad (2.16)$$

$$\Delta T_{radiation} = T_j^4 - T_i^4 \quad (2.17)$$

Work has been performed on the determination of thermodynamic properties for the design process of an oven. Tapia et. al. did a study on determining a single oven resistance and capacitance for the walls of an oven of various geometries and determined the equations below [22]. Equations 2.18 through 2.21 presents the functions of thermal resistances and capacitances in terms of geometry and thermodynamic properties for ovens that are in the form of cubes and rectangular prisms where l is the length of a side, δ is the wall thickness, and C_x is the capacitance of the air within the oven or heated enclosure.

$$R_{rectangular} = \frac{\delta\bar{h} + k}{kh[2(l_1l_2 + l_2l_3 + l_1l_3) + 4(l_1 + l_2 + l_3)\delta + 12\delta^2]} \quad (2.18)$$

$$R_{cube} = \frac{\delta\bar{h} + k}{kh[6l^2 + 12l\delta + 12\delta^2]} \quad (2.19)$$

$$C_{rectangular} = C_{x,rectangle} + c_p\rho g(8\delta^3 + 4(l_1 + l_2 + l_3)\delta^2 + 2(l_1l_2 + l_2l_3 + l_1l_3)\delta) \quad (2.20)$$

$$C_{cube} = C_{x,cube} + c_p\rho g(8\delta^3 + 12l\delta^2 + 6l^2\delta) \quad (2.21)$$

The use of the lumped capacitance method has seen extensive use in academia and industry alike. As the conversation on applied numerical analysis was limited to temperature modeling of an oven, this discussion will also be restricted to kitchen ovens. An application of where the transient analysis of a professional oven is

performed with the lumped capacitance method is in [12]. A model is shown where the author discretized the oven into several elements of equivalent thermal resistances and capacitances and the results of this model matches well with the experimental values of air temperature that were obtained to validate the model. The one portion of their analysis where it stepped outside the bounds of modeling solely using the equations produced from analysis, was when the average convective heat transfer coefficient of the oven walls had to be determined. To do this, they performed a CFD analysis of the oven cavity to study the air flow characteristics of the oven and find the convective heat transfer coefficient that way. The author also had to tune the coefficient after the CFD analysis by comparing the thermodynamic properties with the results of the model. It was successfully tuned once the values converged with satisfactory error.

Other work on the topic was performed by Ramirez-Laboreo et. al. who studied and developed an eighth-order discrete lumped capacitance model of a commercial electric oven [23]. In addition to modeling the temperatures in the oven, the work also focused on modeling the cooking process of food which includes mass transfer associated with the evaporation of water from the cooking food. The authors obtained the thermal model by first discretizing the oven into individual components and arranging the electrical analog accordingly. Due to the complexities associated with obtaining the particular thermodynamic properties of the individual components, system identification was performed by using a large array of thermocouples on every component as well as measuring the room temperature with a thermocouple. Knowing the heat flux flowing through the system as well as the heat associated with vaporizing the water out of the food sample, which was represented by a porous material saturated with water for experimental controllability and repeatability, the thermal resistances and capacitances can be

determined experimentally.

Experiments were also performed by Abraham et. al. for the determination of a general model for a load situated in an electrically heated oven via natural convection and radiation [24]. Various geometries, materials, and surface finish emissivities were experimented with to validate the model. Like Ramirez-Laboreo, the oven temperature profiles were determined by using thermocouples throughout the oven cavity with the only difference being a larger array of thermocouples were utilized. There was only a theoretical analysis to determine the temperature response of the thermal load in the oven with only the oven cavity temperature acting as an input. The rest of the data, including the oven air and wall temperatures, were determined experimentally. This follows the same trend as most authors on the subject due to the complexity of oven modeling or any other modeling associated with a heated and enclosed space. Generally, it is only practical to try to theoretically model an isolated single component as complexities associated with heat transfer creates great difficulty in modeling without any experimental data to base the model on.

Experimental modeling

In addition to modeling the temperature within an enclosed space using theoretical analysis or numerical simulation, there exists the widespread use of determining the thermodynamics of the system utilizing experimental data. As mentioned in the previous sections, it is a challenge to find an accurate theoretical or numerical model mainly due to aspects that fall under mass flow characterization of the system, such as the average convective heat transfer coefficient inside a heated enclosure. These models had to be tuned with the use of experimental data and later verified to prove accuracy. Unklesbay et. al. analyzed a convection oven solely through the use of experimental data and statistical methods to determine

the transfer function and the dynamics of the thermal response [25]. The model that was determined from the experimental data was measured against actual data from further tests to determine the accuracy and repeatability of this method and it was concluded to accurately track and predict the temperature within the oven.

2.2 Humidity Control

Humidity control is the area of study concerning the control of moisture in air and is often defined as psychrometrics. Moist air is a homogeneous mixture of water vapour and dry air and is important for the application of this environmental control chamber. This section goes over the factors and mechanisms pertinent to this project.

2.2.1 Mechanics of Humidification

The mechanics of humidity is essentially based on the ratio of water vapour in air compared to how much water vapour the volume of air in interest can handle before precipitating. The amount of water vapour in air is typically expressed in terms of the partial pressure of water vapour but can also be expressed as the mass of water vapour per unit volume of air. Humidity of air can be expressed as specific humidity ω which is the mass ratio of water vapour m_v per unit of dry air m_a or relative humidity ϕ where the ratio is expressed as a ratio of the partial pressure of water vapour p_v and the saturation vapour pressure of water p_s in air for a given dry bulb temperature. These relationships are expressed in Equations 2.22 and 2.23 respectively where the additional variable p is the total pressure of the gaseous mixture [26]. In regards to Equation 2.22, the right-most formulation was derived using the ideal gas law and 0.622 is solely the ratio of the molecular weight of water vapour to the molecular weight of dry air.

$$\omega = \frac{m_v}{m_a} = \frac{0.622p_v}{p - p_v} \quad (2.22)$$

$$\phi = \frac{p_v}{p_s} \times 100\% \quad (2.23)$$

When analyzing systems that manipulate the physical properties of a mixture, it is important to obey the theories of conservation of mass and the conservation of energy to determine the thermodynamics of humidification. The addition of water vapour at a given temperature to a stream of dry air will alter the humidity and temperature of air depending on the humidification mechanism utilized. Such mechanisms are thermally driven methods such as steam or mechanically driven methods, both of which are described more in detail in later sections. For analyzing the energy of the system, the mixture enthalpy is determined and is defined as the sum of the enthalpy of dry air and water vapour as shown in Equation 2.24 where H is defined as enthalpy and h is enthalpy per unit mass [26]. Subscripts a labels the parameter for dry air and subscript v is for parameters associated with the water vapour. Another useful formulation is the energy balance equation for humidification and dehumidification systems is illustrated in Equation 2.25 where the subscript w indicates a value associated with liquid water, 1 for one end of the humidifier and 2 represents the opposite end. This equation is used for mass flow problems where there is an inlet and outlet involved such as a duct and the goal of the analysis is to determine the thermodynamics at the inlet and outlet of the control volume [26].

$$\frac{H}{m_a} = h_a + \omega h_v \quad (2.24)$$

$$0 = q + \dot{m}_a[(h_{a1} - h_{a2}) + \omega_1 h_{v1} + (\omega_2 - \omega_1)h_w - \omega_2 h_{v2}] \quad (2.25)$$

The modeling of temperature, relative, humidity, and even light was expressed in [27]. Focusing on humidity modeling, the authors took the modeling approach

by modeling the absolute humidity in the chamber in order to decouple the response from the dry bulb temperature. State variables used in this approach were temperatures of important components and the air as well as the absolute humidity of the air. Ignoring the effects of condensation yields a linear control scheme. The system analyzed in [27] used on-off control through the use of relays of various components. Upon validating the models after system identification was performed, the comparison between experimental data and the predictive model resulted in a fit between approximately 62-73% for each state variable including temperatures and absolute humidity.

In addition to solving a relative humidity problem analytically, one can use CFD to solve for relative humidity inside of a control volume numerically. There exists a myriad of complex humidification systems that involve sources and sinks of water vapour which are best modeled through the use of CFD. Teodosiu et. al. utilized CFD to model relative humidity, air velocity, and temperature profiles in offices which included aspects that affect a room's relative humidity such as climate control and the transpiration of human workers [28]. Although this was a highly inclusive model of relative humidity, the general theories behind the modeling reflected the theoretical formulations based upon conservation of mass and energy principals stated previously. Therefore, CFD can be used as an additional tool in the analysis and/or design of control systems aimed at manipulating and controlling relative humidity systems.

The modeling of saturation vapour density or pressure is based off of empirical data for various dry bulb temperatures. A fitted polynomial curve of this data was used to predict this metric and there exists several polynomial fits for various air dry bulb temperature ranges. If it is desired to measure the saturation vapour content in terms of partial pressures, the formulation by [29] gives a few

eighth-order approximations of the saturation vapour pressure for various temperature ranges as well as whether the air in question is over liquid water or ice. The approximation stated in [29] allows for the determination of saturation vapour pressure in terms of Pascals and is presented as Equation 2.26. This eighth-order polynomial approximation is used for the dry bulb temperature range of 0 to 100 °C and is plotted versus dry bulb temperature in Figure 2.1 for this range. The determination of saturation vapour pressure allows for the analysis of the thermodynamics and humidification of humidifiers and dehumidifiers using previously discussed mathematical relationships.

$$\begin{aligned}
 p_s = & 6.11213476 + 0.444007856T + 0.143064234 \times 10^{-1}T^2 + 0.264461437 \times 10^{-3}T^3 \\
 & + 0.305903558 \times 10^{-5}T^4 + 0.196237241 \times 10^{-7}T^5 + 0.892344772 \times 10^{-10}T^6 \\
 & - 0.373208410 \times 10^{-12}T^7 + 0.209339997 \times 10^{-15}T^8
 \end{aligned}
 \tag{2.26}$$

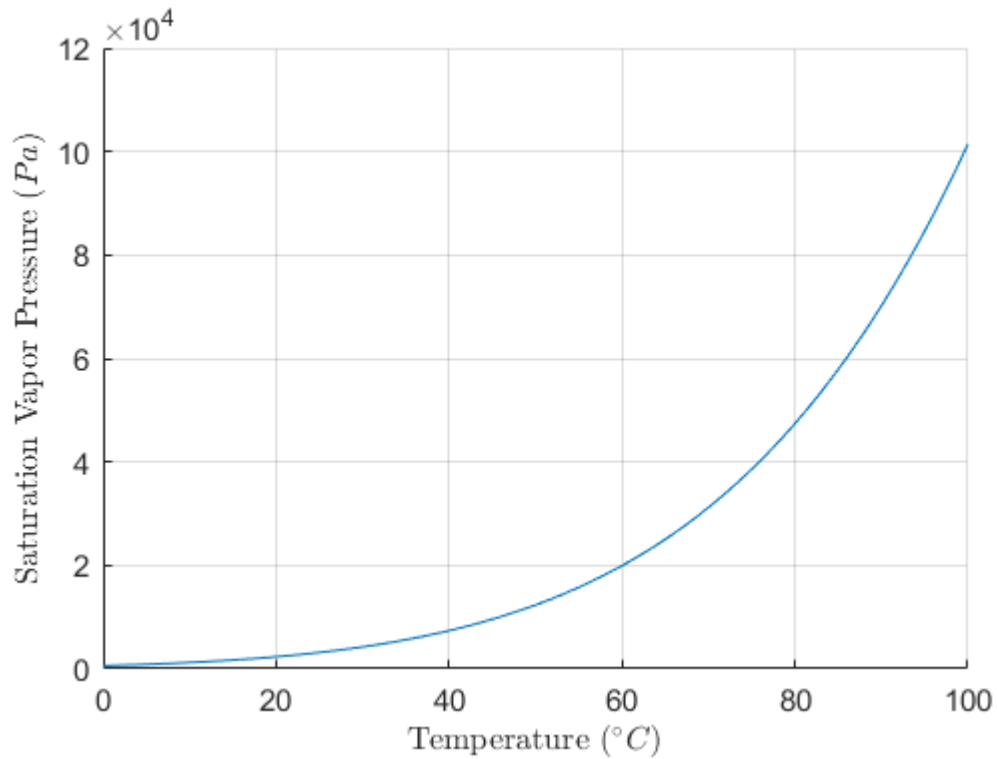


Figure 2.1. Eighth-order polynomial fit for saturation vapour pressure of water vapour in air versus dry bulb temperature based off of the Hyland-Wexler formulation.

In addition to studying the saturation vapour pressure for humidification analysis, there exists psychrometric charts for the determination of various thermodynamic variables for moist air including dry bulb temperature, wet bulb temperature, specific humidity, relative humidity, specific volume, and specific enthalpy. Knowing any two values of these properties in addition to knowing the constant pressure of the mixture enables for the determination of the other variables. An example of a psychrometric chart for atmospheric pressure is featured in [30] and [26] goes over the use of psychrometric charts as well as including specific examples. The use of these charts are widely used in industry for an approximation of variables pertinent to heating, ventilation, and air conditioning applications and has a use for analyzing an environmental control chamber.

2.2.2 Humidification Methods

Steam

One of the most common humidification methods is to heat and vaporize liquid water into steam. This method increases the specific humidity and the dry bulb temperature of air since both thermal energy and mass of water vapour in air are introduced to the virgin air [26]. Utilizing steam in this manner is simple but for design, it may not be favorable for applications that involve the control of temperatures elevated above the zero-input temperature as this method may increase the temperature above a desired threshold.

Evaporative

Another method to increase the specific humidity of air is to utilize the natural evaporation of water without the need to add external energy to the system. This method capitalizes on the natural tendency for water to evaporate in low relative humidity environments [31]. This is due to the state between liquid water and air not being in equilibrium with each other. The water is evaporated through random molecular collisions where some molecules gain enough energy to escape the bulk of liquid water and mix with the dry air. Equilibrium is established once the water vapour pressure reaches saturation. Implementation and enhancement of this mechanic is produced by employing a wick and a fan that introduces a stream of air to the moist wick. The wick increases the surface area of water to air as well as positioning the water into the stream of air. Exposing the moist wick to the flowing air increases the rate of humidification [32]. This method offers humidification without introducing unwanted heat to the system and produces fine and filtered water molecules. However, this method does have a limiting factor for use since at higher relative humidity as it is more difficult for the water to be evaporated from the wick. If it is desired to have a cool humidifier that does not

need to produce high levels of humidity in the surrounding air without increasing temperature, then this method may be superior.

Ultrasonic

In addition to the previous methods, there is a way to mechanically introduce atomized water to air in order to increase humidity via the use of an ultrasonic humidifier. Ultrasonic humidifiers consist of a piezoelectric vibrating plate submerged in a reservoir of liquid water. The piezoelectric plate emits vibrations into the surrounding water a high ultrasonic frequency which displaces and disrupts the surface tension of the water. This process atomizes the liquid water into water vapour during this displacement without the need to heat the water to promote evaporation [33]. Just like evaporative humidifiers, ultrasonic humidifiers will produce a cool mist for humidification. A drawback of this method is that it naturally does not have a filter for filtering out minerals within the water which causes a more translucent mist compared to other humidifiers [32].

List of References

- [1] J. Hanania, J. Jenden, S. Kosasih, K. Stenhouse, J. Toor, and J. Donev. Energy Education. “Heat transfer mechanisms.” [Online]. Available: http://energyeducation.ca/encyclopedia/Heat_transfer_mechanisms
- [2] Britannica. “Thermal conduction.” [Online]. Available: <https://www.britannica.com/science/thermal-conduction>
- [3] J. Hanania, J. Jenden, S. Kosasih, K. Stenhouse, J. Toor, and J. Donev. The Engineering Toolbox. “Conductive heat transfer.” 2003. [Online]. Available: https://www.engineeringtoolbox.com/conductive-heat-transfer-d_428.html
- [4] F. White, *Heat and Mass Transfer*. Addison-Wesley Publishing Company, 1988, pp. 119–170.
- [5] F. White, *Heat and Mass Transfer*. Addison-Wesley Publishing Company, 1988, pp. 270–271.
- [6] F. White, *Heat and Mass Transfer*. Addison-Wesley Publishing Company, 1988, p. 272.

- [7] F. White, *Heat and Mass Transfer*. Addison-Wesley Publishing Company, 1988, pp. 285–417.
- [8] Engineers Edge. “Convective heat transfer coefficient.” [Online]. Available: https://www.engineersedge.com/thermodynamics/convective_heat_transfer.htm
- [9] F. White, *Heat and Mass Transfer*. Addison-Wesley Publishing Company, 1988, pp. 17–18.
- [10] Auburn University College of Engineering. “Radiation exchange between surfaces.” [Online]. Available: <http://www.eng.auburn.edu/~dmckwski/mech7210/radexchange.pdf>
- [11] C. J. M. Lasance. Electronics Cooling. “Thermal capacitance.” 2003. [Online]. Available: <https://www.electronics-cooling.com/2003/05/thermal-capacitance/#>
- [12] F. Burlon, E. Tiberi, D. Micheli, R. Furlanetto, and M. Simonato, “Transient model of a professional oven,” *Energy Procedia*, vol. 126, pp. 2–9, 2017. [Online]. Available: <https://doi.org/10.1016/j.egypro.2017.08.045>
- [13] Wikipedia. “OpenFOAM.” [Online]. Available: <https://en.wikipedia.org/wiki/OpenFOAM>
- [14] Wikipedia. “COMSOL Multiphysics.” [Online]. Available: https://en.wikipedia.org/wiki/COMSOL_Multiphysics
- [15] F. White, *Heat and Mass Transfer*. Addison-Wesley Publishing Company, 1988, p. 363.
- [16] F. White, *Viscous Fluid Flow*. McGraw-Hill, 2005, pp. 183–205.
- [17] F. White, *Fluid Mechanics*. McGraw-Hill, 2015, pp. 225–246.
- [18] H. Mistry, Ganapathi-subbu, S. Dey, P. Bishnoi, and J. L. Castillo, “Modeling of transient natural convection heat transfer in electric ovens,” *Applied Thermal Engineering*, vol. 26, no. 17-18, pp. 2448–2456, 2006. [Online]. Available: <https://doi.org/10.1016/j.applthermaleng.2006.02.007>
- [19] A. F. Robertson and D. Gross, “An electrical-analog method for transient heat-flow analysis,” *Journal of Research of the National Bureau of Standards*, vol. 61, no. 2, pp. 105–115, 1958. [Online]. Available: <http://dx.doi.org/10.6028/jres.061.016>
- [20] Dartmouth College. “System analogies.” [Online]. Available: https://www.dartmouth.edu/~sullivan/22files/System_analogy_all.pdf

- [21] F. White, *Heat and Mass Transfer*. Addison-Wesley Publishing Company, 1988, pp. 48–99.
- [22] S. Tapia and J. A. del Río. Universidad Nacional Autónoma de México. “One temperature model for effective ovens.” 2011. [Online]. Available: <https://arxiv.org/pdf/1109.0664.pdf>
- [23] E. Ramirez-Laboreo, C. Sagues, and S. Llorente, “Dynamic heat and mass transfer model of an electric oven for energy analysis,” *Applied Thermal Engineering*, vol. 93, pp. 683–691, 2016. [Online]. Available: <https://doi.org/10.1016/j.applthermaleng.2015.10.040>
- [24] J. P. Abraham and E. M. Sparrow, “A simple model and validating experiments for predicting the heat transfer to a load situated in an electrically heated oven,” *Journal of Food Engineering*, vol. 62, no. 4, pp. 409–415, 2004. [Online]. Available: [https://doi.org/10.1016/S0260-8774\(03\)00265-6](https://doi.org/10.1016/S0260-8774(03)00265-6)
- [25] K. Unklesbay, A. Boza-Chacon, and N. Unklesbay, “Air temperature transfer function of a convection oven,” *Food Control*, vol. 8, no. 1, pp. 39–43, 1997. [Online]. Available: [https://doi.org/10.1016/S0956-7135\(96\)00045-X](https://doi.org/10.1016/S0956-7135(96)00045-X)
- [26] M. J. Moran, H. N. Shapiro, D. D. Boettner, and M. B. Bailey, *Fundamentals of Engineering Thermodynamics*. Wiley, 2014, pp. 753–784.
- [27] J. Dostál and L. Ferkl, “Model predictive control of climatic chamber with on-off actuators,” *IFAC Proceedings Volumes*, vol. 47, no. 3, pp. 4423–4428, 2014. [Online]. Available: <https://doi.org/10.3182/20140824-6-ZA-1003.01571>
- [28] C. Teodosiu, V. Ilie, and R. Teodosiu, “Modeling of water vapor sources in enclosures,” *International Journal of Structural and Civil Engineering Research*, vol. 4, no. 2, pp. 212–217, 2015. [Online]. Available: <http://www.ijscer.com/uploadfile/2015/0922/20150922014808395.pdf>
- [29] P. J. Flatau, R. L. Walko, and W. R. Cotton, “Polynomial fits to saturation vapor pressure,” *Journal of Applied Meteorology*, vol. 31, no. 12, pp. 1507–1513, 1992. [Online]. Available: [https://doi.org/10.1175/1520-0450\(1992\)031%3C1507:PFTSVP%3E2.0.CO;2](https://doi.org/10.1175/1520-0450(1992)031%3C1507:PFTSVP%3E2.0.CO;2)
- [30] Z. Zhang and M. B. Pate, *A Methodology for Implementing a Psychrometric Chart in a Computer Graphics System*. ASHARE Transactions, 1988, vol. 94.
- [31] Luma Comfort. “See how an evaporative humidifier works.” [Online]. Available: <http://www.lumacomfort.com/article/how-evaporative-humidifier-works.htm>
- [32] M. Mifflin. The Spruce. “Ultrasonic vs evaporative portable humidifiers.” [Online]. Available: <https://www.thespruce.com/humidifiers-ultrasonic-vs-evaporative-humidifiers-1908160>

- [33] Holmes. “How does an ultrasonic humidifier work?” [Online]. Available: <http://www.holmesproducts.com/blog/archive/2014/october/how-does-an-ultrasonic-humidifier-work%3F.html>

CHAPTER 3

Methodology

3.1 Electronics and Software Design

The electrical system for the prototype was designed in coordination with the other sub-systems involved in the prototype, including the temperature and humidity control sub-systems. Since the combination of software and electronics affects other portions of the prototype, the overall design is first discussed to give a better understanding of how each sub-system was melded together for a complete system design.

3.1.1 Firmware

Another portion of the project that required coding is the microcontroller that was used in the system's electronics which will be talked about in a later section. The utilized microcontroller is the ATMEGA328P-PU and this particular microcontroller was chosen due to its compatibility with the open-source Arduino IDE and its ease of programming with a dedicated programmer.

The purpose of this microcontroller is solely for fan control of the humidifier and heater. Although it is not required to use PWM fans for these sub-systems, this architecture allows for greater hardware flexibility for these sub-systems. The microcontroller receives an analog signal from the data acquisition card's digital to analog output pins for control of the heater and humidifier fans and translates the analog voltage to a PWM duty cycle of a set frequency specified in the firmware's code. It also receives feedback from the tachometers of the heater fans to determine the rotational speed of the fans for the purpose of optional safety protocols for heater failure. The firmware generated for this project only variably controls PWM duty cycle and measures heater fan rotational speeds. Besides reading the

frequency of tachometers, the reason why this method of PWM control was used instead of using the more traditional PWM generator circuit that consists of a triangular wave generator and a comparator was due to being able to set the frequency via programming.

The firmware code was generated in the Arduino IDE environment and can be programmed with the in system programmer of the later discussed circuit board. Since the microcontroller and the base Arduino environment can only support a few specified PWM frequencies, there needed to be a solution to set any frequency for the PWM signals. Luckily, an open-source solution for this problem was found at [1]. By adding this code to the Arduino IDE library, this enabled for greater flexibility and functionality for the previously discussed application. The complete firmware code is found in Appendix A.1.

3.1.2 Software

The overall control of the system is governed by a PC with software coded in Visual Basic. Users are able to operate the software to specify a desired set point for the temperature and the relative humidity of the enclosure as well as monitor these parameters over time. This is accomplished by discretizing analog voltage signals from hardware and storing the data in established data arrays in the Visual Basic source code. The GUI shows the data arrays for air temperature and relative humidity in the enclosure through the use of line graphs where the vertical axis represents the parameter value and the horizontal axis represents time in seconds. The status of heater temperature and ambient air temperature are also shown in the GUI but does not visually record that information in a plot. The user can also tune fan speeds to a specified duty cycle if there is a need to limit air speed in the enclosure as well as set a specified duration of time for the control task after which the system's hardware will turn off. A graphic of the GUI is shown in Figure 3.1

below.

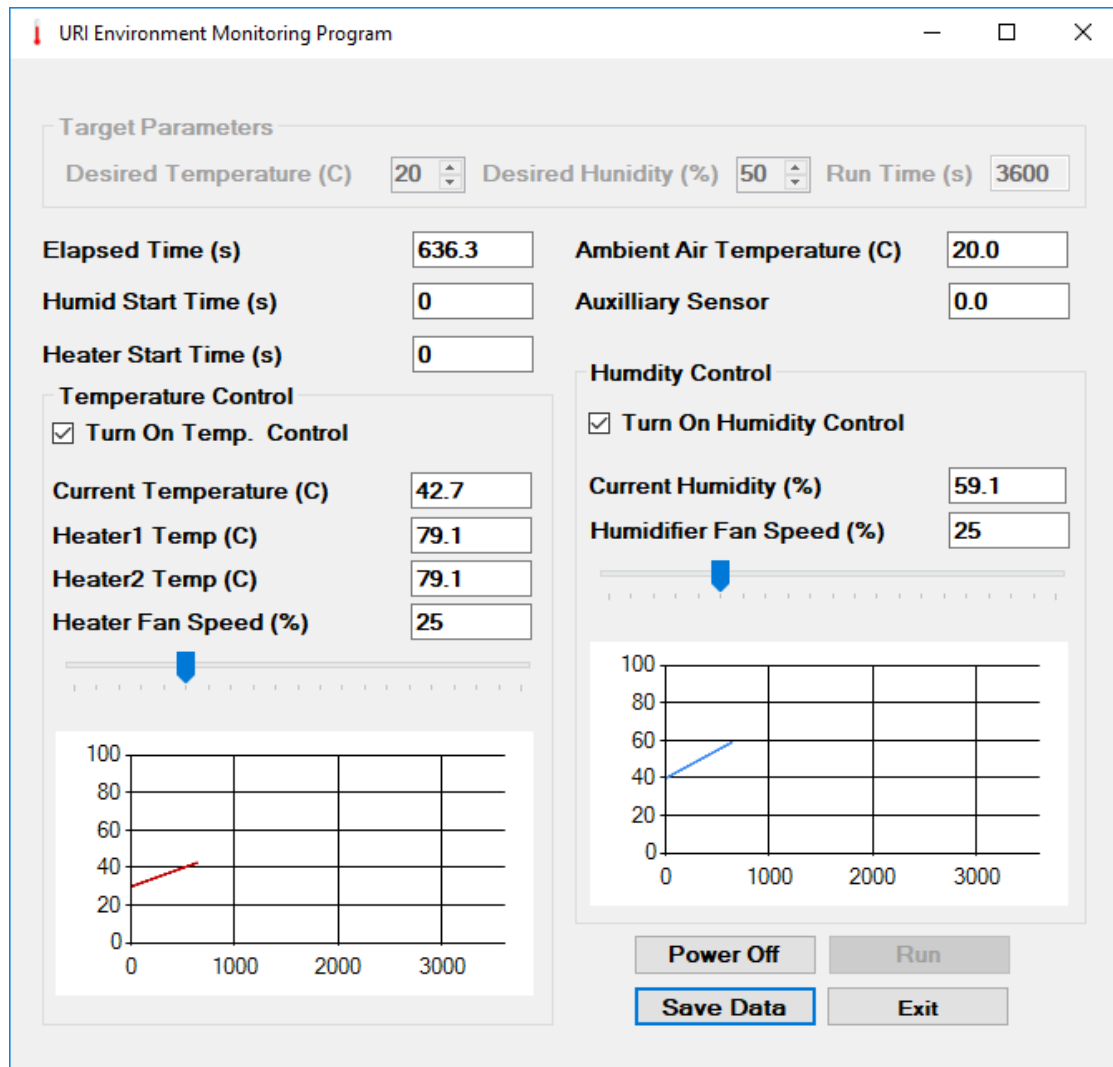


Figure 3.1. Graphical user interface for control of temperature and humidity.

In addition to viewing this information live, the user can also save the data to a .txt file for additional analysis or for any other reason that requires system data to be recorded. This function not only records the temperature and relative humidity, but also records other parameters that are valuable for looking at the data at a later date. This data includes logical values that specify whether the heater and/or humidifier was active and the PWM duty cycles of the fans in addition to the previously mentioned temperature and relative humidity data. For

further details of the Visual Basic source code used in this project, please refer to Appendix A.2.

In order to interface the software with the required hardware, all communications were accomplished with the use of a data acquisition card. Specifically, the USB-1408FS-Plus was employed as the intermediate component between system hardware and the PC and occupies a single USB port on the computer. It has 8-bit digital input, 8 channels of 13-bit resolution analog to digital converters, 8-bit digital output and 2 digital to analog converters. The analog pins are capable of recording or transmitting signals at 50000 samples per second [2].

3.1.3 Electronics

In addition to the development of software and firmware for the system, there was a need to design and build electrical hardware for proper application of the software. A printed circuit board (PCB) was used to provide the necessary signal processing and power delivery for all of the sub-systems involved. The large problem the PCB solved was the generation of accurate and low noise analog signals that were free from any loading effects from the sub-systems that draw a large amount of electrical power. Therefore, the design of the PCB allowed for proper measurement of state variables, power delivery that does not affect sensor measurements, control of all electrical parts, and communication to the PC's software. To better follow along with the discussion of the electronics of this section, refer to the provided schematics located in Appendix B.1.

The measurement of all state variables was accomplished by employing analog sensors to measure parameters. These analog sensors consist of sensors measuring state properties such as temperature, relative humidity, and position of numerous components. Temperature of the air inside the enclosure as well as the ambient air temperature was measured using LM35 temperature sensors which are a silicon-

based integrated circuit that produces a linear analog voltage signal that scales with temperature and has an overall temperature response range from -55 to 150 Centigrade depending on the particular sensor [3]. The LM35 sensors used in the prototype have a range from 0 to 110 Centigrade. Adafruit PT100 platinum RTD sensors were used for monitoring the temperature in the heaters since this sensor has a wide temperature operating range and a maximum measurable temperature of 550 Centigrade [4]. Relative humidity was measured with a Honeywell HIH-4021 relative humidity sensor in the initial prototype. This sensor operates similarly to the LM35 temperature sensor since it is also a silicon based device that produces an analog voltage signal that scales with the measured relative humidity [5]. This sensor was replaced in the final design with a Vaisala HMP110 temperature and relative humidity sensor probe due to better relative humidity accuracy for the most-often used case where the enclosure will be operated below 40 Centigrade [6]. The Actuonix L12-50-50-12-P linear actuator that was used in the final application contains a potentiometer that measured the extension by producing an analog voltage signal [7]. The actuator was used in the final Cryo-TEM prototype for controlling a door that separates the enclosure from the dewar and was used to protect the thermodynamics of the system.

All of the circuits containing the previously mentioned analog circuits as well as any other analog sensors the user would like to use are in series with analog signal processing components. The LM35 temperature sensors' analog output pin are directly connected to the input of a non-inverting operational amplifier with an output gain of 10 in order for the data acquisition card to read the signal and be outside its uncertainty error range of about ± 11 mV [2]. Taking into consideration that the LM35's analog voltage signal scales at 10 mV per degree centigrade, the gain was necessary in order to prevent any signal noise caused by measurement

uncertainty [3]. The RTDs were placed as a resistor in a wheatstone bridge in order to take the difference of the voltage between two fixed 1 kilohm resistors and the voltage between the RTD and another 1 kilohm resistor. This technique reduces the effect of any problems that may occur due to fluctuations in the 5 VDC power rail. The outputs of the wheatstone bridge are connected to an active low-pass filter prior to the two signals being processed by a differential operational amplifier in an effort to reduce the number of pins needed for the data acquisition card to read. There are also two customizable analog sensor circuits that can utilize either 24 VDC or 5 VDC analog sensors and contain a non-inverting operational amplifier with trim potentiometers located between the inverting input and the output of the amplifier for hardware control of the amplifier gain. In parallel with the potentiometer, a SPST switch is used to short the potentiometer in case the user decides to not have any gain on these sensor signals. This is the case for the HIH-4021 relative humidity sensor due to its voltage output range. As for the circuit designed for the HMP110 sensor, it does not contain any components to manipulate the output signal save for some buffering due to circuitry inboard of the sensor. All of the aforementioned circuits contain active low-pass filters at or near the input to the data acquisition card which all have a cutoff frequency of about 23 Hz which was chosen in conjunction with the sampling frequency of the software. These active filters also have the benefit of having the sensors not subject to any loading effects due to the operational amplifier's low impedance output. The analog outputs of the circuitboard is connected to a DC-37 female D-sub connector which is connected to the data acquisition card.

In an effort to decrease the noise in measurement signals, a linear power supply is used for the measurement circuits. Linear power supplies offer low output voltage ripple as opposed to switching power supplies which often generate high frequency

noise without filtering. The only downside with linear power supplies is that they are not ideal for high power circuits. To get the benefits of both of these power supplies, a circuitboard that utilize both a linear and a switching power supply for specific applications will be able to have both a noiseless voltage supply for sensitive components and enough power to drive high power components such as heaters. To achieve this, the power supplies and their respective components need to be electrically isolated from one another and can only communicate with each other through the use of optocouplers. Specifically, the switching power supply used for the heaters, humidifiers, and other high power components is a 350 Watt power supply built by Delta [8]. The linear power supply for measurements and system logic can be a fixed output power supply or a lab bench linear power supply that is capable of supplying 24 VDC. In order to bridge the gap between the circuits powered by the separate power supplies, LTV-847 optocouplers are used to communicate digital logic, PWM, and other square waves from individual sub-systems back to the PC or the microcontroller.

As mentioned earlier, an ATMEGA328P-PU microcontroller was used for fan control and fan monitoring of the heaters and humidifier as their control and monitoring is based on square waves. The foundation of utilizing this microcontroller in the circuitboard is based off of the open-source Arduino Uno Rev 3 platform whose schematic is found at [9]. This design was altered to better serve the application at hand. Besides the fans, the microcontroller is able to communicate with the PC through an 8-bit parallel connection to the data acquisition card's digital input pins via the aforementioned D-sub connector. The motivation behind this was that the microcontroller is in a good position for being utilized as both a controller and a safety mechanism by having the option of telling the computer any warnings that the firmware can be coded for this application.

For controlling the numerous high-power components in the total system, it was determined that transistors were the better choice for switching instead of relays. The main consideration in this decision was that transistors are capable of switching at a higher frequency whereas electromechanical relays would quickly wear out for this application. There exists high frequency switching due to the narrow deadband of the on-off control of temperature. The narrow deadband was deemed necessary to keep the temperature close to the desired temperature. Normally the reason why on-off control is used is to prevent wear on components, however since the heaters do not have any mechanical components, excluding the fans, there will not be any significant wear due to the high-frequency switching. The fans themselves are PWM controlled fans and were designed for such high frequency therefore, the entire heater system with the transistors allow for a narrow deadband control. The same logic can also be extended to the humidifier since it is also controlled by a transistor in an on-off control system and has a similar fan in terms of operation and an ultrasonic humidifier that operates at high frequencies. The transistor used for this application is a Vishay IRL540 MOSFET which has the capacity of handling up to 20 Amps of electrical current when the die is at 100 degrees Centigrade. When the transistor is saturated, the drain-source on-state resistance between the drain and the source is 0.077 Ohms [10]. These characteristics make these transistors suitable for controlling the high-power devices in the system. An array of six of these transistors are utilized in the final circuit board. Cooling for the heater's transistor is needed due to approximately 10 Amps of current flowing through it causes the transistor to dissipate about 8 Watts of heat. Therefore a heat sink capable of dissipating this amount of heat with natural convection was used to preserve the transistor.

3.2 Prototype Enclosure Design

The prototype enclosure built for preliminary evaluations is simply put, a cube with 10 inch sides built with 7/32 inch thick polycarbonate sheets. To form the enclosure, the polycarbonate was machined and assembled into two pieces, one being the lid and the other piece being the main body of the enclosure that consists of five pieces of polycarbonate glued together with plastic cement. The interior of the enclosure was sealed with a bead of silicone sealant along the interior edges to mitigate the escape of hot and humid air. The panels consists of machined features to facilitate the addition of hardware necessary for properly sealing the enclosure which includes but is not limited to holes for tube fittings, gaskets, and sealed cord grips.

Heating and humidifying the enclosure necessitates features for interfacing the heaters and humidifier. The enclosure has two tube fittings for fitting a closed-loop humidifier outside of it. This allows for one fitting to act as an inlet to the enclosure and the other to be the return. In addition to the tube fittings, two sealed cord grips were installed into one of the walls of the enclosure in order to feed electrical wires into the interior of the enclosure without compromising the sealing of the enclosure. An additional hole is used to fit a probe that contains sensors for measuring relative humidity and temperature of the enclosure's cavity. Gaskets were also installed in portions of the enclosure where there is a possibility for significant air to escape the inside of the enclosure including the lid, tube fittings, and the sensor probe. Additional details of the construction of the enclosure can be found in Appendix B.2 and a 3-D rendering of the enclosure assembly is shown in Figure 3.2 below.



Figure 3.2. 3-D CAD model of enclosure assembly without heaters or humidifier.

3.3 Temperature Control

This section goes over the theoretical analysis of the thermal system and goes over the design process of the necessary components.

3.3.1 Heater Design

The first step in the design phase is to design and build adequate heaters for the system. It was decided that the heater has to conform to a size envelope, to use electric heaters that run on 24 VDC for power delivery, and to be relatively safe for its application. Prior to doing any sort of analysis, a proof of concept prototype was designed with the knowledge that forced convection was to be employed to have a compact heater size and with the idea that the prototype should be easily altered as far as modifying the properties of heat transfer. This section goes over the design process of the heater.

To conform with the size and electrical requirements, the decision was made to use ceramic cartridge heaters for the heat source. Specifically, the cartridge heaters

used were designed for and utilized in 3-D printer nozzle heater assemblies and an example of such a cartridge heater is shown in [11]. These heaters are 20 millimeters long with a 6 millimeters diameter and are capable of producing a heat rate of 40 Watts per unit which allows for the potential of a compact array of these heaters connected in parallel to deliver sufficient heat for the enclosure. When using these heaters it is important to note the thermal limitations of the cartridges. Although a thorough internet search did not yield any readily available documentation for these heaters directly, an observation of an exhibit of where these heaters are used such as in [12], it is stated that the maximum temperature for the extruder is 260 °C so this will be the metric to analyze the heater temperature against. Measuring the temperature of the heaters will be performed by an RTD temperature sensor which outputs an analog voltage signal that can be measured by a PC.

The previously mentioned cartridge heaters may be able to deliver a heat rate of 40 Watts each, however it is required to have them implemented in a manner to not overheat and destroy the heaters or at the very least, have them implemented in a safe way. To do this, the cartridge heaters were embedded into a metallic piece to draw heat away from the heaters themselves. The style of this design was inspired by how CPUs are cooled in computers. Typically CPUs are cooled using a heat exchanger or some form of a heat sink both of which are enhanced with force convection induced by a fan that is mounted directly or near the heat sink itself. With this in mind, the cartridge heaters and RTD were installed in-between two metallic plates with grooves that match the diameter of these parts in order to provide the best interface for heat conduction. The assembled plates with heaters and RTD are to be referred to as the heater block. The material used for these plates was determined to be copper due to its high thermal conductivity and relatively low specific heat. The heat transfer performance was enhanced through

the use of a heat sink and a PWM controlled 24 VDC brushless fan that directs air towards the heater. A detailed drawing is provided in Appendix B.3 which includes all of the parts used in the design. A cross section of the design is provided for in Figure 3.3 below for a quick reference.

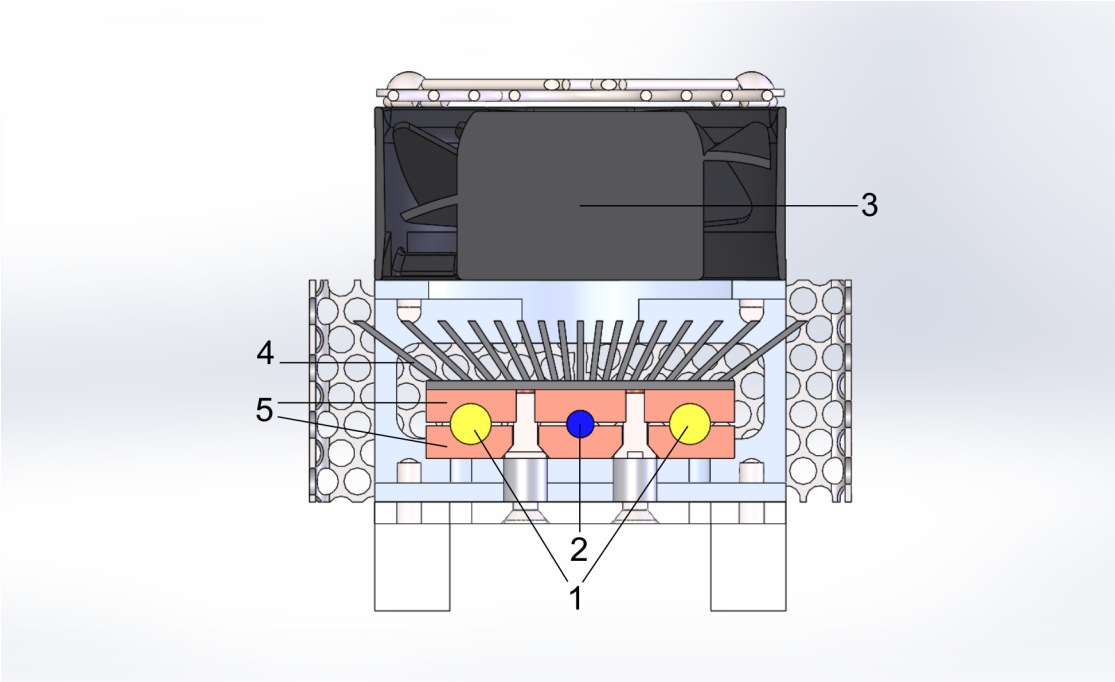


Figure 3.3. Cross section of heater sub-assembly showing the cavities for cartridge heaters and RTD temperature sensor. 1. cartridge heaters, 2. RTD, 3. fan, 4. heat sink fins, 5. copper blocks.

The previously discussed heater sub-assembly was utilized in a modular fashion for the ease of manufacturability and scalability. To keep the heaters together and to provide a platform for eliminating excess wiring within the enclosure, the sub-assemblies were mounted onto a 3-D printed mounting bracket. Also included on the mounting bracket is a fixture for mating a prototype PCB for connecting the fans, cartridge heaters, sensors, and any other auxiliary electrical components. For this enclosure, two heater blocks were to be used to provide up to 240 Watts of heat rate or more. A 3-D CAD model of the finished assembly is depicted in

Figure 3.4 at the end of this paragraph. A complete set of technical documents associated with the heaters are found in Appendices B.3, D.1, and D.2.

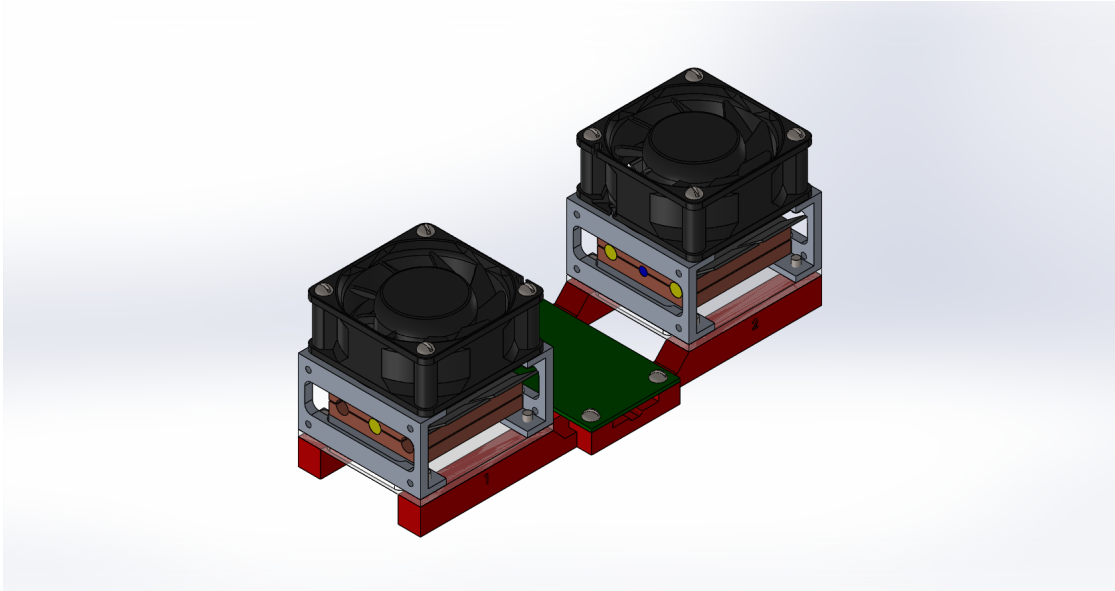


Figure 3.4. A 3-D CAD image of the heater assembly which consists of two heater sub-assemblies capable of delivering 240 Watts of heat via forced convection.

Theoretical analysis was performed on the previously mentioned heater design. The steady state analysis is done first to determine a maximum operating heater wattage that will not damage the system. This is a simple analysis for the heaters since it can be accurately modeled by a first-order system. The heater's equivalent thermal resistance is determined by the sum of the thermal resistances of the heat sink and the heater block. For this analysis, the heat transfer properties will be determined with the heater's fan set to a 25% duty cycle as this was to be used in the final system. At this duty cycle, the air velocity against the heat sink was determined to be 7.05 m/s which was determined by referring to the datasheet included in Appendix D.2 to find the volumetric flow rate for this duty cycle as well as using the cross sectional area of the fan's duct from the manufacturer's CAD file. Cross referencing this velocity to the heat sink's datasheet in Appendix D.1, it can be found via interpolation that the thermal resistance at this velocity is

approximately 1.10 K/W. For the heater block, it is assumed that the majority of the heat transfer is through the heat sink. Assuming this, the thermal resistance through the block is calculated using Equation 2.14 with the thermal conductivity of copper being 400 W/mK as found in [13] and was calculated to be 0.00530 K/W. Summing the heat sink thermal resistance and the heater block thermal resistance adds up to the total thermal resistance of the heater which is 1.10 K/W.

The thermal capacitance of the heater is simply the sum of the capacitances of the heat sink and the heater block. Using Equation 2.6, the thermal capacitance of each component is calculated knowing the masses and specific heat of the components. SolidWorks allows for the determination of the mass of the copper heater block and the aluminum heat sink which is 0.156 kg and 0.026 kg respectfully. The data for the specific heats of the mentioned materials were gathered from [14] where the specific heat of copper was 0.39 kJ/kgK and 0.91 kJ/kgK for aluminum. With this information, the total theoretical capacitance was found to be 85 J/K.

A model for the heater was developed with the previously determined thermal resistance and capacitance of the heater. By treating the ambient temperature and heat dissipation rate through the heaters as inputs to this system, a first-order differential equation can be used to model the heater's behavior. An electrical analog for this system is visually represented in Figure 3.5 and its mathematical form is presented in Equation 3.1 below. Being a linear equation, it lends itself to be suitably simulated in Matlab with the `lsim` function, details of the simulation are shown in the Matlab function script located in Appendix C.1. The results of this simulation for a single heater, not the whole dual-heater assembly, with an actual input of 116 Watts and the heater exposed to ambient room temperature air are shown in Figure 3.6 with temperature change versus time. This heat rate input represents the use of three 40 Watt cartridge heaters in the heater block and

the reason for why this does not lead to a heat rate input of 120 Watts is due to electric power dissipation through the IRL540 MOSFET used to control the heater. The transistor's drain-source on-state resistance is 0.077Ω at 5 VDC and this value was used to determine power loss in the heater circuit due to a lack of information for the transistor at 24 VDC. The Matlab script was written to take the transistor's resistance into consideration and effectively models the dynamics with a heat input as a function of the equivalent electrical resistance of the heaters and is only meant for use in a 24 VDC system.

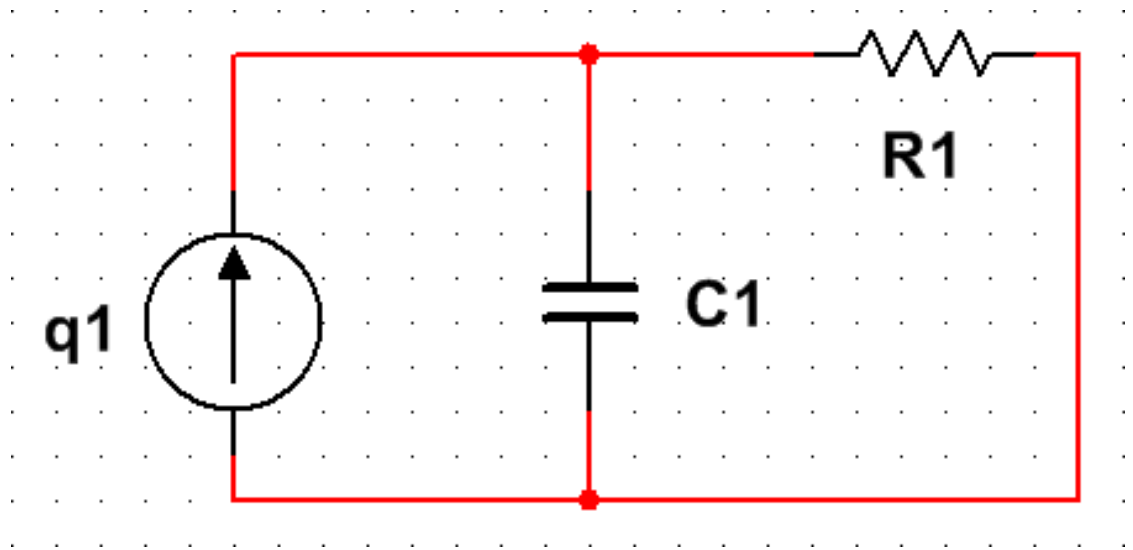


Figure 3.5. Electrical analog for heater thermal dynamics.

$$\dot{T}_1 = \frac{-1}{R_1 C_1} T_1 + \frac{q_1}{C_1} + \frac{T_a}{R_1 C_1} \quad (3.1)$$

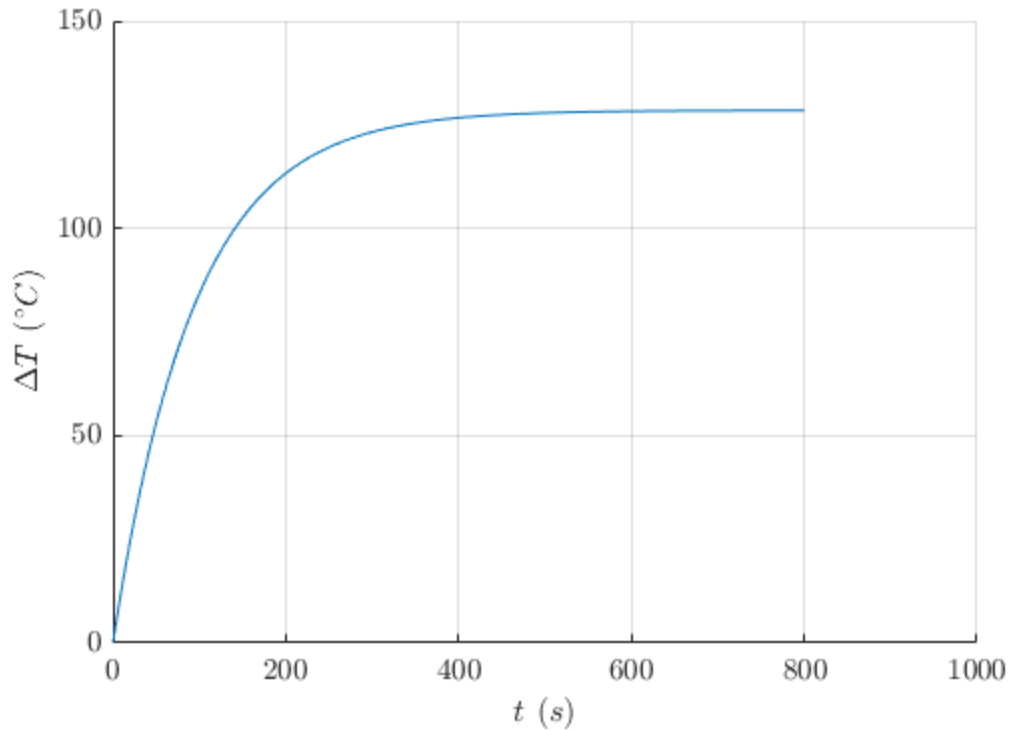


Figure 3.6. Heater model simulation for $v=7.05$ m/s air stream and three cartridge heaters in heater block with a 116.2 Watt step input. Heater temperature is relative to ambient temperature.

The remaining enclosure to be modeled does not lend itself well to modeling purely by theory. The rationale behind this statement is due to the fluid transport within and outside the enclosure. As shown in Equation 2.4, without the knowledge of the velocity profiles of the airflow and how heat transfer is determined for odd shapes, the convective heat transfer coefficient cannot be theoretically calculated accurately. Without an extensive simulation performed by a finite element or finite difference calculations, analysis is limited to identifying the thermal system experimentally. Although the numerical values for the thermodynamic parameters involved may not be able to be calculated, it is still possible to determine the general structure of the state-space equation associated with the enclosure and its components with the lumped capacitance method. The following section on the

state-space representation goes over some more of the specifics of the modeling process.

3.3.2 Thermal State Space Representation

As discussed in the former section, the best way to model the entire system’s thermal performance is experimentally through system identification and the lumped capacitance method. Prior to determining the exact values of thermal resistance and thermal capacitance for each individual component, the general form of the state-space equation needed to be determined.

The portions of the system where thermal state variables are measured are the heaters, enclosure air, walls, and the exterior boundary between the wall and the ambient environment. This leads to a fourth-order system due to four transient first-order systems put in series with each other which is shown illustratively as an electrical analog in Figure 3.7 where the subscript 1 represents variables associated with the heater, 2 for the air within the enclosure’s interior, 3 for the enclosure’s walls, and 4 for the film of air on the exterior of the enclosure. The temperatures in the system are located between the resistors or between a resistor and a heat flow within its electrical analog. Treating heat flow q_1 and ambient temperature T_a as inputs, the continuous state space representation of the model can be determined and is shown in Equation 3.2 below. The ambient temperature to be treated as an input is the air temperature far from the prototype.

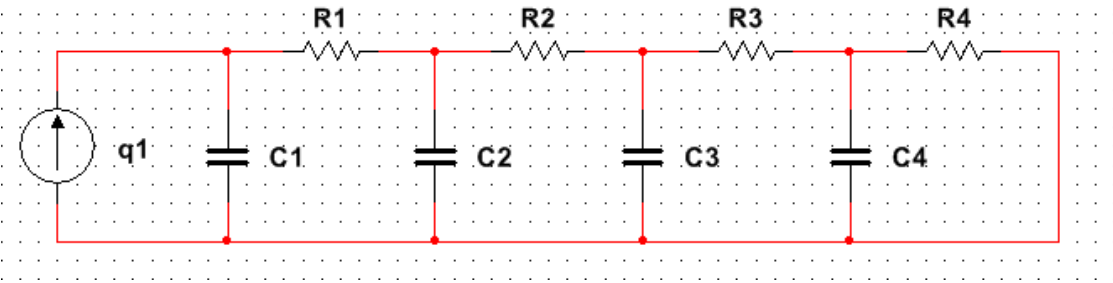


Figure 3.7. Electrical analog for a fourth-order thermal system.

$$\begin{aligned}
\begin{bmatrix} \dot{T}_1 \\ \dot{T}_2 \\ \dot{T}_3 \\ \dot{T}_4 \end{bmatrix} &= \begin{bmatrix} -\frac{1}{C_1 R_1} & \frac{1}{C_1 R_1} & 0 & 0 \\ \frac{1}{C_2 R_1} & -\frac{1}{C_2 R_1} - \frac{1}{C_2 R_2} & \frac{1}{C_2 R_2} & 0 \\ 0 & \frac{1}{C_3 R_2} & -\frac{1}{C_3 R_2} - \frac{1}{C_3 R_3} & \frac{1}{C_3 R_3} \\ 0 & 0 & \frac{1}{C_4 R_3} & -\frac{1}{C_4 R_3} - \frac{1}{C_4 R_4} \end{bmatrix} \begin{bmatrix} T_1 \\ T_2 \\ T_3 \\ T_4 \end{bmatrix} \\
&+ \begin{bmatrix} \frac{1}{C_1} & 0 & 0 & 0 \\ 0 & 0 & 0 & 0 \\ 0 & 0 & 0 & 0 \\ 0 & \frac{1}{C_4 R_4} & 0 & 0 \end{bmatrix} \begin{bmatrix} q_1 \\ T_a \\ 0 \\ 0 \end{bmatrix}
\end{aligned} \tag{3.2}$$

To identify the various parameters of the state-space equation, measurements of the transient and steady-state response of each separate component must be performed. By running an experiment or several experiments to collect data reflecting the state variables, the parameters of thermal resistances and capacitances can be identified. Specifically, by using the data for a certain temperature node as an input and isolating the system prior to the node, it is possible to tune the system parameters to yield the proper transient and steady-state response for each component. For example, since it is known what the thermal resistance and capacitance of the heater are and that there was an experiment to measure each of the temperature nodes, the adjacent resistance-capacitance element can be determined. Using the state-space equation associated with element 1 and 2 in Figure 3.7 and treating the enclosure air temperature as an input along with heat flow, the thermal parameters can be found. The thermal resistance is the first item to be determined since the steady state response needs to be determined prior to the transient response which is affected by thermal capacitance. Tuning the thermal resistance to get the model to match the measured data to a satisfactory error allows for the thermal resistance determination of each component. The same can be done for determining the thermal capacitance of the system or if the scenario allows for it, typical system dynamic formulations can be used for characterizing the transient response.

The first element of the thermal system has already been theoretically modeled earlier for this application due to its simplicity. Since there are two heater blocks in the constructed prototype, the thermodynamic parameters R_1 and C_1 can be determined for the dual heaters by treating the heater blocks to be in parallel with one another. In other words, the heat rate input to the system is shared by the two heater blocks symmetrically. The thermodynamic properties have already been determined in Section 3.3.1 earlier therefore, to determine the thermodynamic values needed for the previously state state-space equation, the previously determined heater thermal resistance was reduced by half and the heater capacitance doubles in value.

Another consideration for this modeling application is the heat rate loss due to the IRL540 transistor since this will result in an error in the calculation. To account for this, the model in Matlab was coded to take this into account. This was easily done by knowing that the heat rate input is a function of the number of cartridge heaters used in the heater. To keep the formulation in general terms, the actual heat rate input associated with any MOSFET transistor in a heater application utilizing cartridge heaters is shown in Equation 3.3 below where V is the DC voltage across the heater in volts, R_{heater} is the electrical resistance of the cartridge heater(s) in Ohms, n is the number of heating elements in parallel with one another, and R_{ds} is the electrical resistance of the drain-source on resistance of the MOSFET transistor used. This equation was derived utilizing a combination of Kirchoff's circuit laws and electrical power formulations to determine the current flowing through the circuit and the power dissipated over the heater array. In the case of the experiments in this thesis, the heat loss from the transistor at 240 Watts, 160 Watts, and 80 Watts of cartridge heater values (ie. 6, 4, and 2 40 Watt heaters in parallel) are 14.7 Watts, 6.60 Watts, and 1.70 Watts respectfully.

This formulation allows for an easy conversion of datasheet heat dissipation rate solely with the heaters to the actual heat dissipation rate in an application with a MOSFET transistor controlling the actuation of heat rate.

$$q = \frac{V^2 R_{heater}}{n(R_{ds} + R_{heater}n^{-1})^2} \quad (3.3)$$

The experiments for the identification of the thermal state-space system utilize the previously discussed LM35 and platinum RTD sensors in Section 3.1.3. To enhance thermal conduction between the critical surfaces of the cartridge heaters and various temperature sensors, Arctic MX-4 thermal compound was utilized [15]. This allows for a proper mating of thermal components to maximize heat flow to associated components without having to worry about the surface conditions of the various sensor and heater mating surfaces and allows for more accurate temperature readings from the temperature sensors. Temperature readings from the enclosure walls, heaters, humidifier, and air were read every second for the duration of the experiments to records the temperature state-variables.

3.4 Humidity Control

This section is dedicated to going over the design and analysis of humidification.

3.4.1 Humidifier Design

The humidifier used in the prototype is a closed-loop design where air is drawn from the enclosure to be humidified and is returned to the enclosure. 3/4 in. inner-diameter tubes were used to transport the water vapour-air mixture between the humidifier and the enclosure. The entire humidifier assembly consists of a 3-D printed cover with ports and fixtures for fans, cabling, and the aforementioned tubing, a reservoir for distilled water, and an ultrasonic humidifying head. Tech-

nical drawings of the humidifier cover are shown in Appendix B.4. The reservoir is a stainless steel food container that is roughly 4 and 13/16 inch diameter and includes a latch to secure the cover in place. A CAD rendering of the humidifier assembly is shown in Figure 3.8.

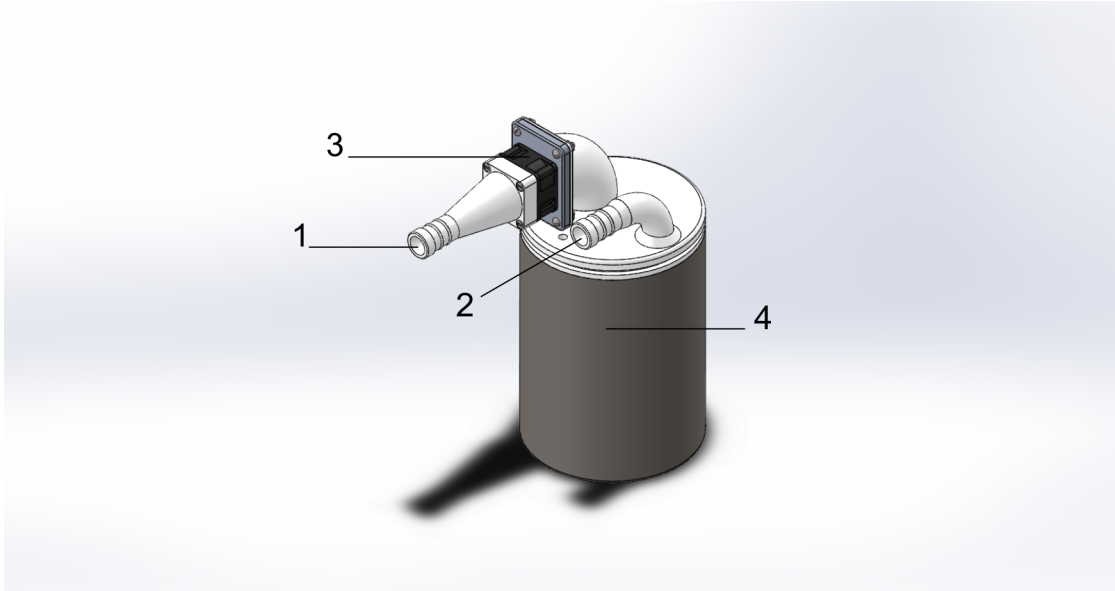


Figure 3.8. Humidifier assembly. 1. intake nozzle, 2. exhaust nozzle, 3. fan, 4. water reservoir.

The ultrasonic humidifying head used in the system is similar to the humidifier found in [16]. This particular humidifier is said to be able to atomize 400 milliliters of water per hour under normal operating conditions. Given that this is an unknown parameter for the application it is used in, the average amount of water atomized will be measured on a mass basis. The fan utilized is a 40 millimeter Mechatronics MD4028V24B-FSR-PC capable of delivering 24.3 CFM of air. The fan was installed on the intake side of the humidifier to reduce the ingress of water to the electrically controlled fan. The humidifier head was loosely installed on the floor of the water reservoir with wiring passing through the cover of the humidifier. A cross section is available in Figure 3.9 to show the placement of the the ultrasonic humidifier.

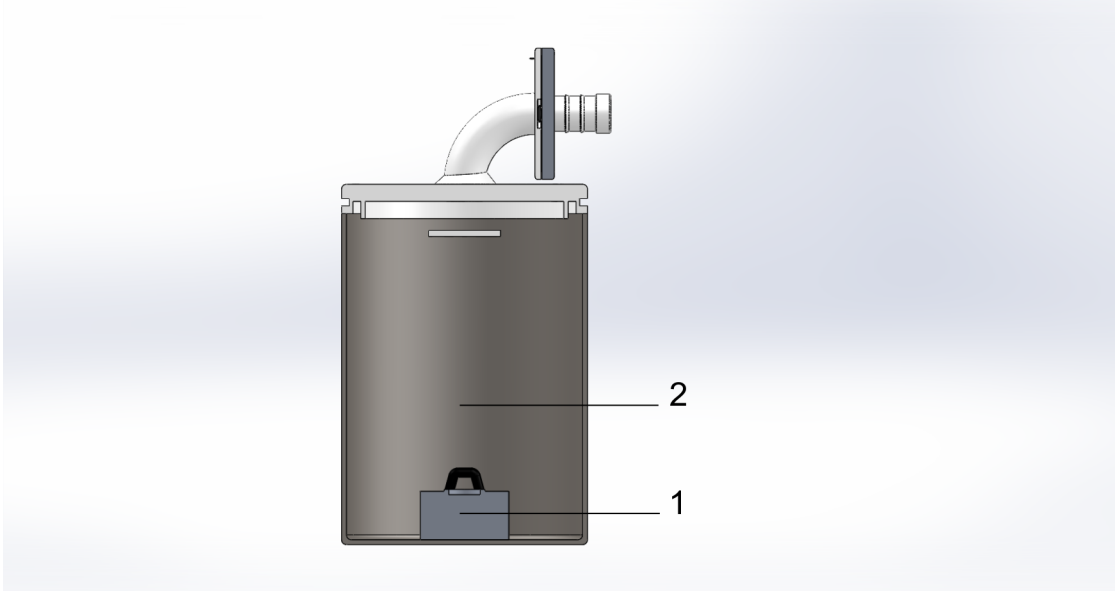


Figure 3.9. Cross section of humidifier. 1. ultrasonic humidifier 2. water reservoir.

3.4.2 Humidifier Characterization

The characterization of the humidification process was done through mass-flow analysis of the water vapour in the system. Utilizing conservation of mass principles allows for the determination of the mass of water vapour in the system over a given amount of time. In addition to mass-flow analysis of the system, the temperature dependent variable of saturation vapour pressure for water vapour in air was performed to calculate relative humidity with known vapour pressures.

Since relative humidity operates on a pressure driven basis of the water vapour partial pressure in the moist air mixture, transient and steady-state parameters were used to generate a first-order predictive model for relative humidity for a known dry-bulb temperature input. The model is shown in Equation 3.4 where P_v is the water vapour partial pressure in the enclosure, P_a is the ambient water vapour pressure of the ambient environment, \dot{m} is the mass flow rate of water vapour from the humidifier, R_n is the pneumatic resistance between the enclosure and the ambient environment, and C_n is the pneumatic capacitance of the enclosure,

if the volume and pressure of the gas mixture remains unchanged, there must be mass flow directed outside of the control volume to have equalized gas pressure [17]. As with all applications of fluid flow, there is a resistance to flow due to drag associated with the fluid coming into contact with the enclosure surfaces. A transient term also exists since the enclosure acts as the sole storage element of water vapour. Due to the combination of the complexity of the system and the scarce amount of information on the transient modeling of relative humidity, both the pneumatic resistance and the pneumatic capacitance had to be empirically determined.

$$\dot{P}_v = \frac{\dot{m}}{C_n} + \frac{1}{R_n C_n} (P_a - P_v) \quad (3.4)$$

To fully characterize the humidification system, measurements of the partial pressures and the mass flow rate of water vapour were performed. Two Honeywell HIH-4021 relative humidity sensors and two LM35 temperature sensors were employed in this exercise to measure the relative humidity and dry bulb temperatures of the air in the enclosure as well as the air of the ambient environment simultaneously. Mass flow rate of water vapour was determined by measuring the mass loss of the humidifier's water reservoir over the duration of an experiment. The measurements from the temperature and relative humidity sensors allows for the calculation of the saturation vapour pressure and the instantaneous water vapour pressure for both points with Equations 2.23 and 2.26 under the valid assumption that the air pressure of the enclosure's interior is equal to the air pressure of the ambient environment. After an experiment was performed to generate data for the water vapour partial pressures of the enclosure and the ambient air, steady-state analysis followed by transient analysis of the observed response led to the determination of the values for pneumatic resistance and capacitance. Pneumatic

resistance is equivalent to the quotient of the water vapour's partial pressure difference between the enclosure and the ambient environment, and the humidifier's water vapour mass flow rate. Pneumatic capacitance was calculated via the knowledge of the time it took for the water vapour partial pressure to reach steady state which is equivalent to five time constants. The quotient of the experimentally derived time constant and the earlier determined pneumatic resistance yielded the experimentally determined pneumatic capacitance [17].

List of References

- [1] "arduino-pwm-frequency-library." [Online]. Available: <https://code.google.com/archive/p/arduino-pwm-frequency-library/downloads>
- [2] Measurement Computing. "Usb-1208fs-plus/ls/1408fs-plus series." [Online]. Available: <https://www.mccdaq.com/usb-data-acquisition/USB-1208FS-LS-1408FS-Series.aspx>
- [3] Texas Instruments. "Lm35 precision centigrade temperature sensors." 2017. [Online]. Available: <http://www.ti.com/lit/ds/symlink/lm35.pdf>
- [4] Adafruit. "Platinum RTD Sensor - PT100 - 3 Wire 1 meter long." [Online]. Available: <https://www.adafruit.com/product/3290>
- [5] Honeywell. "Hih-4010/4020/4021 series." 2007. [Online]. Available: <https://sensing.honeywell.com/honeywell-sensing-hih4010-4020-4021-series-product-sheets-009020-1-en.pdf>
- [6] Vaisala. "HUMICAP humidity and temperature probe HMP110." 2018. [Online]. Available: https://www.vaisala.com/sites/default/files/documents/HMP110-Datasheet-B210852EN_1.pdf
- [7] Phidgets Inc. "Miniature linear motion series L12." 2016. [Online]. Available: https://www.phidgets.com/productfiles/3540/3540_0/Documentation/3540_0.Datasheet.pdf
- [8] Delta Electronics. "PMT panel mount power supply." 2018. [Online]. Available: <http://www.deltapsu.com/products/download/Datasheet/PMT-24V350W1AK>
- [9] Arduino. "Arduino UNO Rev3." [Online]. Available: https://www.arduino.cc/en/uploads/Main/Arduino_Uno_Rev3-schematic.pdf

- [10] Vishay. “Power MOSFET.” [Online]. Available: <https://www.vishay.com/docs/91300/91300.pdf>
- [11] Amazon. “Balitensen 24v 40w ceramic cartridge heater 620 for 3d printer rewrap prusa mendel pack of 5.” [Online]. Available: https://www.amazon.com/BALITENSEN-Ceramic-Cartridge-Heater-Printer/dp/B078SQ4BPR/ref=sr_1_2_sspa?ie=UTF8&qid=1526408204&sr=8-2-spons&keywords=3d+printer+heater+24v&psc=1
- [12] Monoprice. “Maker select 3d printer v2.” [Online]. Available: https://www.monoprice.com/product?p_id=13860
- [13] The Engineering Toolbox. “Thermal conductivity of common metals and gases.” [Online]. Available: https://www.engineeringtoolbox.com/thermal-conductivity-d_429.html
- [14] The Engineering Toolbox. “Specific heats for metals.” [Online]. Available: https://www.engineeringtoolbox.com/specific-heat-metals-d_152.html
- [15] Amazon. “Arctic MX-4 - thermal compound paste, carbon based high performance, heatsink paste, thermal compound cpu for all coolers, thermal interface material - 4 grams.” [Online]. Available: https://smile.amazon.com/ARCTIC-MX-4-Compound-Performance-Interface/dp/B0045JCFLY/ref=sr_1_1_sspa?ie=UTF8&qid=1529001107&sr=8-1-spons&keywords=mx-4+thermal+compound&psc=1
- [16] Amazon. “AGPtEK aluminum mist maker fog maker for water fountain pond rockery fishtank vase birdbath.” [Online]. Available: https://smile.amazon.com/Aluminum-Fountain-Rockery-Fishtank-Birdbath/dp/B00PAK245E/ref=sr_1_23_sspa?ie=UTF8&qid=1528913523&sr=8-23-spons&keywords=ultrasonic+humidifier+head&psc=1
- [17] W. Palm III, *System Dynamics*. McGraw-Hill, 2013, pp. 402–430.

CHAPTER 4

Findings

4.1 System Performance

The following chapter covers the experiments and analysis performed on the preliminary prototype. Experiments were performed for system identification and model validation for the systems relating to thermal control and relative humidity.

4.1.1 Thermal Performance

As stated previously in Section 3.3.1, the accuracy of the heater models allows for the initial formation of the state-space equations. Utilizing the parameters found in the aforementioned section allows for the simulation of the thermal response of the heaters for a given heat rate input and ambient temperature. Testing the heaters was done with three cartridge heaters in each heater block, totaling 116 Watts of heat rate, while the enclosure's exterior was subjected to room temperature and using a fan PWM duty cycle of 25%. The temperature measurement of the heater blocks was done for approximately 13 minutes where the heaters reached steady state. The two temperatures associated with the two heater blocks of the heater assembly are plotted against the model in Figure 4.1. The plots of the two heater blocks follow the model within 1.5% steady state error and transient error within 10% of the model's value. Given the accuracy, this model can be utilized in the overall model of the system with minimal changes associated with convection factors due to installation inside the enclosure.

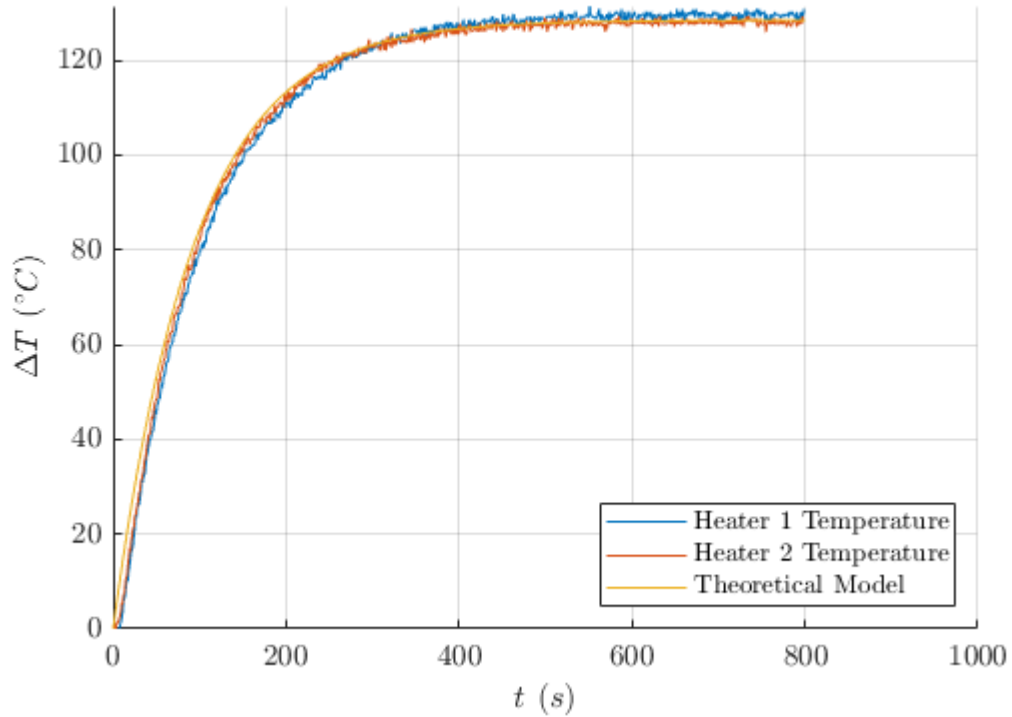


Figure 4.1. Comparison of heater model with actual test data for $v=7.05$ m/s air stream, and 116 Watt step input of heat in each heater block with heater assembly in open air. Values are relative to room temperature at time of test.

After these tests, the heater assembly was installed inside the enclosure to test and identify the model for the enclosure's thermal resistances and capacitances. The capacitance of the air volume inside the enclosure can be theoretically calculated with Equation 2.6 since the volume of the enclosure's interior, dry air specific heat and the density of dry air are known values. The values for the interior air resistance, wall resistance and capacitance, and external air film resistance and capacitance had to be identified via experimentation. By thermally isolating the individual components via inputting the temperature prior to the component and knowing that the heat rate input is the same for every component, thermal resistance and capacitance can be calculated with the knowledge of the temperature difference across the components and the time constant of the response. Most of

the time, this knowledge is enough to calculate the thermal properties, if not then it is a good starting point for tuning the parameters until the response error is satisfactory.

For greater detail, two thermal models for the system were produced for conditions consisting of when the humidifier is not connected to the enclosure and one for when the humidifier is attached and the only the humidifier fan is on. In the tests with the humidifier attached, the humidifier element was not powered resulting in only dry air circulating through the humidifier and returning to the enclosure with its specific humidity unchanged. The reason for this is due to noticeable differences in thermal resistance and capacitance between the two conditions. Plots of the experimental results and the model's simulation for both cases are depicted in Figures 4.2 and 4.3. From the close correspondence between the real and simulated results, this method has produced an accurate steady state and transient model for the prototype. Further analysis of the two models are illustrated in Figures 4.4 and 4.5 which show the state variables in terms of percentage of the steady state value over time. The thermodynamic values used to produce this model is shown in Tables 4.1 and 4.2 and were utilized in Equation 3.2 to form the Matlab functions found in Appendices C.2 and C.3 respectfully.

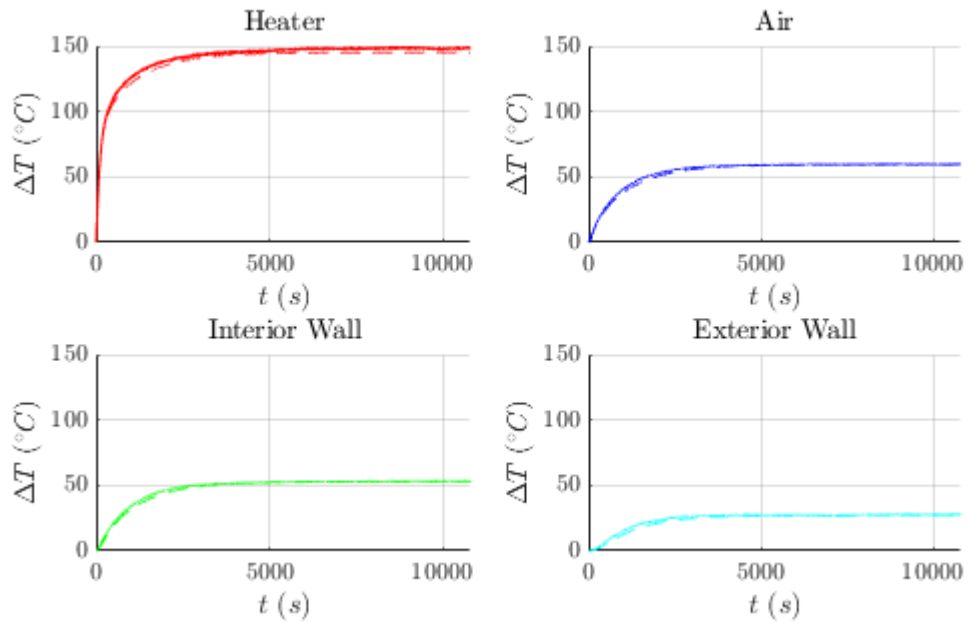


Figure 4.2. Plots for the four state variables associated with the thermal system with a heat rate input of 153 Watts and humidifier not connected. Plots compare the model (dashed line) and the actual results (solid line).

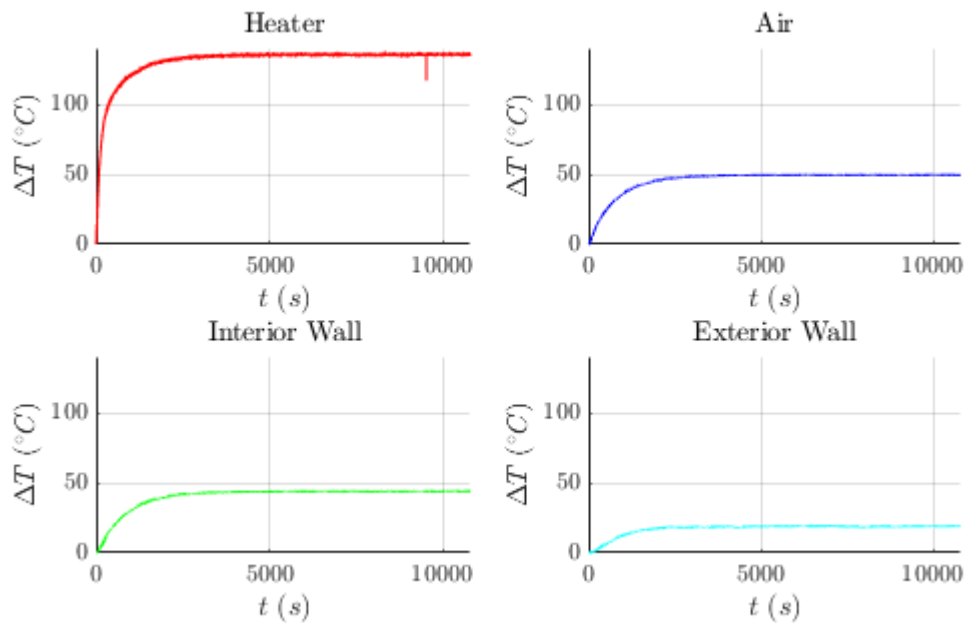


Figure 4.3. Plots for the four state variables associated with the thermal system with a heat rate input of 153 Watts and only humidifier fan on. Plots compare the model (dashed line) and the actual results (solid line).

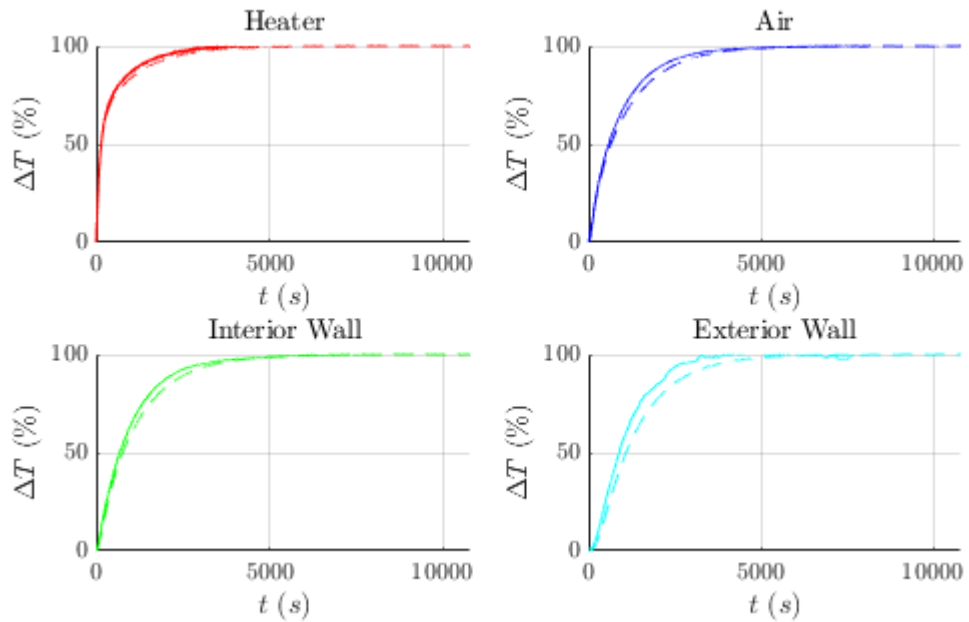


Figure 4.4. Plots of the thermal system state variables with heat rate input of 153 Watts and no humidifier attached in terms of percentage of model's steady state value. Plots compare the model (dashed line) and the actual results (solid line).

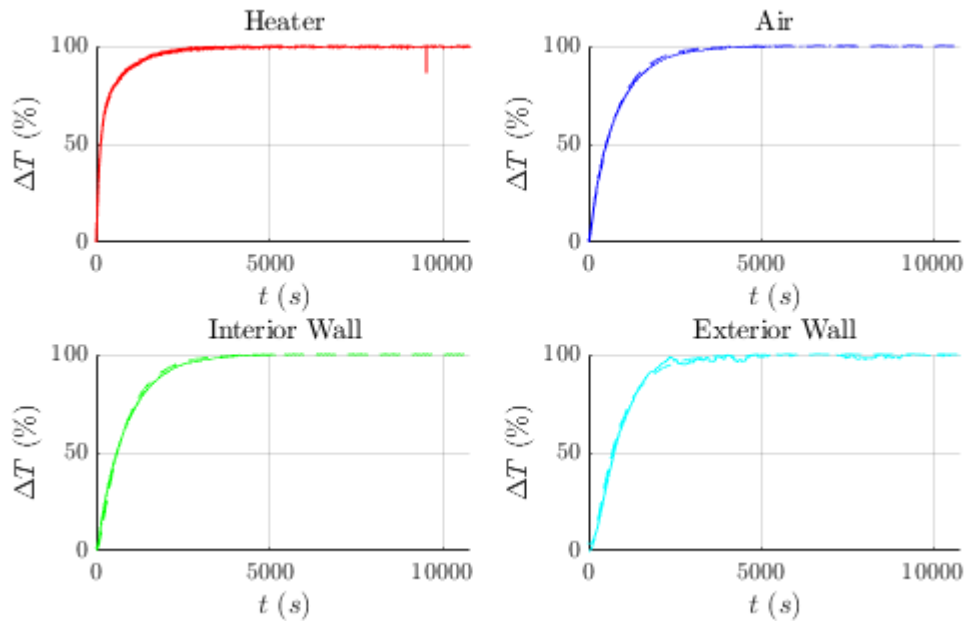


Figure 4.5. Plots for the thermal system with a heat rate input of 153 Watts and only humidifier fan on in terms of percentage of model's final steady state value. Plots compare the model (dashed line) and the actual results (solid line).

i	$R_i \left(\frac{K}{W} \right)$	$C_i \left(\frac{J}{K} \right)$
1	0.560	170
2	0.0432	12.3
3	0.168	1900
4	0.178	3380

Table 4.1. Model values for enclosure without humidifier attached.

i	$R_i \left(\frac{K}{W} \right)$	$C_i \left(\frac{J}{K} \right)$
1	0.560	170
2	0.0379	12.3
3	0.162	2200
4	0.123	1000

Table 4.2. Model values for enclosure with humidifier attached with the humidification element turned off.

For further analysis of the model's validity, altering the thermodynamic properties and changing the heat rate input of the model were performed to study its effect. Testing was performed under the condition that the humidifier was on with zero moisture produced. This will give insight on how the model performs when the enclosure is utilized in differing applications.

The first test consisted of changing the heat rate input to 78.3 Watts by allowing to have only one cartridge heater installed in each heater block. Testing was performed over the same amount of time as the original identification tests. Figure 4.6 depicts the results of the test and the simulation for each state variable. A look into the error of the model is illustrated in Figure 4.7 in terms of percentage of the model's steady state value. The heater and air temperature plots show that the model is still in good agreement although there is increased error when comparing to the previous identification tests. Thermal resistance of the wall increased as shown by the higher temperature difference of the interior of the wall

and the exterior of the wall when comparing Figure 4.3 and 4.6. When looking at Figure 4.7, there is a large discrepancy between the model for the exterior wall and the measured data. Measured values shows that the measured temperature was approximately 66% of the model during steady state operation which suggests a decreased thermal resistance for this state variable. This is the case since thermal resistance is the only parameter that governs steady state conditions. The rationale behind this change in resistance is due to a change in the convective heat transfer coefficient along the walls which is dependent upon the temperature gradient present.

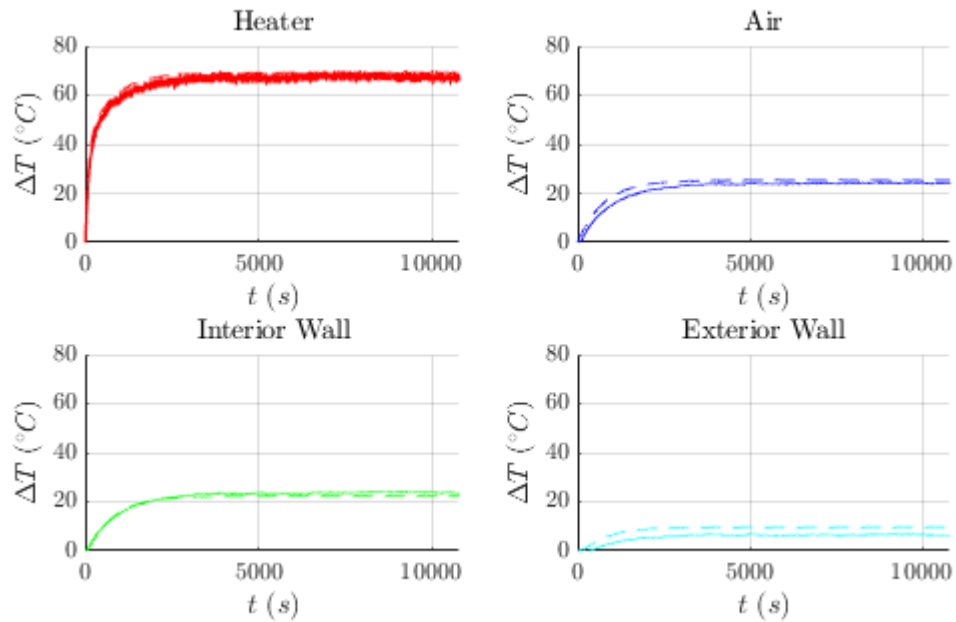


Figure 4.6. Plots for the thermal system with a heat rate input of 78.3 Watts and only the humidifier fan turned on. Plots compare the model (dashed) and the actual results (solid).

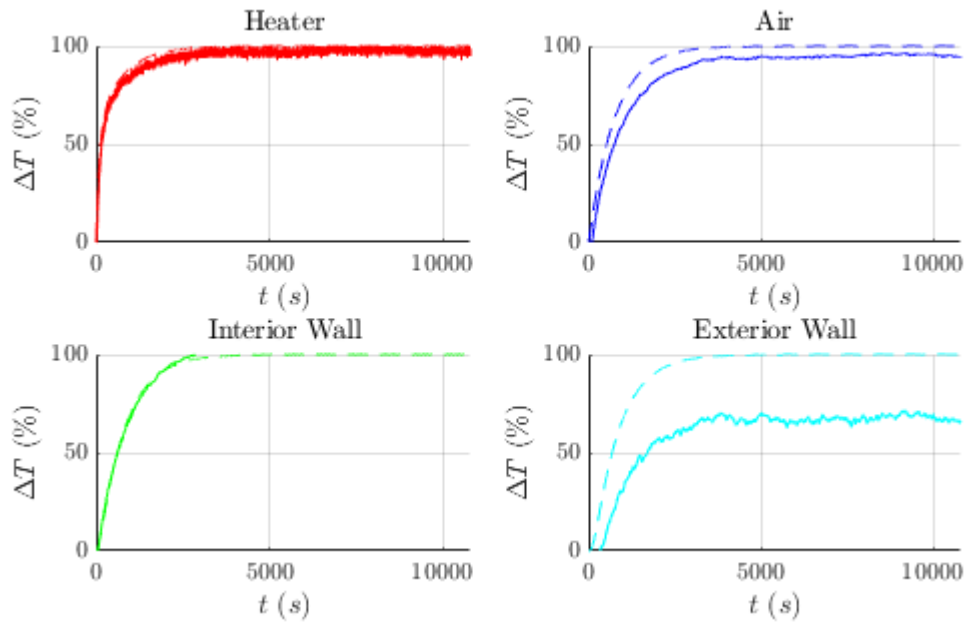


Figure 4.7. Plots for the thermal system with a heat rate input of 78.3 Watts and only humidifier fan turned on in terms of percentage of model’s final steady state value. Plots compare the model (dashed) and the actual results (solid).

Altering parameters consisted of vertically placing a 1 inch diameter, 6 inch long, 304 stainless steel cylinder adjacent to the heater in the enclosure. This in theory will mostly change the effective capacitance of the enclosure with minimal changes to the thermal resistance due to being a part of the interior. Adding the thermal capacitance of the steel rod to the air portion of the fourth order model was used to study the effects of this alteration. Results of this change is shown in Figure 4.8 below along with its experimental results. The plots show the effects of how the air temperature’s dynamics were affected by this addition since that is the prominent state variable for this design. The plot does show the significantly increased capacitance associated with the air or interior temperature of the enclosure and the slight offset of the steady state value. This reflects the prediction well since more energy can be stored inside the interior and the rod will alter the heat flow to maintain a steady state temperature for the entirety of the

system.

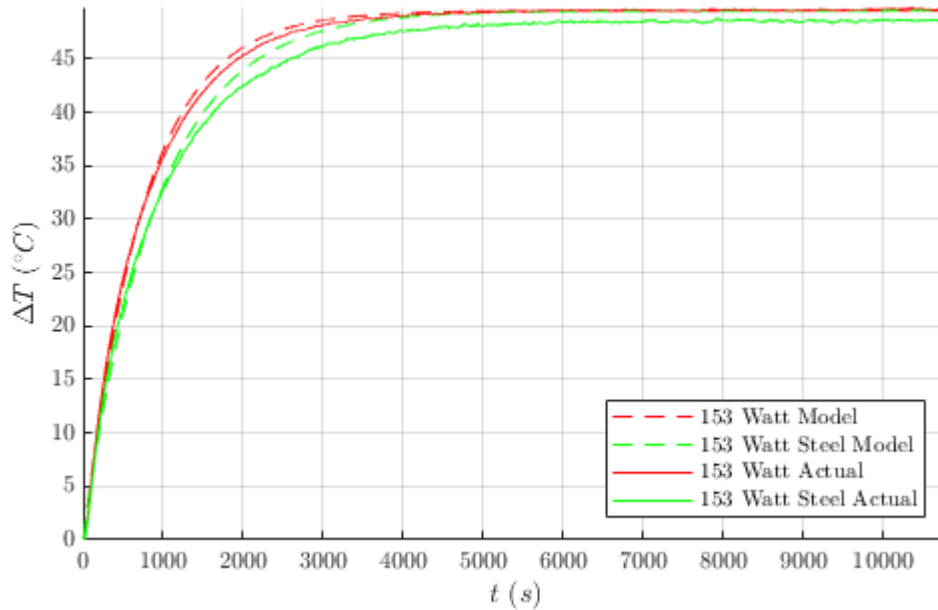


Figure 4.8. Enclosure air temperature change comparison between original model and differing the thermodynamics via adding a stainless steel cylinder. All tests have the humidifier attached and only the humidifier fan turned on.

4.1.2 Humidity Performance

As previously mentioned in Section 3.4.2, the system parameters that define the transient and steady-state response of relative humidity required empirical data. System identification was performed during the steady-state period for the thermal response during 153 Watts of heat rate step input. In other words, the enclosure was heated until the temperature state variables reached steady state condition. For consistency, the control software was programmed to trigger the humidifier once 4000 seconds have elapsed since the beginning of the heat rate step input. The total test time lasted three hours for each experiment where at time 0, a constant heat rate input was applied to the system. Following the procedure for identifying the system stated in Section 3.4.2 yielded the pneumatic values for water vapour capacitance, resistance, and mass flow rate found in Table

4.3 and were utilized in Equation 3.4. The Matlab function associated with this model can be found in Appendix C.4. The mass flow rate of water vapour from the humidifier ended up to be approximately half of what the ultrasonic humidifier’s datasheet claimed and was most likely caused by not being in it’s intended operating environment; an open reservoir.

$\dot{m} \left(\frac{kg}{s}\right)$	$R_n \left(m^{-1}s^{-1}\right)$	$C_n \left(ms^2\right)$
5.32×10^{-5}	1.38×10^8	2.89×10^{-6}

Table 4.3. Model values for the enclosure’s humidity response. Used for predicting response of water vapour partial pressure for a given input.

Experimental trials were performed to evaluate the effectiveness of the relative humidity model. Besides the 153 Watt experiment used to identify the model, two experiments at 116 and 78.3 Watts were performed. Plots comparing the experimental data and the predicted relative humidity for a measured temperature profile are shown in Figures 4.9 to 4.11. By visual inspection, the model is in fairly good agreement considering the wide variability inherent with humidification and a minimum of 3 percent measurement error given by the HIH-4021 relative humidity sensor. Further comparison of the model and experimental values in terms of percent difference is shown in Figure 4.12 where it can be seen that the percent difference is mostly below 10 percent off showing fairly good agreement between the model and measured values. Fluctuations in the model values are due to employing experimental dry bulb temperature values to convert the water vapour partial pressure to relative humidity. This was performed by dividing the partial pressure value by the saturation vapour pressure value for the given temperature.

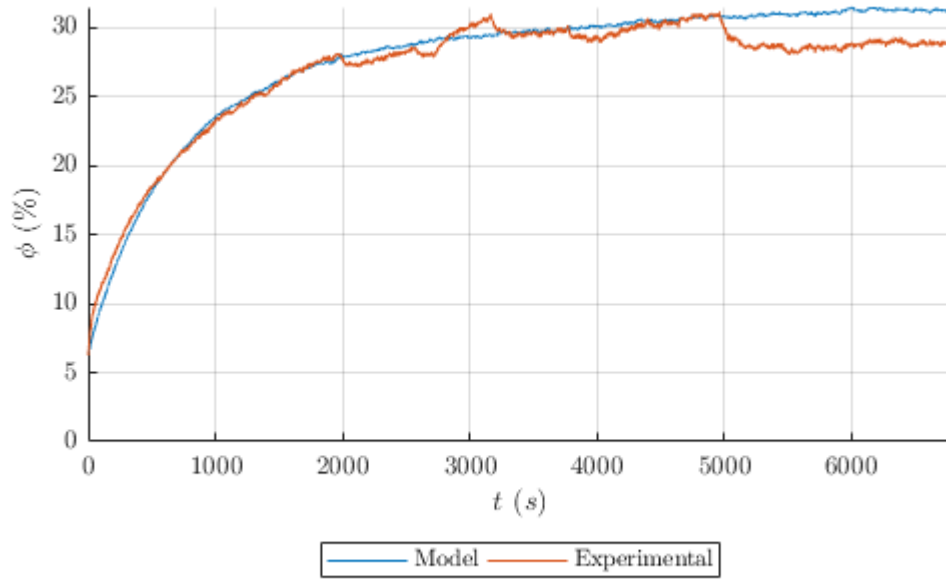


Figure 4.9. Plots for relative humidity performance. Data collection started after 4000 seconds from applying 153 Watt heat rate input.

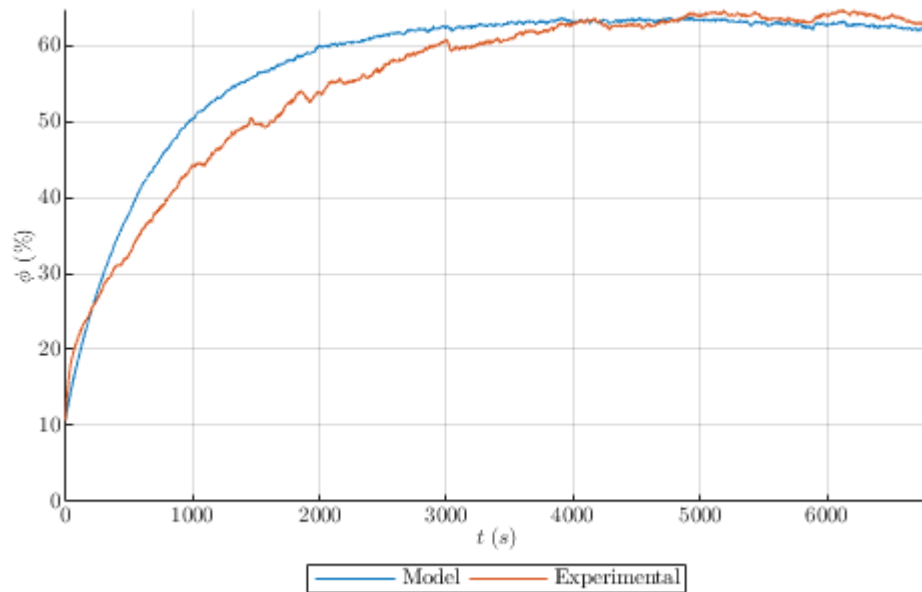


Figure 4.10. Plots for relative humidity performance. Data collection started after 4000 seconds from applying 116 Watt heat rate input.

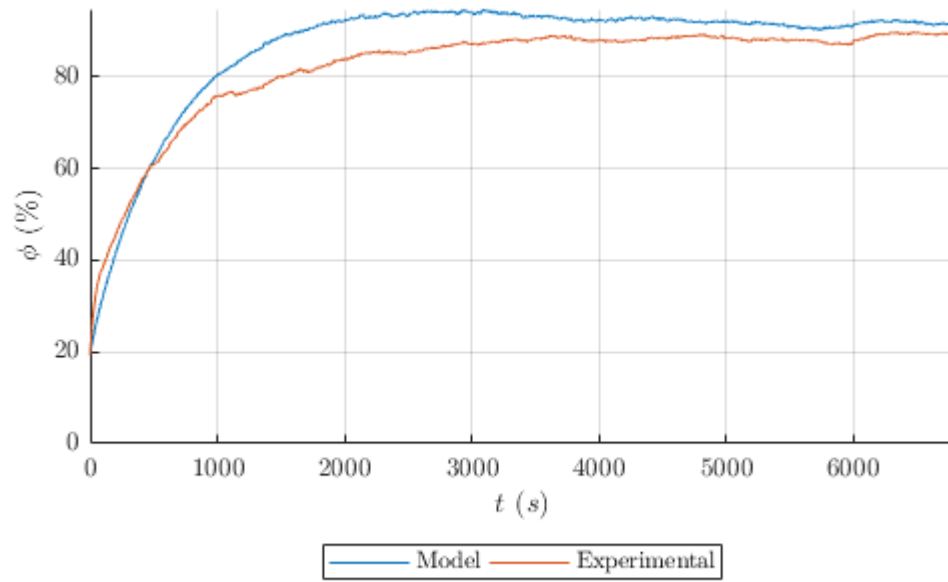


Figure 4.11. Plots for relative humidity performance. Data collection started after 4000 seconds from applying 78.3 Watt heat rate input.

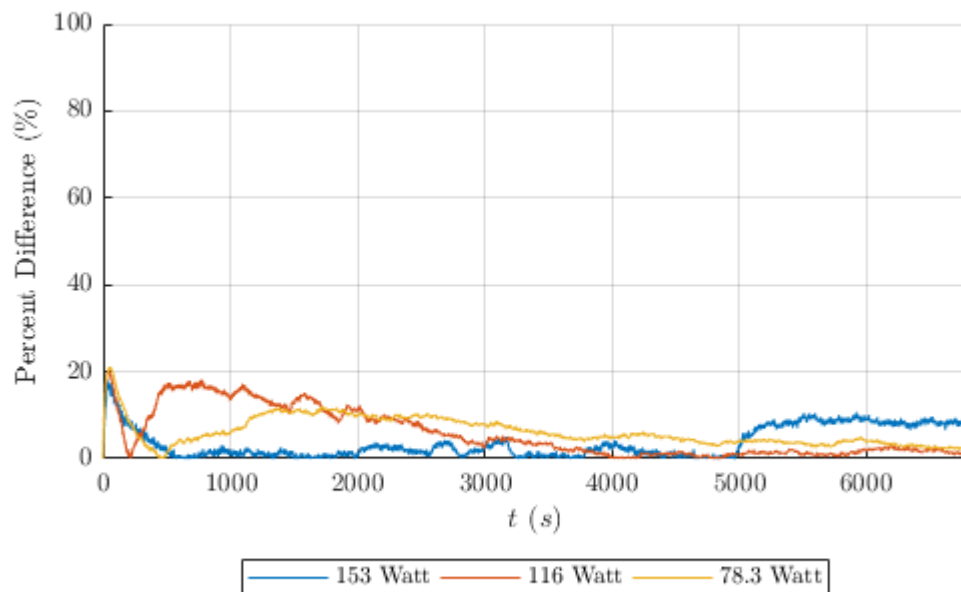


Figure 4.12. Percent difference of relative humidity model to experimental data.

Viewing the dynamics of the humidifying system under the constraint of change over time allows for typical system analysis as was performed. Since relative humidity is both a function of partial pressure or mass of water vapour and dry bulb temperature, observing relative humidity versus dry bulb temperature allows for a different perspective for the underlying mechanics. Figure 4.13 shows the relationship of relative humidity and temperature over the range of a typical temperature profile from the tests. The resulting swan shape in this depiction is due to a change in control inputs. The first portion of the plot where relative humidity is decreasing while dry bulb temperature is increasing resulted from purely heating the air in the enclosure. As expected, the relative humidity decreases with temperature if the water vapour content of the air remains constant due to the saturation pressure increasing with the increase in temperature. The other portion where humidity is increasing and temperature is decreasing is the result of the same heat rate input as well as having the humidifier turned on for the remaining duration of the plot. Temperature decreases with the increase in humidity due to the inclusion of cold water vapour and reaches a steady state condition once the relative humidity reaches steady state. The increase in humidity at the first portion of the plot is caused by an unknown factor inherent in the prototype. Probable causes are the fact that more humid air is less dense than dry air causing the moist air to settle at the top of the enclosure and forced passed the humidity sensor when the heater's fans are turned on, or cooler air being forced passed the sensors which has higher relative humidity due to having a smaller water vapour saturation partial pressure [1].

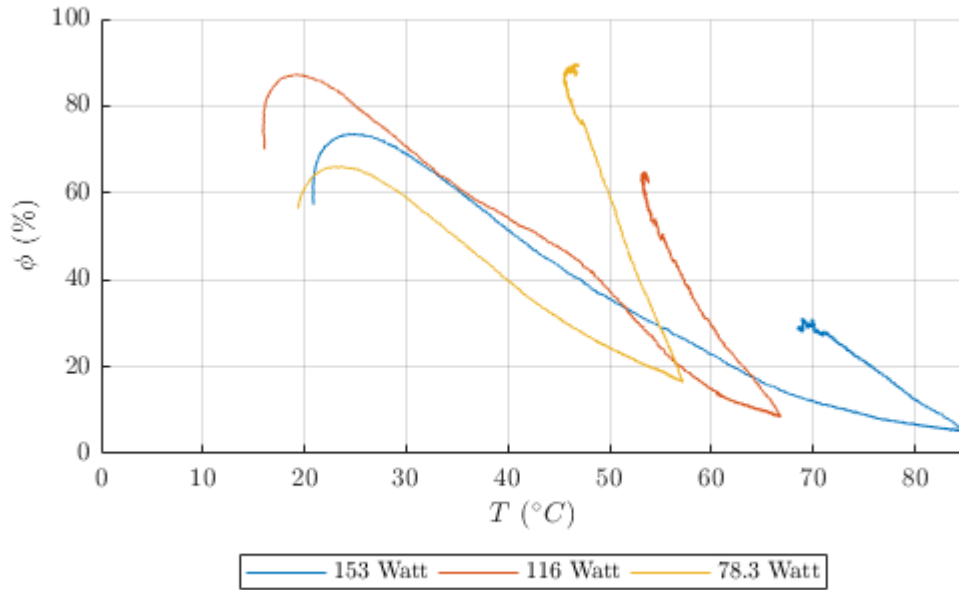


Figure 4.13. Plots of relative humidity versus dry bulb temperature for various heat rate inputs.

The aforementioned relative humidity model was used again to verify the model’s behavior against the swan plots of relative humidity versus temperature in Figure 4.13. The inputs of the model are depicted in Table 4.4 below where \dot{m} refers to the mass flow of water vapour caused by the humidifier, ϕ_a is the relative humidity of the ambient environment, T_a is the temperature of the ambient air, ϕ_o is the initial condition for relative humidity inside the enclosure, T is the resulting temperature profile of the enclosure’s air for a given heat rate input, and t_{delay} is the programmed time for humidification to begin. All of the table entries containing “From data” are an array of values that was measured from real world testing in an effort to isolate any issues of the humidity model to only be caused by humidity factors. This includes barring any temperature modeling that is also dependent on the humidification of the system. The temperature profiles chosen are respective of their defined constant heat rate step inputs over the duration of the model and

test. Initial conditions for relative humidity inside the enclosure were chosen on a basis to reflect that of the data collected from tests. Specifically, the relative humidity initial condition was chosen at the peak of the first leg of the plot in an effort to ignore the anomaly causing the initial jump in relative humidity.

q (W)	\dot{m} ($\frac{kg}{s}$)	ϕ_a (%)	T_a ($^{\circ}C$)	ϕ_o (%)	T ($^{\circ}C$)	t_{delay} (s)
78.3	5.32×10^{-5}	From data	From data	65	From data	4000
116	5.32×10^{-5}	From data	From data	87	From data	4000
153	5.32×10^{-5}	From data	From data	73	From data	4000

Table 4.4. Inputs for relative humidity model resulting in the plots found in Figure 4.14.

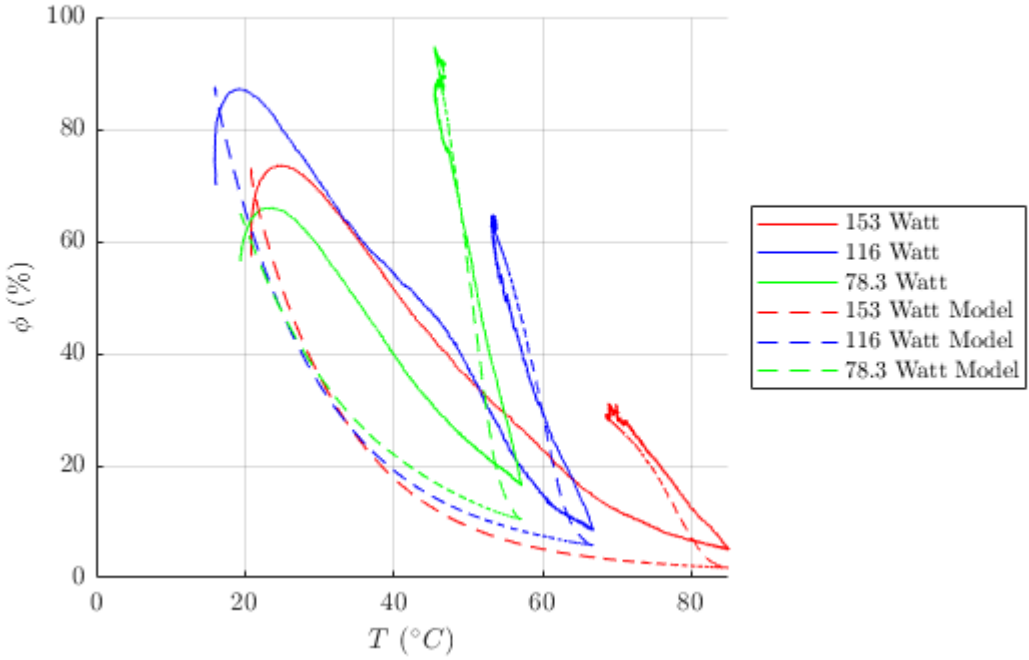


Figure 4.14. Plots of relative humidity versus dry bulb temperature for various heat rate inputs, includes model of relative humidity for comparison.

Comparing the data and the models' results found in Figure 4.14 shows how the model parallels actual data. If the hump at the first leg of the measured results are ignored, then it can be seen that both the model and the real world values have

a similar relationship to one another in terms of being proportionate to one another. The first leg consists of an exponential decay of relative humidity as temperature increases which both the model and the measured values agree with. They also agree with the relative humidity and temperature converging to a similar contour regardless of the initial conditions or heat rate input to the system. Agreement also exists for the second leg of the plot where humidification is occurring resulting in a polynomial pattern for all cases. The model also converges to the same final value after the three hour simulation. Another experiment was in order to sort out the issue of the beginning hump.

In an effort to notice how the model behaves without the hump, the enclosure was humidified to 100% relative humidity and then heated with 153 Watts of heat rate. Specifically, the experiment consisted of a constant mass flow rate of water vapour for the duration of the one hour test and heat applied starting at 300 seconds after test start and remaining constant for the remainder of the experiment. Results of the model and the experiment are detailed in Figure 4.15 and shows good agreement between the model and the experiment.

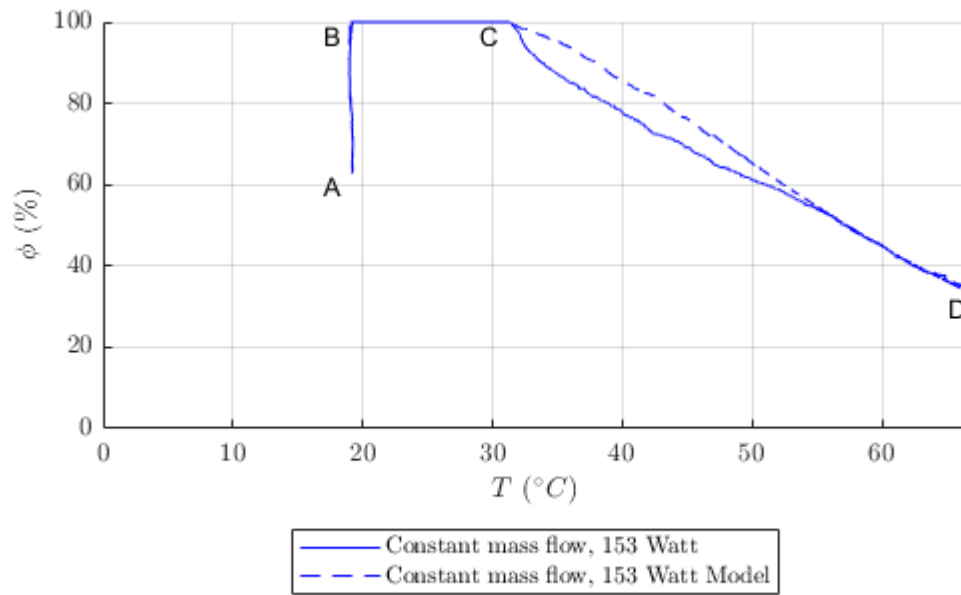


Figure 4.15. Plots of relative humidity versus dry bulb temperature for constant water vapour mass flow rate with 153 Watts of heat rate input for a portion of the test.

It is important to note that while utilizing this model for design, the user must be aware that once the relative humidity reaches 100%, the water vapour partial pressure will no longer increase assuming the dry bulb temperature does not change. Any additional water vapour added to the control volume will result in condensation which this model does not cover. Therefore, the model for Figure 4.15 was performed in a step-wise fashion due to the model being outside of its scope during condensing conditions. The initial step from point A to point B in Figure 4.15 consisted of the model with an initial condition identical to the experiment and was simulated until the model reached 100% humidity. Relative humidity remains constant from point B to C until the experimental value for relative humidity started to decrease. At this point, the model was simulated again with the initial condition set to 100% relative humidity from point C to D.

With the proven effectiveness of the humidity model, one can apply the model for design purposes. The model should not be used by itself for accurate applications since it requires dry bulb temperature information for determining relative humidity. If the only goal is to determine the water vapour partial pressure, then temperature is not important for modeling. If a model is to be used for generating dry bulb temperature information, it is important to include how the humidity dynamics of the system alter the thermodynamics in the system. Assuming the dry bulb temperature model takes water vapour content into consideration, this relative humidity model can be utilized in design or analysis.

List of References

- [1] The Engineering Toolbox. "Density of dry air and water vapor - moist or humid air." [Online]. Available: https://www.engineeringtoolbox.com/density-air-d_680.html

CHAPTER 5

Conclusion

5.1 Conclusions

Design of the thermal and humidification systems for the preliminary Cryo-TEM sample preparation prototype was heavily based from experimental data. Utilizing lumped systems to express the thermal and humidification systems allowed for the fairly accurate state space representation. The benefit of this method is the low capital cost and low amount of time required to obtain an accurate model for design assuming the system being identified for a certain application is in its final geometric state. This would prevent exceeding the limitations presented by this methodology which is especially present in cases where convection is a mechanic. Low capital cost is associated with only having the need for the device being modeled to be present (ie. an oven or in this case, a prototype for Cryo-TEM sample preparation), sensors, and data acquisition hardware and software. Utilizing a CFD based approach to this problem faces extreme upfront costs for designers since such software is astronomically expensive by itself and requires technical skills and knowledge in order to simulate successfully. Therefore, this method allows for engineers or anyone in need of modeling systems the ability to build a state space model for control applications.

For scenarios where a device is being designed for thermal or humidity control prior to construction, it is advised to not use this method due to the shear amount of unknowns. This is especially true for systems where fluids are involved where if it is not known what the fluid's mechanics are, then this method will not yield an accurate result. This can be seen in this study since past the heater design, every component had to modeled experimentally. Experimental design is not an available approach for design prior to construction. For this case, it is best to

model via CFD and obtain the state space system in that manner to reduce the probability of redesign. Worst case scenario is the need to slightly tweak the model to increase accuracy as previously cited literature also claim.

However, there are cases where this lumped capacitance method excels at in thermal systems. Predictive models prior to experimentation are possible for thermal systems where the heat transfer mechanic is through thermal conduction. As shown in Section 4.1.1, the predictive model for the heaters was nearly an exact fit to the real world performance. It is likely that the same method can be applied to hermetically sealed humidification systems only to study the humidity model by itself. Therefore, for systems that are isolated from the ambient environment or where the parameters that are easily calculated from textbook values, the lumped systems method is a good tool.

5.2 Future Work

Future work consists of further efforts in modeling and applying said models. The goal of all of this modeling is not only to study the methods of how it is accomplished, but for application in actual devices. This future work should be done in parallel with one another to achieve the best result.

To further work on the relative humidity model, a new rig needs to be designed and built. It is suspected that leakage paths from the system may negatively affect the predictive model. To rectify this, it is proposed to construct a new enclosure design that is hermetically sealed and allows for the interior to be subjected to positive air pressures. This removes any possibility for mass flow, and any energy flow associated with said flow, into the surrounding environment. A known and isolated control volume would be the best path forward for more analysis into the humidity model where more literature on the subject is needed.

In addition, work needs to be performed on generating a humidity model which

includes the mechanic of condensation. Condensation was noticeable during the previous experiments which may have had a considerable effect on the performance of the humidification system. Not only is this an important factor to know for control design, knowing the condensation mechanic allows for knowledge of how to control this potentially damaging effect of humidification. Water collection in an enclosed space if not drained can cause damage to electrical components or the enclosure itself if improper materials are used.

A complete model that forms a state space system to encompass both the thermal and relative humidity mechanics of the system is needed for the development of control schemes. Humidification causes the thermodynamic parameters of the system to change depending on the quantity of water vapour present in the enclosure. Therefore, a model that is responsive to these changes is required to be developed to gain a practical understanding of how to control the thermodynamics and the mixture of the air in the enclosure.

APPENDIX

Programs

A.1 Arduino Code

```
1 #include <PWM.h>
2 int32_t frequency1=25000; //(freq)
3 int32_t frequency2=60; //(freq)
4 int tach1=8;
5 int tach2=12;
6 int fanpwm1=9; // pin 15 on MCU
7 int fanpwm2=10; // pin 16 on MCU
8 int heat=0; // pin 23 on MCU
9 int humid=1; // pin 24 on MCU
10 double FanP1;
11 double FanP2;
12 double FanSpeed1;
13 double FanSpeed2;
14 double HzToRPM=11000/350;
15 void setup()
16 {
17 //initialize all timers except for 0, to save time ...
    keeping functions
18 InitTimersSafe();
19 // Serial.begin(9600);
20
```

```

21 //sets the frequency for the specified pin
22 bool success1 = SetPinFrequencySafe(fanpwm1, ...
    frequency1);
23 bool success2 = SetPinFrequencySafe(fanpwm2, ...
    frequency2);
24
25 //if the pin frequency was set successfully, turn ...
    pin fanpwm1 and fanpwm2 on
26 if(success1) {
27     pinMode(tach1, INPUT);
28     pinMode(fanpwm1, OUTPUT);
29     digitalWrite(fanpwm1, HIGH);
30 }
31 if(success2){
32     pinMode(tach2, INPUT);
33     pinMode(fanpwm2, OUTPUT);
34     digitalWrite(fanpwm2, HIGH);
35 }
36 }
37 void loop()
38 {
39     //Reads analog signal from PC
40     float a1=analogRead(heat);
41     float a2=analogRead(humid);
42     float b1=((1023-a1)/1023)*255;
43     float b2=((1023-a2)/1023)*255;

```

```

44
45 //Sends PWM signal to fans
46 pwmWrite(fanpwm1, b1); // converts heater's pwm ...
    pin to 5V output
47 pwmWrite(fanpwm2, b2); // converts humidifier's ...
    pwm pin to 5V output
48 //Reads half period of tach signal in microseconds
49 FanP1 = pulseIn(tach1, LOW, 100000);
50 FanP2 = pulseIn(tach2, LOW, 100000);
51 // Serial.print(b1);
52 // Serial.print("\t");
53 // Serial.print(b2);
54 // Serial.println();
55 // Translates to frequency
56 if (FanP1==0)
57 {
58     FanSpeed1=0;
59 }
60 else
61 {
62     FanSpeed1=HzToRPM*pow(10, 6) / (2*FanP1);
63 }
64 if (FanP2==0)
65 {
66     FanSpeed2=0;
67 }

```

```
68  else
69  {
70      FanSpeed2=HzToRPM*pow(10,6)/(2*FanP1);}}
```

A.2 Visual Basic Code

```

...ironment Monitoring Program\WindowsApplication13\Form1.vb 1
1 Imports System.IO
2 Public Class Form1
3     Dim Simulation As Boolean = False
4     Dim deltat As Single = 0.5
5     Dim tmr As PerformanceTimer
6     Dim TempLM351 As Short = 1 'Channel that reads LM35 #1 ↗
7     Dim TempLM352 As Short = 0 (ambient air temperature) 'Channel that reads LM35 #2 ↗
8     Dim HumidSen As Short = 7 (enclosure air temperature) 'Channel that reads Humidity
9     Dim HumidSen2 As Short = 6 Humidity 'Channel that reads Ambient ↗
10    Dim TempLM353 As Short = 1 'Channel that reads outside side ↗
11    Dim TempLM354 As Short = 7 wall temperature
12    Dim RTD1 As Short = 3 'Channel that reads temperature
13    Dim RTD2 As Short = 4 'Channel that reads RTD1 sensor
14    Dim Heater As Short = 0 'Channel that reads RTD2 sensor
15    Dim Humidifier As Short = 1 heaters 'Channel that controls both ↗
16    Dim Tupdate As Single = 1.0 'Channel that controls humidifier
17    Dim StartTime As Double 'Control Intererval in seconds
18    Dim StartTimeText As Double 'Specifies start time of control
19    Dim StartTimeHumidity As Double 'Specifies start time of control, ↗
20    Dim EnclTemp As Single used for accurarate time recording
21    Dim EnclHumid As Single 'Time at which closed loop ↗
22    Dim AmHumid As Single humidity control started
23    Dim AmbientTemp As Single 'Enclosure temp in C
24    Dim SideTemp As Single 'Relative Humidity in %
25    Dim RTD1Temp As Single 'Ambient Relative Humidity in %
26    Dim RTD2Temp As Single 'Ambient Air Temperature in C
27    Dim PortValue As Short = 0 'Value of sensor
28    Dim Volt2Temp As Single = 10 'RTD1 temp in C
29    Dim Volt2RTD As Single = 1 'RTD2 temp in C
30    Dim DesEnclTempLast As Single = 20 'Variable that keeps track of the ↗
31    Dim RunTime As Single output digital port
32    Dim data(0, 9) As Single 'Conversion factor from voltage ↗
33    Dim pwmh As Integer to temp in C for LM35
34    Dim pwmhum As Integer 'Conversion factor from voltage ↗
35    Dim heaterstatus As Integer = 0 to RTD temp in C
36    Dim humidifierstatus As Integer = 0 'Last desired enclosure air ↗
37    Dim count As Integer temperatrure
38    Dim Vs As Single = 5.018 'Runs environment control for a ↗
39    Dim R As Single = 1000 'specified time in seconds
    Dim data(0, 9) As Single 'Array for control data
    Dim pwmh As Integer 'PWM value of heater fans
    Dim pwmhum As Integer 'PWM value of humidifier fan
    Dim heaterstatus As Integer = 0 'Status of heater
    Dim humidifierstatus As Integer = 0 'Status of humidifer
    Dim count As Integer 'Counter
    Dim Vs As Single = 5.018 'RTD wheatstone bridge supply ↗
    Dim R As Single = 1000 'RTD wheatstone bridge fixed ↗

```

```

    resistor values
40 Dim Rl As Single = 0           'RTD lead wire resistance
41 Dim Rt As Single = 0.385      'RTD thermal coefficient
42 Dim Rto As Single = 50        'RTD resistance at 0 celsius
43 Dim Vo1 As Single             'RTD output voltage 1
44 Dim Vo2 As Single             'RTD output voltage 2
45 Dim C1 As Single = 259.74     'RTD 1 offset
46 Dim C2 As Single = 0          'RTD 2 offset
47 Dim a As Integer = 0          'Control variable
48 Dim HumidStart As Integer     'Controls humid control trigger
    time
49 Dim HeaterStart As Integer    'Controls heater control trigger
    time
50 Dim TimeElapsed As Single     'Time elapsed
51 Dim HeaterEnabled As Boolean = True
52 Private Sub cmdExit_Click(sender As Object, e As EventArgs) Handles
    cmdExit.Click
53     HumidifierControl(False)
54     HeaterControl(False)
55 End
56 End Sub
57 Public Sub InitializeTimer()
58     'A routine to initialize the QueryPerformanceTimer
59     tmr = New PerformanceTimer
60     tmr.StartTimer()
61 End Sub
62 Public Function GetTimeNow() As Double
63     tmr.ReadCurrentTimer() ' Read the timer value
64     GetTimeNow = tmr.TimeElapsed(PerformanceTimer.PerformanceValue.pvSecond)
65 End Function
66
67 Private Sub cmdRun_Click(sender As Object, e As EventArgs) Handles
    cmdRun.Click
68     a = 1
69     RunTime = RunTimeTxt.Text
70     ReDim data(RunTime / Tupdate, 10) ' Column 0 - time, Column 1 - Encl.
        temp, Column 2 - Humidity, Column 3 - Heater temp1, Column 4 - Heater
        temp2, Column 5 - Ambient Air Temp, Column 6 - Heater fan PWM, Column 7
        - Humidifier fan PWM, Column 8 - Heater status, Column 9 - Humidifier
        status, Column 10 - Outside side wall temperature
71     'CheckBoxTempControl.Enabled = False
72     'CheckBoxHumidityControl.Enabled = False
73     GroupParameters.Enabled = False
74     cmdWriteDatatoFile.Enabled = True
75     cmdRun.Enabled = False
76     HumidStart = HumidStartText.Text
77     HeaterStart = HeaterStartText.Text
78     If Simulation = False Then
79         Call Initialize_IO()
80         Send_IO(PortValue)
81     End If
82     If Simulation = True Then

```

```

83         For i As Integer = 0 To RunTime / Tupdate
84             data(i, 0) = i * Tupdate
85             data(i, 1) = 30 + 0.02 * i
86             data(i, 2) = 40 + 0.03 * i
87             data(i, 3) = 60 + 0.03 * i
88             data(i, 4) = 60 + 0.03 * i
89             data(i, 5) = 20
90             data(i, 6) = 25
91             data(i, 7) = 25
92             data(i, 8) = 0
93             data(i, 9) = 1
94         Next
95     End If
96     count = 0
97     StartTime = GetTimeNow()
98     StartTimeText = GetTimeNow()
99     Call SetupCharts()
100    While count <= RunTime / Tupdate And a = 1
101        System.Windows.Forms.Application.DoEvents() ' Allows background processing
102        Call ControlTask()
103    End While
104    Call cmdPowerOff.PerformClick()
105    TextTimeElapsed.Text = "OVER"
106 End Sub
107
108 Private Sub ControlTask()
109     TextTimeElapsed.Text = Format((GetTimeNow() - StartTimeText), "###0.0")
110     TimeElapsed = TextTimeElapsed.Text
111     If ((GetTimeNow() - StartTime) >= Tupdate) Then
112         If Simulation = True Then
113             EnclTemp = data(count, 1)
114             EnclHumid = data(count, 2)
115             RTD1Temp = data(count, 3)
116             RTD2Temp = data(count, 4)
117             AmbientTemp = data(count, 5)
118             pwmh = data(count, 6)
119             pwmhum = data(count, 7)
120             heaterstatus = data(count, 8)
121             humidifierstatus = data(count, 9)
122         Else
123             EnclTemp = Read_AD(TempLM352) * Volt2Temp - 2.4
124             AmbientTemp = Read_AD(TempLM351) * Volt2Temp - 1.9
125             EnclHumid = (161.2903 * Read_AD(HumidSen) / 5 - 25.8095) /
126                 (1.0546 - 0.00216 * EnclTemp)
127             AmHumid = (161.2903 * Read_AD(HumidSen2) / 5 - 25.8095) / (1.0546
128                 - 0.00216 * AmbientTemp)
129             'Read_AD(TempLM354) * Volt2Temp
130             SideTemp = Read_AD(TempLM353) * Volt2Temp
131             Vo1 = (Read_AD(RTD1))
132             RTD1Temp = ((R * ((Vs - 2 * Vo1) / (Vs + 2 * Vo1)) - R1 * (4 *

```

```

132         Vo1 / (Vs + 2 * Vo1))) / Rt - C1) - 17 + 11.9
133         Vo2 = (Read_AD(RTD2))
133         RTD2Temp = ((R * ((Vs - 2 * Vo2) / (Vs + 2 * Vo2)) - R1 * (4 *
134         Vo2 / (Vs + 2 * Vo2))) / Rt - C2) - 229 - 48.1 - 3.2
134         data(count, 0) = count * Tupdate
135         data(count, 1) = EnclTemp
136         data(count, 2) = EnclHumid
137         data(count, 3) = RTD1Temp
138         data(count, 4) = RTD2Temp
139         data(count, 5) = AmbientTemp
140         data(count, 6) = pwmh
141         data(count, 7) = pwmhum
142         data(count, 8) = heaterstatus
143         data(count, 9) = humidifierstatus
144         data(count, 10) = AmHumid
145     End If
146     count = count + 1
147
148     TextBoxActualHumidity.Text = Format(EnclHumid, "##0.0")
149     TextBoxActualTemp.Text = Format(EnclTemp, "##0.0")
150     TextHeater1temp.Text = Format(RTD1Temp, "##0.0")
151     TextHeater2temp.Text = Format(RTD2Temp, "##0.0")
152     AmbientText.Text = Format(AmbientTemp, "##0.0")
153     TempBox1.Text = Format(AmHumid, "##0.0")
154
155
156
157     If (count > RunTime / Tupdate) Then
158         Chart1.Series(0).Points.RemoveAt(1)
159         Chart2.Series(0).Points.RemoveAt(1)
160     End If
161     Chart1.Series(0).Points.AddY(EnclTemp)
162     Chart2.Series(0).Points.AddY(EnclHumid)
163
164
165     If ((CheckBoxTempControl.Checked = True) And (HeaterEnabled = True))
166     Then
167         If EnclTemp >= (NumericUpDownDesTemp.Value + deltat) Then
168             HeaterControl(False)
169             heaterstatus = 0
170         ElseIf EnclTemp <= (NumericUpDownDesTemp.Value - deltat) And
171         HeaterStart <= TimeElapsed Then
172             HeaterControl(True)
173             heaterstatus = 1
174         Else
175             HeaterControl(False)
176             heaterstatus = 0
177         End If
178     Else
179         HeaterControl(False)
180         heaterstatus = 0
181     End If

```

```

180     If TimeElapsed = HumidStart Then
181         My.Computer.Audio.Play("C:\Users\Aaron\OneDrive\Documents\Masters Thesis Work\Visual Basic Programs\Sound\Navy Sub Alarm.wav")
182     End If
183
184     If CheckBoxHumidityControl.Checked = True Then
185         If EnclHumid >= (NumericUpDownDesHum.Value + deltat) Then
186             HumidifierControl(False)
187             humidifierstatus = 0
188         ElseIf EnclHumid <= (NumericUpDownDesHum.Value - deltat) And HumidStart <= TimeElapsed Then
189             HumidifierControl(True)
190             humidifierstatus = 1
191         Else
192             HumidifierControl(False)
193             humidifierstatus = 0
194         End If
195     Else
196         HumidifierControl(False)
197         humidifierstatus = 0
198     End If
199     StartTime = GetTimeNow()
200 End If
201 End Sub
202
203
204 Private Sub Form1_Load(sender As Object, e As EventArgs) Handles MyBase.Load
205     InitializeTimer()
206     GroupHeater.Enabled = True
207     GroupHumidifier.Enabled = True
208     cmdWriteDatatoFile.Visible = True
209     RunTimeTxt.Text = 3600
210     heatbar.Value = 25
211     humidbar.Value = 25
212     heatspeedtxt.Text = heatbar.Value
213     pwmh = heatbar.Value
214     pwmhum = humidbar.Value
215     heatbar.Maximum = 100
216     heatbar.Minimum = 0
217     heatbar.TickFrequency = 5
218     heatbar.SmallChange = 5
219     heatbar.LargeChange = 5
220     humidspeedtext.Text = humidbar.Value
221     humidbar.Maximum = 100
222     humidbar.Minimum = 0
223     humidbar.TickFrequency = 5
224     humidbar.SmallChange = 5
225     humidbar.LargeChange = 5
226     HumidStartText.Text = 0
227     HeaterStartText.Text = 0
228 End Sub
229

```

```
230 Private Sub SetupCharts()  
231 Chart1.Series(0).Points.Clear()  
232 Chart1.ChartAreas(0).AxisX.Minimum = 0  
233 Chart1.ChartAreas(0).AxisX.Maximum = RunTime  
234 Chart1.ChartAreas(0).AxisY.Minimum = 0  
235 Chart1.ChartAreas(0).AxisY.Maximum = 100  
236 Chart1.Series(0).ChartType = SeriesChartType.Line  
  
237  
238 Chart2.Series(0).Points.Clear()  
239 Chart2.ChartAreas(0).AxisX.Minimum = 0  
240 Chart2.ChartAreas(0).AxisX.Maximum = RunTime  
241 Chart2.ChartAreas(0).AxisY.Minimum = 0  
242 Chart2.ChartAreas(0).AxisY.Maximum = 100  
243 Chart2.Series(0).ChartType = SeriesChartType.Line  
  
244 End Sub  
245  
246 Private Sub HeaterControl(ByVal setting As Boolean)  
247 If setting = True And cmdRun.Enabled = False Then  
248 If Simulation = False Then  
249 PortValue = PortValue Or (2 ^ Heater)  
250 Send_IO(PortValue)  
251 Write_DA(0, (pwmh / 100) * 10)  
252 End If  
253 LabelHeater.Visible = True  
254 Else  
255 If Simulation = False Then  
256 PortValue = PortValue And (255 - 2 ^ Heater)  
257 Send_IO(PortValue)  
258 Write_DA(0, 0)  
259 End If  
260 LabelHeater.Visible = False  
261 End If  
262 End Sub  
263  
264 Private Sub HumidifierControl(ByVal setting As Boolean)  
265 If setting = True And cmdRun.Enabled = False Then  
266 If Simulation = False Then  
267 PortValue = PortValue Or (2 ^ Humidifier)  
268 Send_IO(PortValue)  
269 Write_DA(1, (pwmhum / 100) * 10)  
270 End If  
271 LabelHumidifier.Visible = True  
272 Else  
273 If Simulation = False Then  
274 PortValue = PortValue And (255 - 2 ^ Humidifier)  
275 Send_IO(PortValue)  
276 Write_DA(1, 0)  
277 End If  
278 LabelHumidifier.Visible = False  
279 End If
```

```

280     End Sub
281     Private Sub cmdPowerOff_Click(sender As Object, e As EventArgs) Handles cmdPowerOff.Click
282         a = 0
283         HeaterControl(False)
284         HumidifierControl(False)
285         CheckBoxTempControl.Enabled = True
286         CheckBoxHumidityControl.Enabled = True
287         cmdRun.Enabled = True
288         GroupParameters.Enabled = True
289         TextTimeElapsed.Text = " "
290     End Sub
291
292     Public Sub WriteDatatoFile()
293         Dim FName$
294         Dim w As StreamWriter
295         Dim StartingIndex As Integer = 0
296         Dim saveFileDialog1 As New SaveFileDialog
297         saveFileDialog1.FilterIndex = 2
298
299         saveFileDialog1.Filter = "txt files (*.txt)|*.txt"
300         saveFileDialog1.RestoreDirectory = True
301
302         If saveFileDialog1.ShowDialog() = DialogResult.OK Then
303             FName$ = saveFileDialog1.FileName
304
305             Dim fs As New FileStream(FName$, FileMode.OpenOrCreate)
306             w = New StreamWriter(fs)
307             Dim i As Long
308
309             For i = StartingIndex To count - 1
310                 w.WriteLine(Str$(data(i, 0)) + " " + Str$(data(i, 1)) + " " +
311                     Str$(data(i, 2)) + " " + Str$(data(i, 3)) + " " + Str
312                     $(data(i, 4)) + " " + Str$(data(i, 5)) + " " + Str$(data
313                     (i, 6)) + " " + Str$(data(i, 7)) + " " + Str$(data(i, 8))
314                     + " " + Str$(data(i, 9)) + " " + Str$(data(i, 10)))
315             Next i
316             w.Close()
317             fs.Close()
318         End If
319     End Sub
320
321     Private Sub cmdWriteDatatoFile_Click(sender As Object, e As EventArgs) Handles cmdWriteDatatoFile.Click
322         Call WriteDatatoFile()
323     End Sub
324
325     Private Sub NumericUpDownDesTemp_ValueChanged(sender As Object, e As EventArgs) Handles NumericUpDownDesTemp.ValueChanged
326         If NumericUpDownDesTemp.Value >= DesEnc1TempLast Then
327             If NumericUpDownDesTemp.Value >= 60 Then

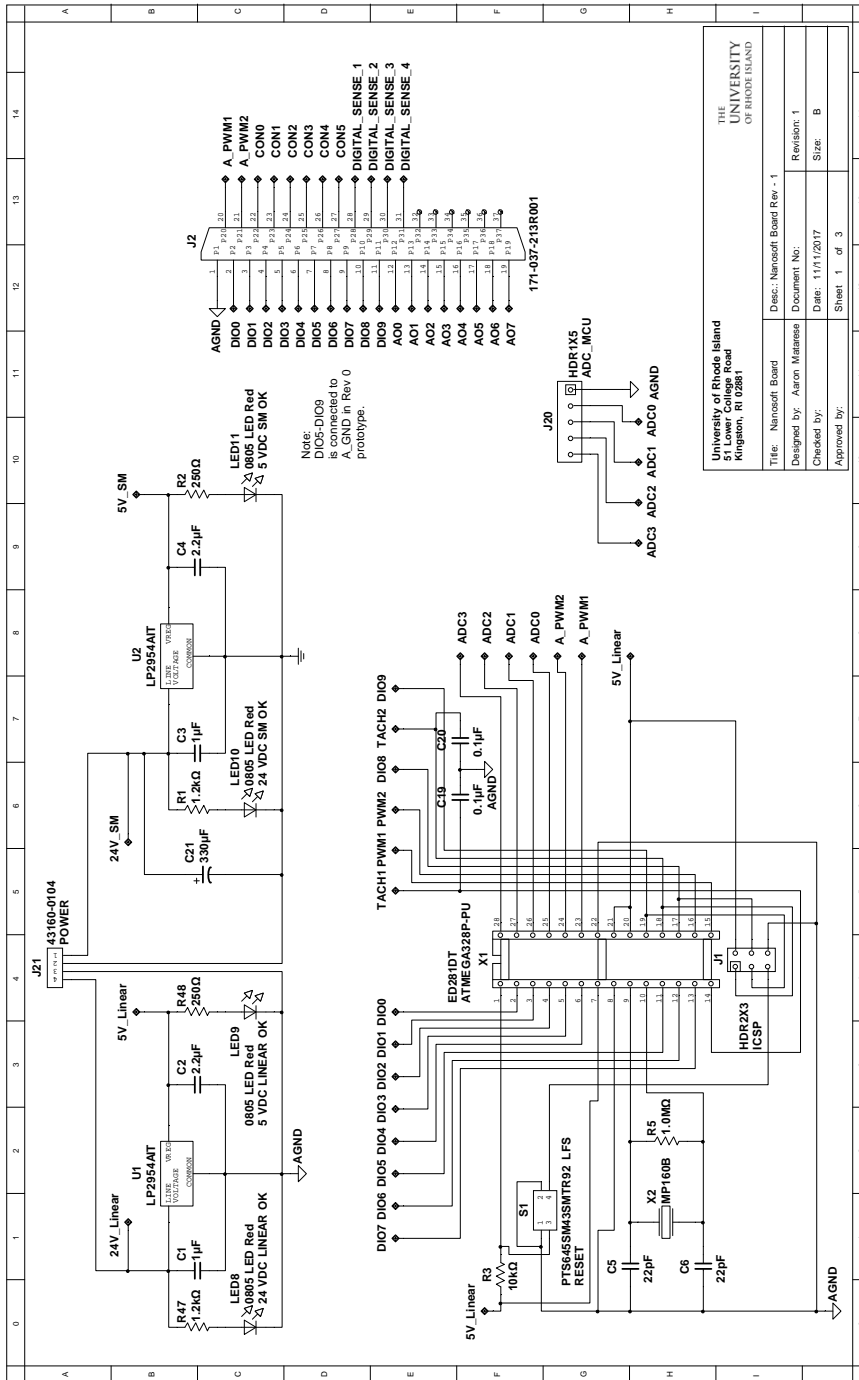
```

```
325         NumericUpDownDesHum.Maximum = 1000
326         ElseIf NumericUpDownDesTemp.Value >= 50 Then
327             NumericUpDownDesHum.Maximum = 1000
328         ElseIf NumericUpDownDesTemp.Value >= 40 Then
329             NumericUpDownDesHum.Maximum = 1000
330         ElseIf NumericUpDownDesTemp.Value >= 30 Then
331             NumericUpDownDesHum.Maximum = 1000
332         ElseIf NumericUpDownDesTemp.Value >= 20 Then
333             NumericUpDownDesHum.Maximum = 1000
334         End If
335     Else
336         If NumericUpDownDesTemp.Value < 30 Then
337             NumericUpDownDesHum.Maximum = 1000
338         ElseIf NumericUpDownDesTemp.Value < 40 Then
339             NumericUpDownDesHum.Maximum = 1000
340         ElseIf NumericUpDownDesTemp.Value < 50 Then
341             NumericUpDownDesHum.Maximum = 1000
342         ElseIf NumericUpDownDesTemp.Value < 60 Then
343             NumericUpDownDesHum.Maximum = 1000
344         End If
345     End If
346     DesEnclTempLast = NumericUpDownDesTemp.Value
347 End Sub
348
349 Private Sub speedbar_Scroll(sender As Object, e As EventArgs) Handles heatbar.Scroll
350     heatspeedtxt.Text = heatbar.Value
351     pwmh = heatbar.Value
352 End Sub
353
354 Private Sub humidbar_Scroll(sender As Object, e As EventArgs) Handles humidbar.Scroll
355     humidspeedtext.Text = humidbar.Value
356     pwmhum = humidbar.Value
357 End Sub
358
359 Private Sub heatspeedtxt_TextChanged(sender As Object, e As EventArgs) Handles heatspeedtxt.TextChanged
360     heatbar.Value = heatspeedtxt.Text
361     pwmh = heatbar.Value
362 End Sub
363
364 Private Sub humidspeedtext_TextChanged(sender As Object, e As EventArgs) Handles humidspeedtext.TextChanged
365     humidbar.Value = humidspeedtext.Text
366     pwmhum = humidbar.Value
367 End Sub
368 End Class
369
```

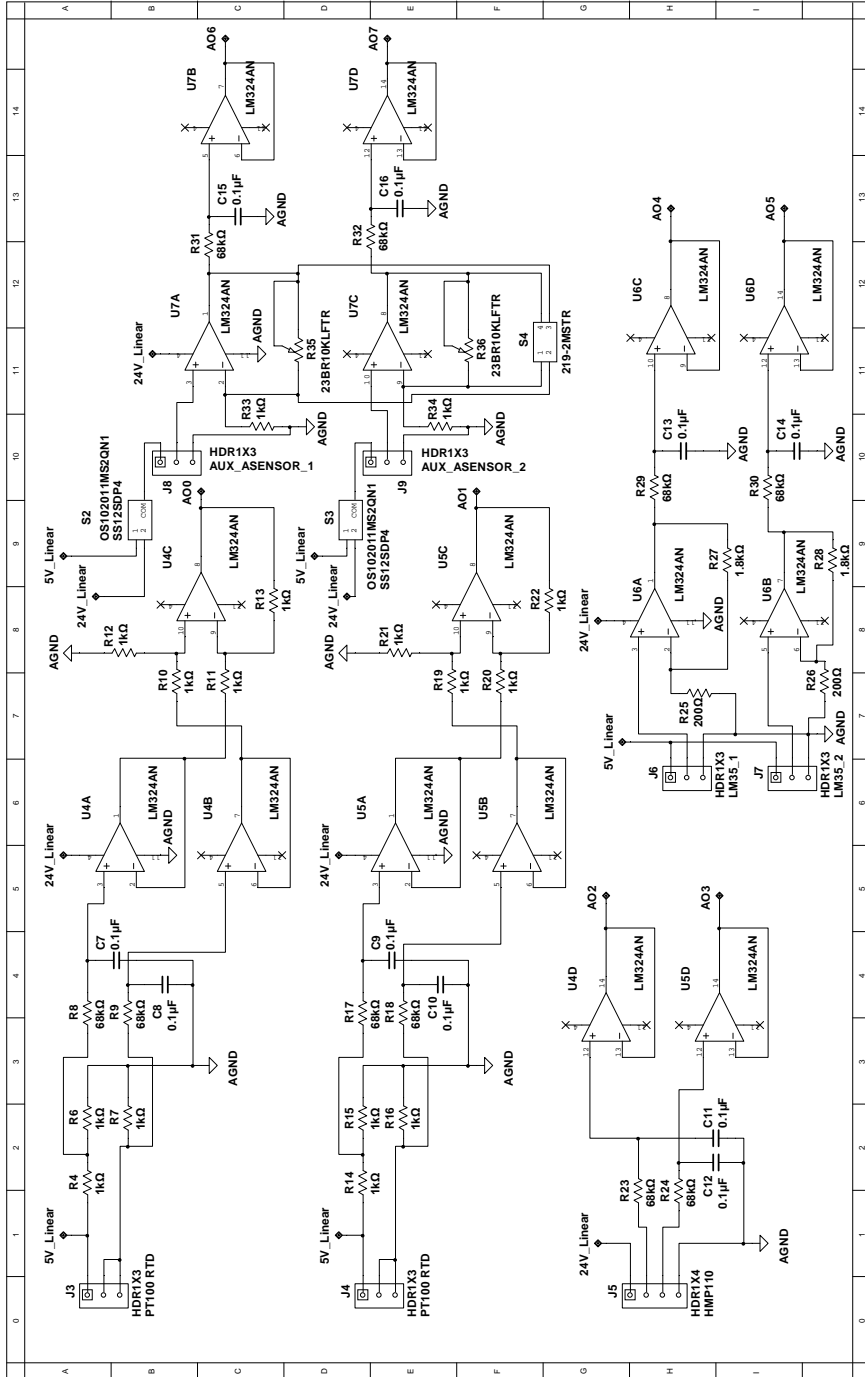
APPENDIX

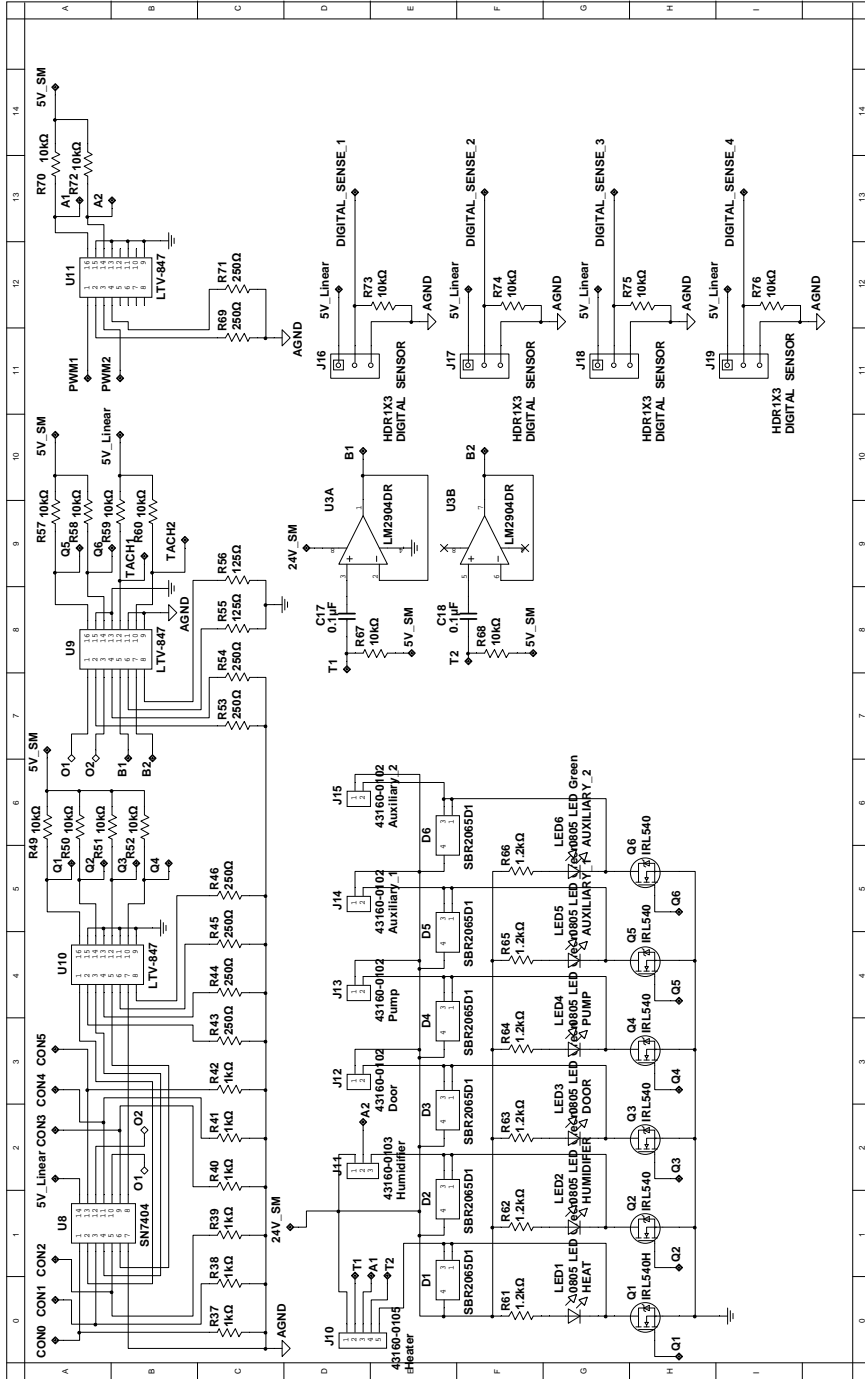
Technical Drawings

B.1 Electronic Schematics

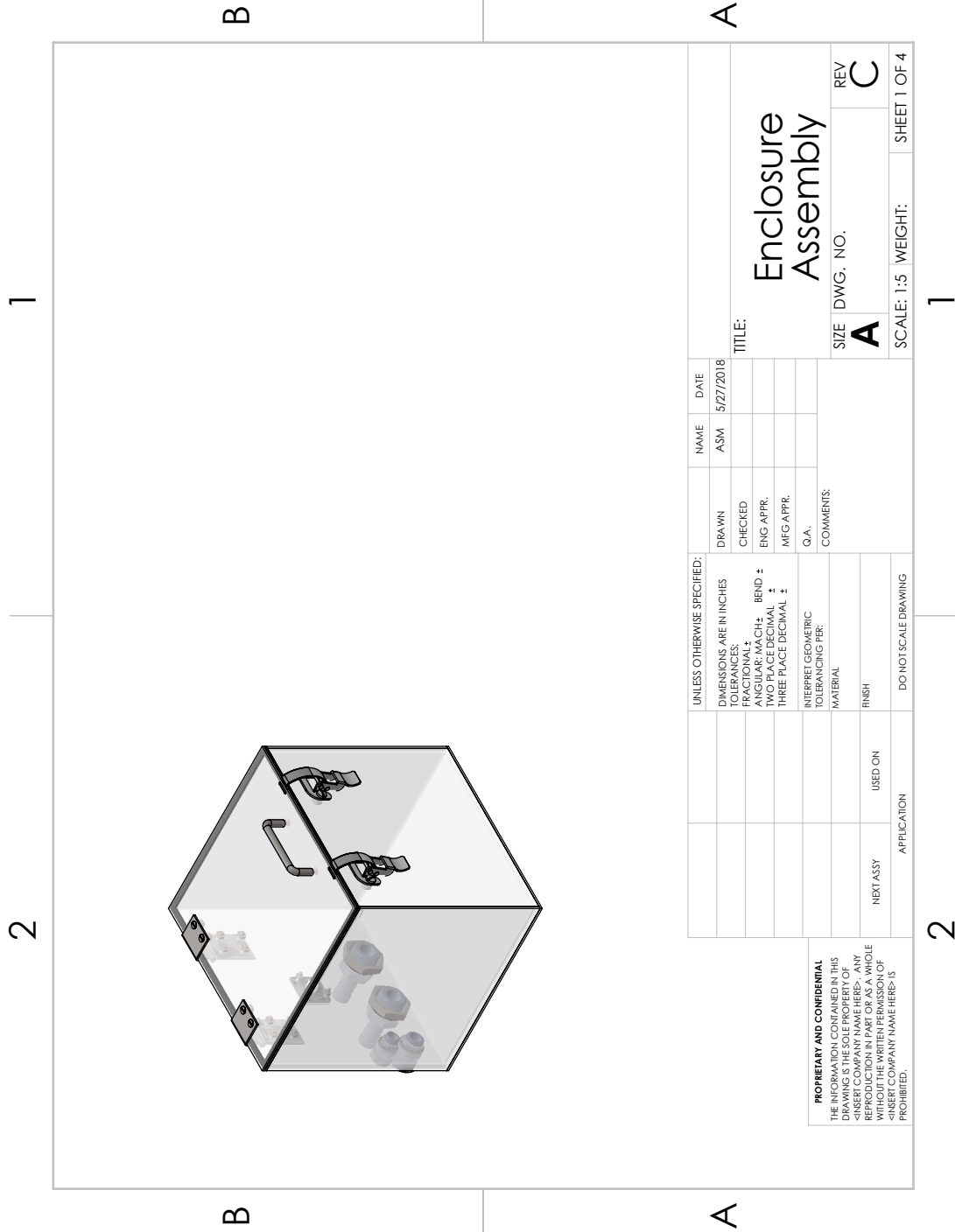


THE UNIVERSITY OF RHODE ISLAND	
University of Rhode Island 100 Flanagan Road Kingston, RI 02881	
Title: NanoSoft Board	Desc: NanoSoft Board Rev - 1
Designed by: Aaron Matrese	Document No:
Checked by:	Date: 11/11/2017
Approved by:	Sheet 1 of 3
Revision: 1	Size: B





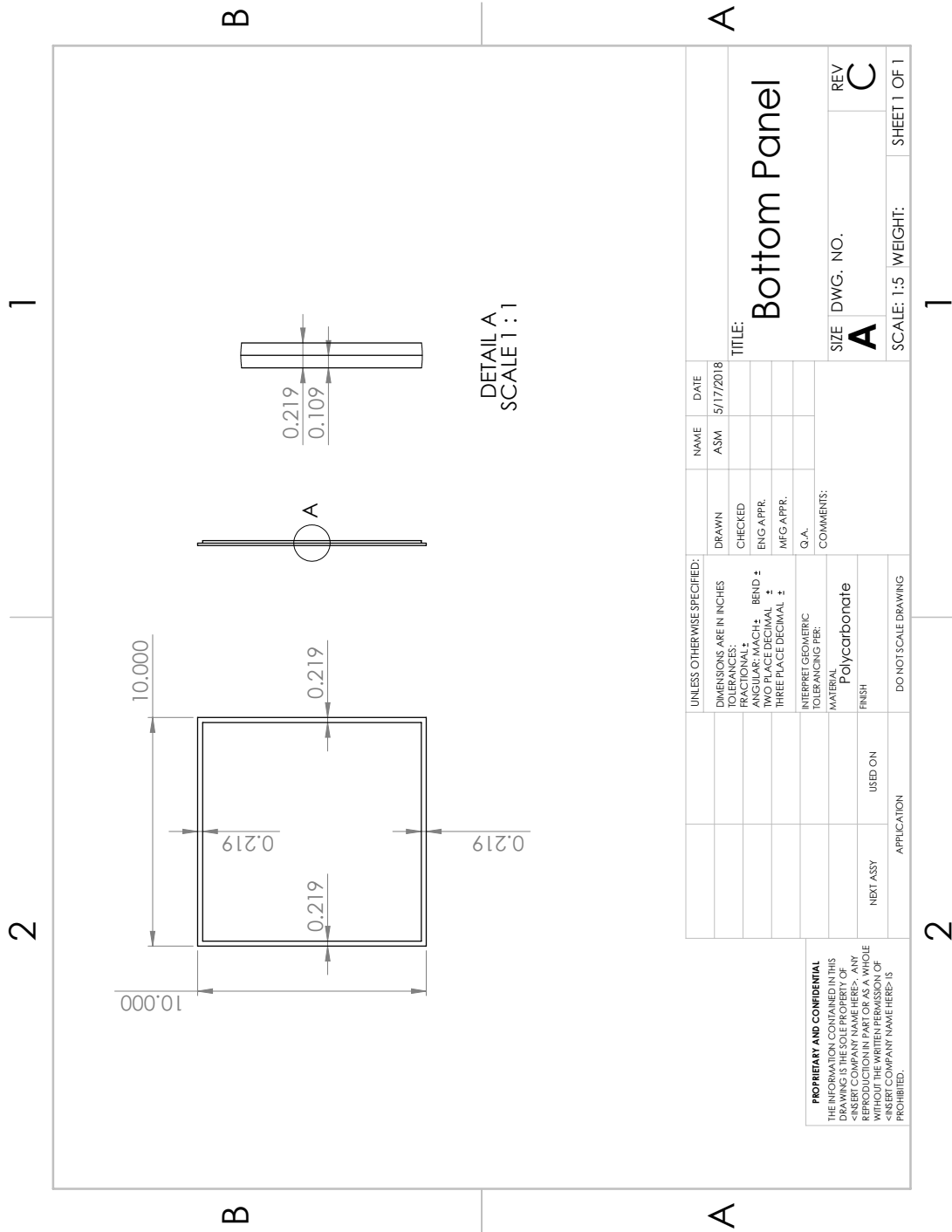
B.2 Enclosure



<p>PROPRIETARY AND CONFIDENTIAL THE INFORMATION CONTAINED IN THIS DRAWING IS THE SOLE PROPERTY OF <INSERT COMPANY NAME HERE>. ANY REPRODUCTION IN PART OR AS A WHOLE WITHOUT THE WRITTEN PERMISSION OF <INSERT COMPANY NAME HERE> IS PROHIBITED.</p>		<p>UNLESS OTHERWISE SPECIFIED: DIMENSIONS ARE IN INCHES TOLERANCES: FRACTIONAL ± ANGULAR: MACH ± BEND ± TWO PLACE DECIMAL ± THREE PLACE DECIMAL ±</p>	<p>DRAWN CHECKED ENG APPR. MFG APPR. Q.A. COMMENTS:</p>	<p>NAME ASM</p>	<p>DATE 5/27/2018</p>
<p>NEXT ASSY</p>	<p>USED ON</p>	<p>INTERPRET GEOMETRIC TOLERANCING PER: MATERIAL FINISH</p>	<p>DO NOT SCALE DRAWING</p>	<p>SCALE: 1:5</p>	<p>WEIGHT:</p>
<p>APPLICATION</p>	<p>REVISIONS</p>	<p>TITLE: Enclosure Assembly</p>	<p>SIZE A</p>	<p>DWG. NO.</p>	<p>REV C</p>
<p>2</p>	<p>2</p>	<p>1</p>	<p>1</p>	<p>1</p>	<p>SHEET 1 OF 4</p>

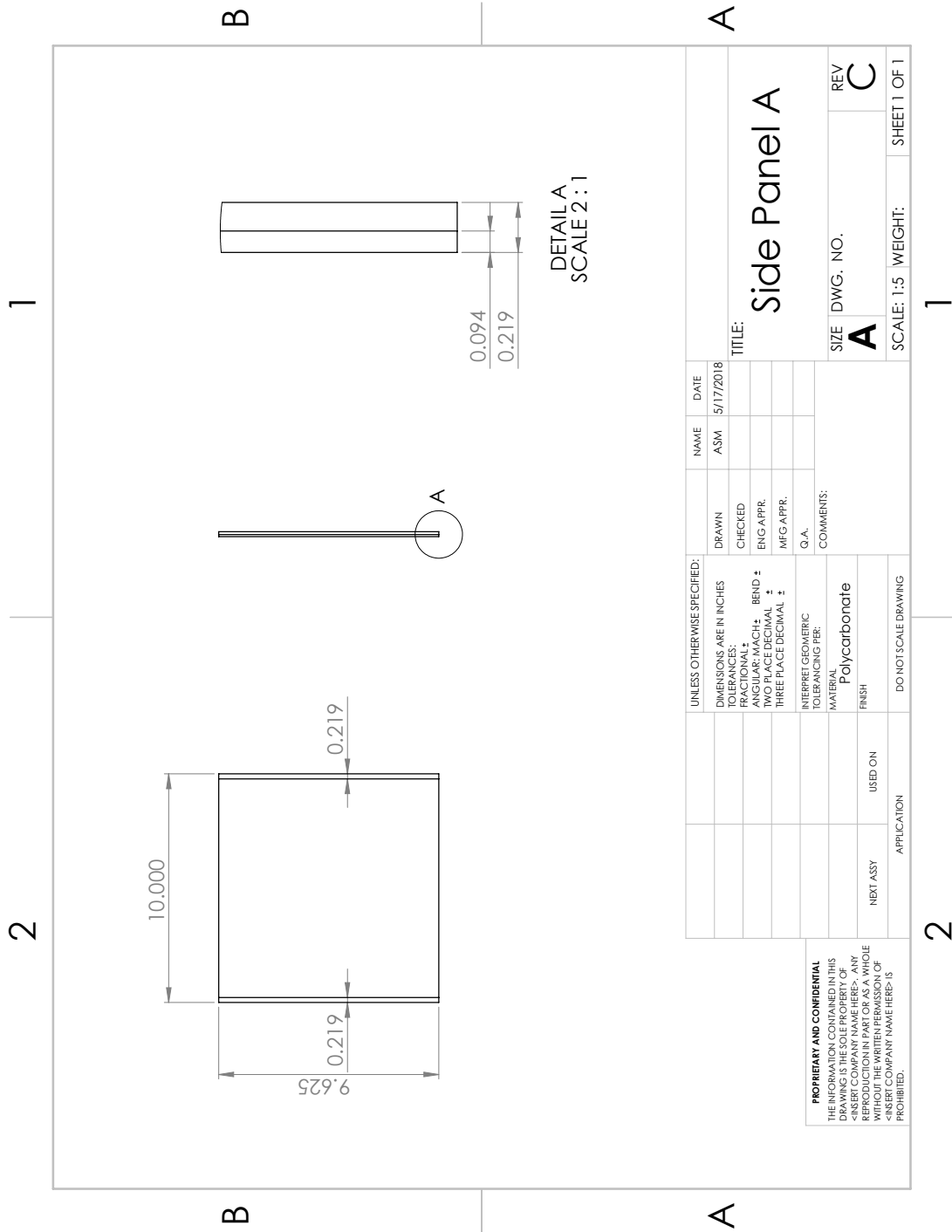
ITEM NO.	PART NUMBER	DESCRIPTION	QTY.
13	McMaster-Carr 91841A011	12-24 Nut	4
14	McMaster-Carr 91792A294S	SL-PHMS 12-24 0.5625x0.5625-N	4
15	McMaster-Carr 5357K46	Barbed Hose Fitting	2
16	McMaster-Carr 4452K676	Threaded Pipe Fitting	2
17	McMaster-Carr 7807K12	Liquid Tight Cord Grip	1
18	McMaster-Carr 7807K57	Liquid Tight Cord Grip	1
19	McMaster-Carr 91841A007	6-32 Nut	4
20	Sensor Probe Gasket - Rev 0		1
21	McMaster-Carr 91781A151	SL-FHMS 6-32 0.75x0.75-N	4
22	Humidifier Nozzle Gasket - Rev 0		2
23	Cord Grip 2 Gasket - Rev 0 - Rev 0		1
24	Sensor Probe - Rev B		1

UNLESS OTHERWISE SPECIFIED: DIMENSIONS ARE IN INCHES TOLERANCES: FRACTIONAL ± ANGULAR: MACH ± BEND ± TWO PLACE DECIMAL ± THREE PLACE DECIMAL ±		DRAWN	CHECKED	NAME	DATE
INTERPRET GEOMETRIC TOLERANCING PER: MATERIAL		ENG APPR.	MFG APPR.	ASM	5/27/2018
FINISH		TITLE: Enclosure Assembly			
NEXT ASSY		SIZE DWG. NO. A			
USED ON		SCALE: 1:5 WEIGHT: SHEET 3 OF 4			
APPLICATION		REV C			



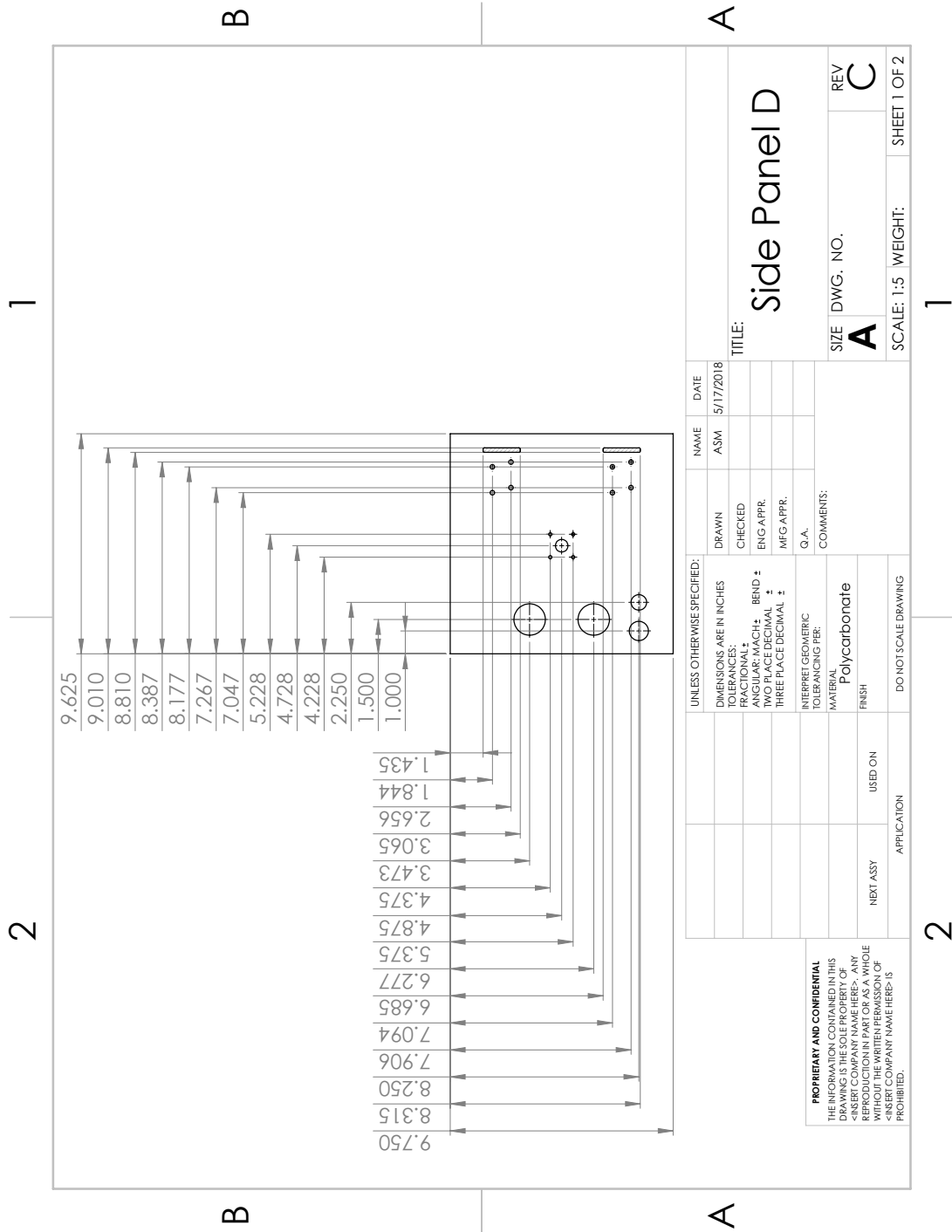
UNLESS OTHERWISE SPECIFIED:		NAME	DATE
DIMENSIONS ARE IN INCHES		ASM	5/17/2018
TOLERANCES:		DRAWN	CHECKED
FRACTIONAL ±		ENG APPR.	MFG APPR.
ANGULAR: MACH ± BEND ±		Q.A.	
TWO PLACE DECIMAL ±		COMMENTS:	
THREE PLACE DECIMAL ±		MATERIAL	
INTERPRET GEOMETRIC TOLERANCING PER:		FINISH	
POLYCARBONATE		NEXT ASSY	
USED ON		APPLICATION	
DO NOT SCALE DRAWING		SCALE: 1:5	
SIZE DWG. NO.		WEIGHT:	
A		SHEET 1 OF 1	
REV		REV	
C		C	

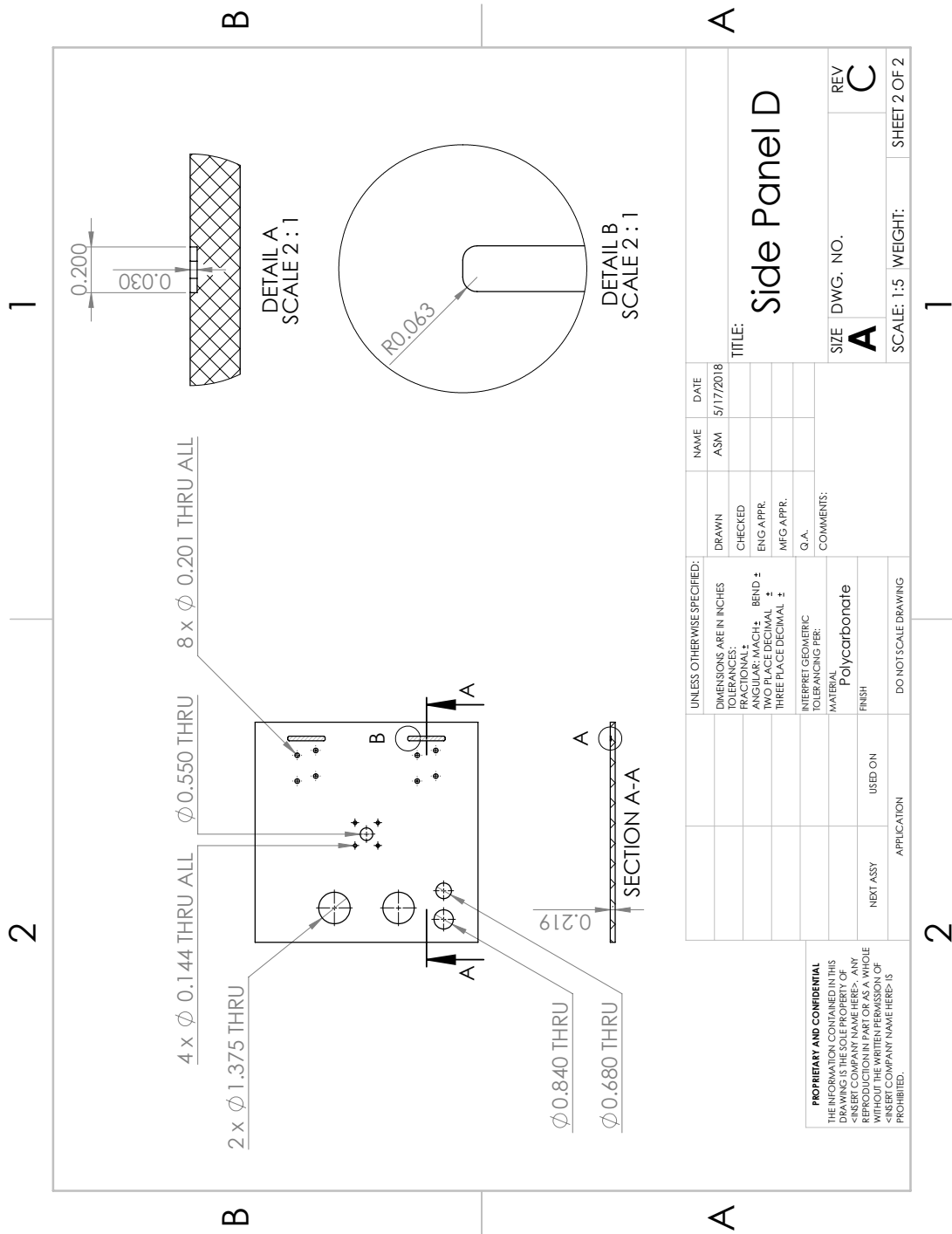
PROPRIETARY AND CONFIDENTIAL
 THE INFORMATION CONTAINED IN THIS DRAWING IS THE SOLE PROPERTY OF <INSERT COMPANY NAME HERE>. ANY REPRODUCTION IN PART OR AS A WHOLE WITHOUT THE WRITTEN PERMISSION OF <INSERT COMPANY NAME HERE> IS PROHIBITED.



UNLESS OTHERWISE SPECIFIED:		NAME	DATE
DIMENSIONS ARE IN INCHES		ASM	5/17/2018
TOLERANCES:		DRAWN	CHECKED
FRACTIONAL ±		ENG APPR.	MFG APPR.
ANGULAR: MACH ± BEND ±		G.A.	
TWO PLACE DECIMAL ±		COMMENTS:	
THREE PLACE DECIMAL ±		INTERPRET GEOMETRIC TOLERANCING PER:	
MATERIAL:		POLYCARBONATE	
FINISH:		USED ON	
NEXT ASSY		APPLICATION	
DO NOT SCALE DRAWING		SCALE: 1:5	
SIZE		DWG. NO.	
A		C	
TITLE:		REV	
Side Panel A		C	
SCALE: 1:5		WEIGHT:	
1		SHEET 1 OF 1	

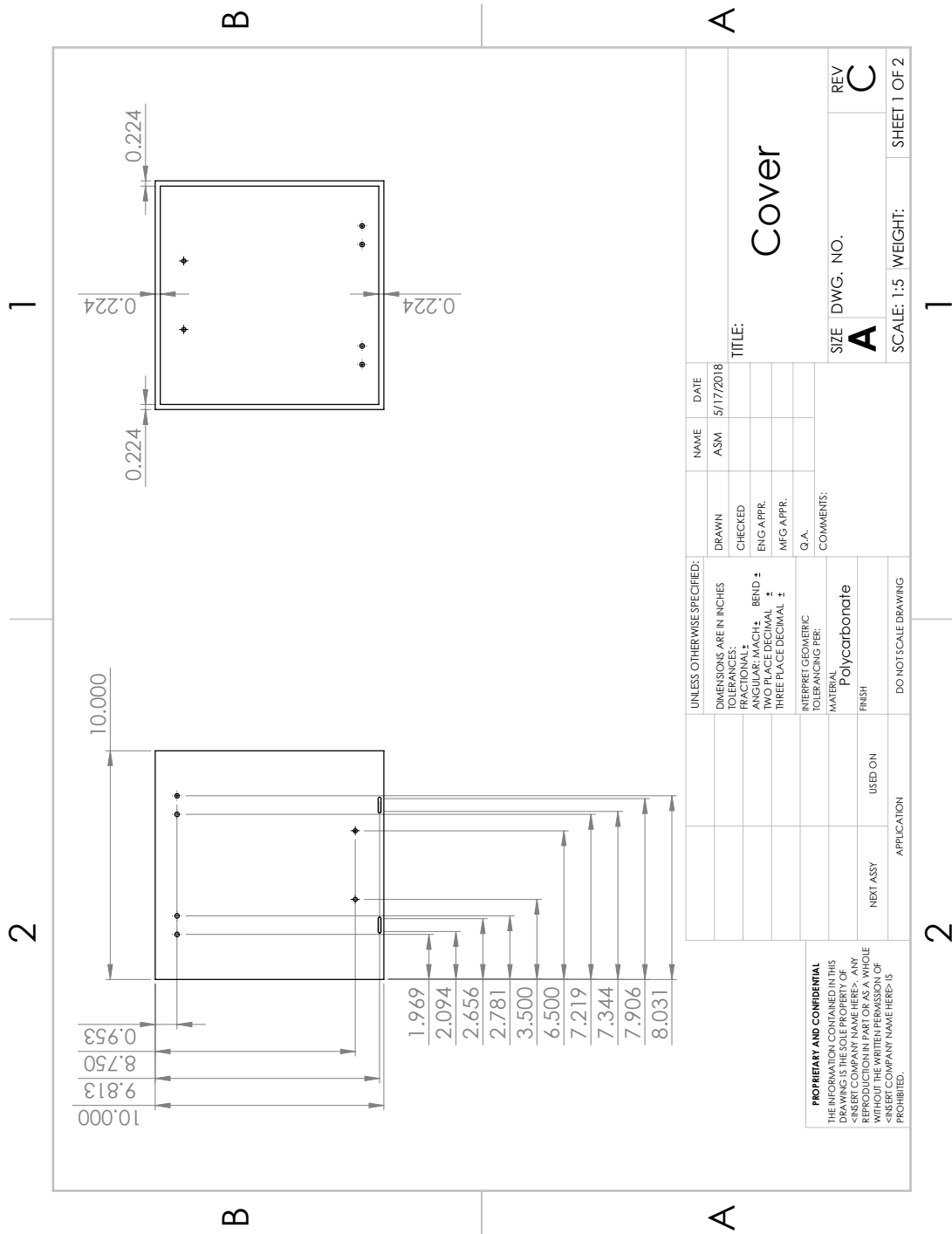
PROPRIETARY AND CONFIDENTIAL
 THE INFORMATION CONTAINED IN THIS DRAWING IS THE SOLE PROPERTY OF <INSERT COMPANY NAME HERE>. ANY REPRODUCTION IN PART OR AS A WHOLE WITHOUT THE WRITTEN PERMISSION OF <INSERT COMPANY NAME HERE> IS PROHIBITED.

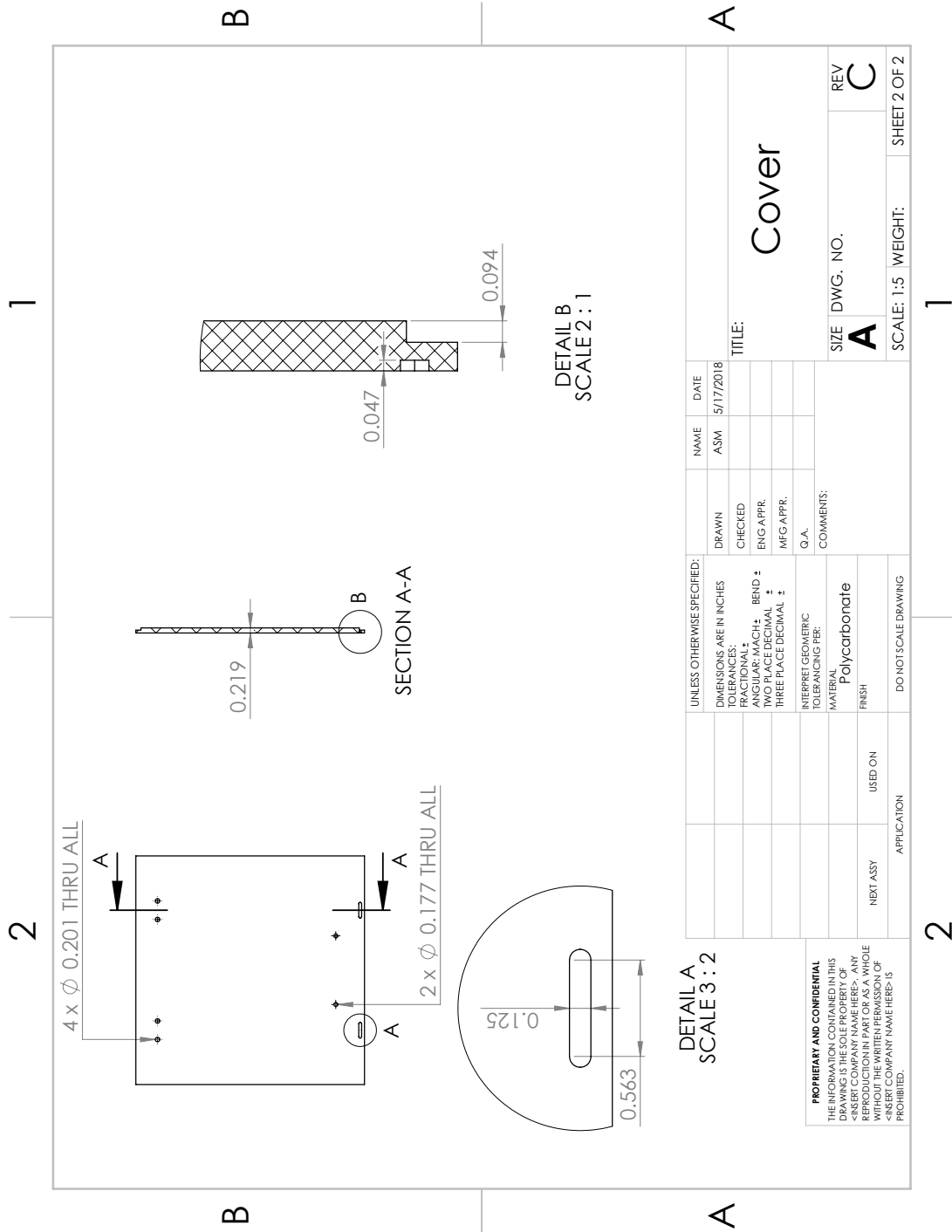


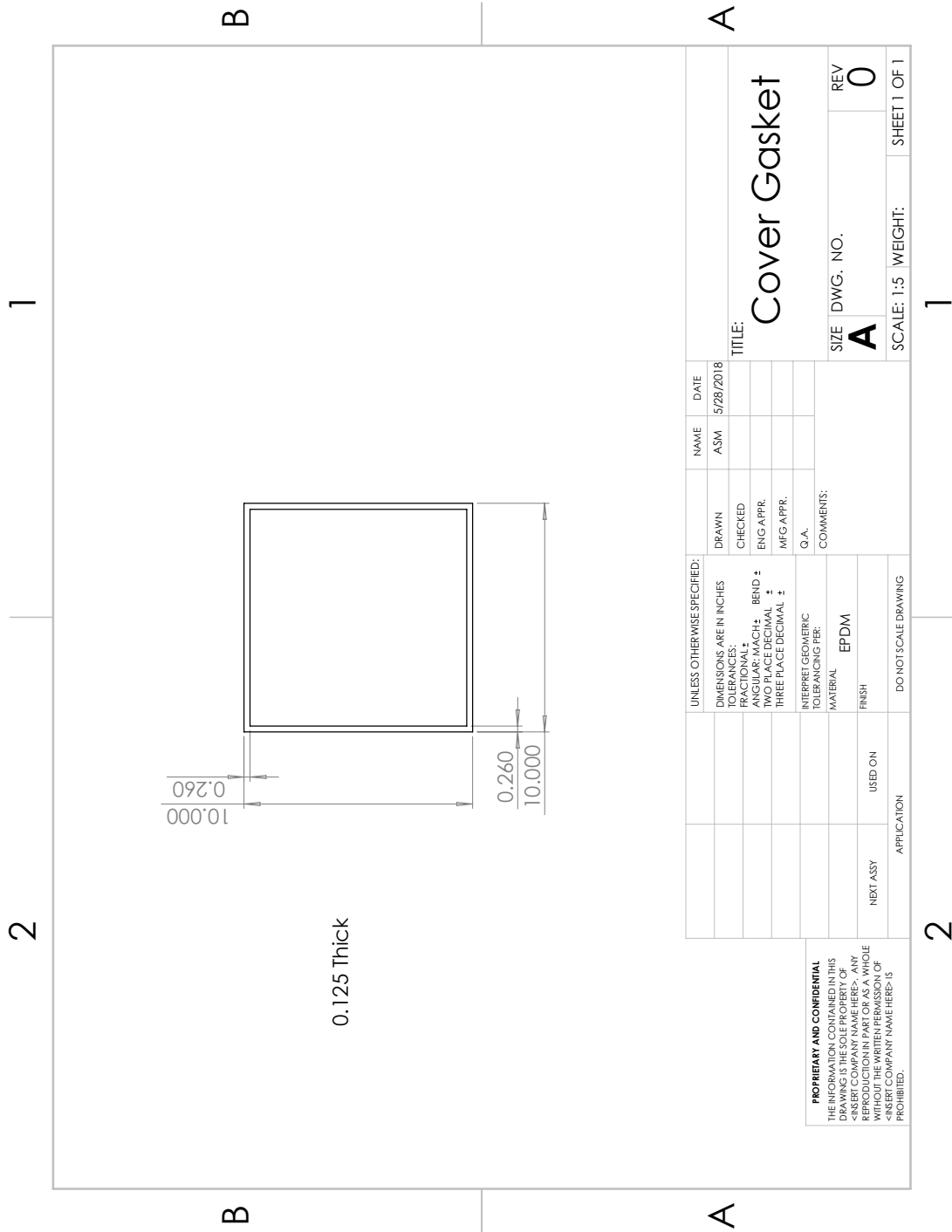


UNLESS OTHERWISE SPECIFIED:		NAME	DATE
DIMENSIONS ARE IN INCHES		ASM	5/17/2018
TOLERANCES:		DRAWN	
FRACTIONAL ±		CHECKED	
ANGULAR: MACH ± BEND ±		ENG APPR	
TWO PLACE DECIMAL ±		MFG APPR	
THREE PLACE DECIMAL ±		Q.A.	
INTERPRET GEOMETRIC TOLERANCING PER:		COMMENTS:	
MATERIAL:		Polycarbonate	
FINISH:			
NEXT ASSY	USED ON	SIZE	DWG. NO.
APPLICATION		A	C
		SCALE: 1:5	WEIGHT:
			SHEET 2 OF 2

Side Panel D







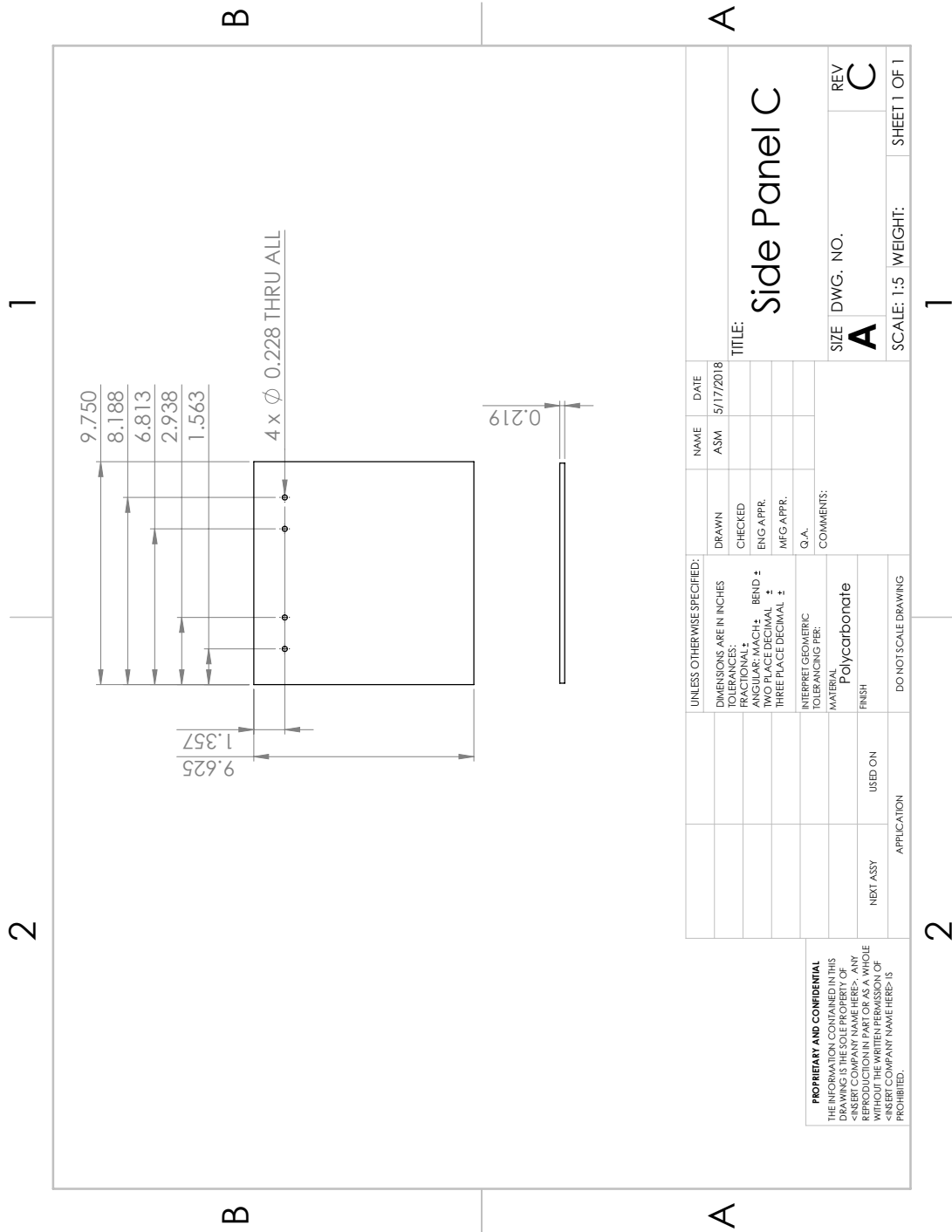
10.000
0.260
0.260
10.000

0.125 Thick

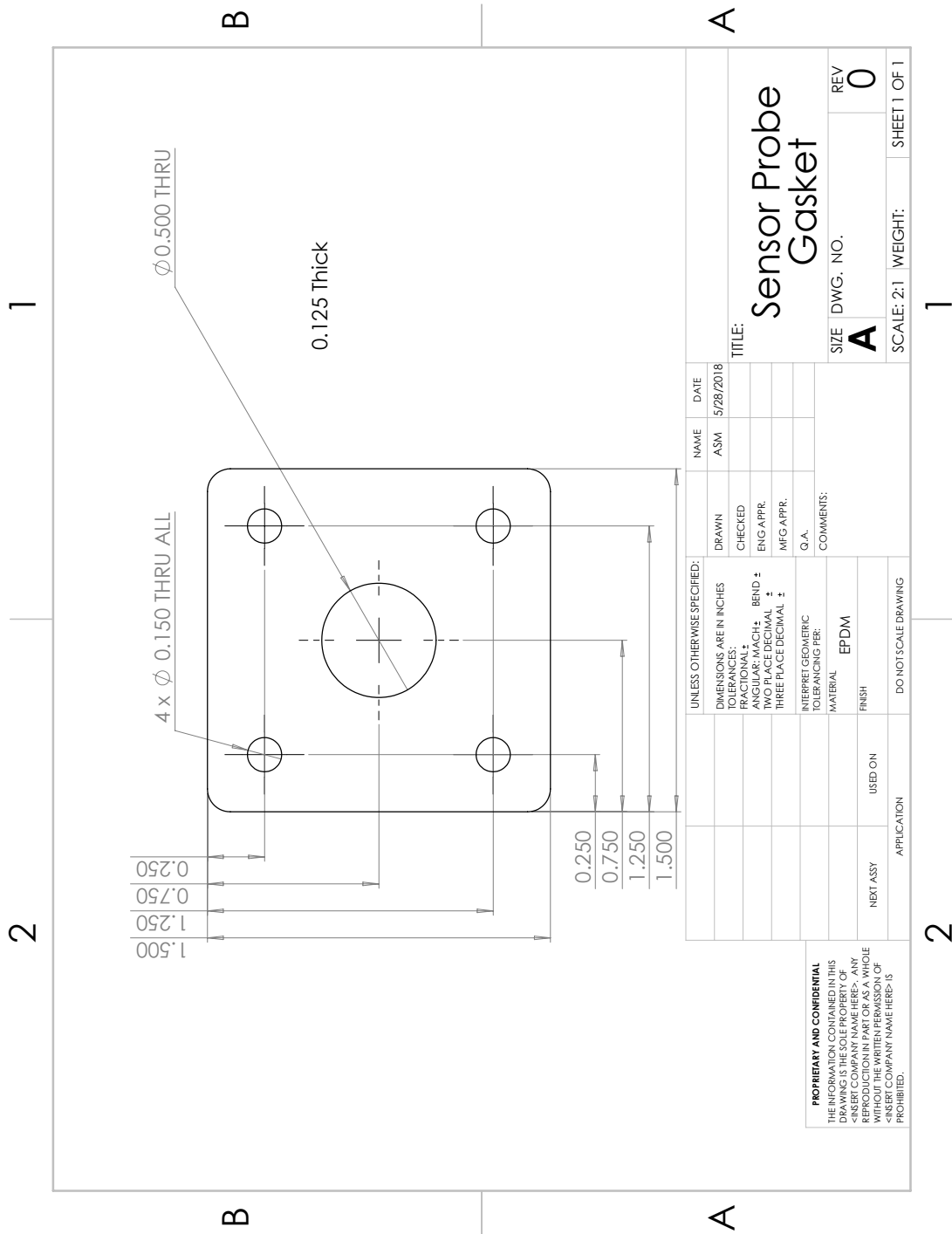
UNLESS OTHERWISE SPECIFIED:		NAME	DATE
DIMENSIONS ARE IN INCHES		ASM	5/28/2018
TOLERANCES:		DRAWN	
FRACTIONAL ±		CHECKED	
ANGULAR: MACH ± BEND ±		ENG APPR.	
TWO PLACE DECIMAL ±		MFG APPR.	
THREE PLACE DECIMAL ±			
INTERPRET GEOMETRIC TOLERANCING PER:		Q.A.	
MATERIAL		COMMENTS:	
FINISH		EPDM	
NEXT ASSY	USED ON	SIZE	DWG. NO.
APPLICATION		A	0
		SCALE: 1:5	WEIGHT:
			SHEET 1 OF 1

TITLE:
Cover Gasket

PROPRIETARY AND CONFIDENTIAL
THE INFORMATION CONTAINED IN THIS DRAWING IS THE SOLE PROPERTY OF <INSERT COMPANY NAME HERE>. ANY REPRODUCTION IN PART OR AS A WHOLE WITHOUT THE WRITTEN PERMISSION OF <INSERT COMPANY NAME HERE> IS PROHIBITED.



<p>PROPRIETARY AND CONFIDENTIAL THE INFORMATION CONTAINED IN THIS DRAWING IS THE SOLE PROPERTY OF <INSERT COMPANY NAME HERE>. ANY REPRODUCTION IN PART OR AS A WHOLE WITHOUT THE WRITTEN PERMISSION OF <INSERT COMPANY NAME HERE> IS PROHIBITED.</p>		<p>UNLESS OTHERWISE SPECIFIED: DIMENSIONS ARE IN INCHES TOLERANCES: FRACTIONAL ± ANGULAR: MACH ± BEND ± TWO PLACE DECIMAL ± THREE PLACE DECIMAL ±</p>		<p>DRAWN CHECKED ENG APPR. MFG APPR. Q.A. COMMENTS:</p>	<p>NAME ASM</p>	<p>DATE 5/17/2018</p>
<p>NEXT ASSY</p>	<p>USED ON</p>	<p>MATERIAL Polycarbonate FINISH</p>	<p>INTERPRET GEOMETRIC TOLERANCING PER:</p>	<p>Q.A. COMMENTS:</p>	<p>TITLE: Side Panel C</p>	<p>SIZE DWG. NO. REV A C</p>
<p>APPLICATION</p>	<p>DO NOT SCALE DRAWING</p>	<p>SCALE: 1:5 WEIGHT: SHEET 1 OF 1</p>	<p>SCALE: 1:5 WEIGHT: SHEET 1 OF 1</p>	<p>SCALE: 1:5 WEIGHT: SHEET 1 OF 1</p>	<p>SCALE: 1:5 WEIGHT: SHEET 1 OF 1</p>	<p>SCALE: 1:5 WEIGHT: SHEET 1 OF 1</p>



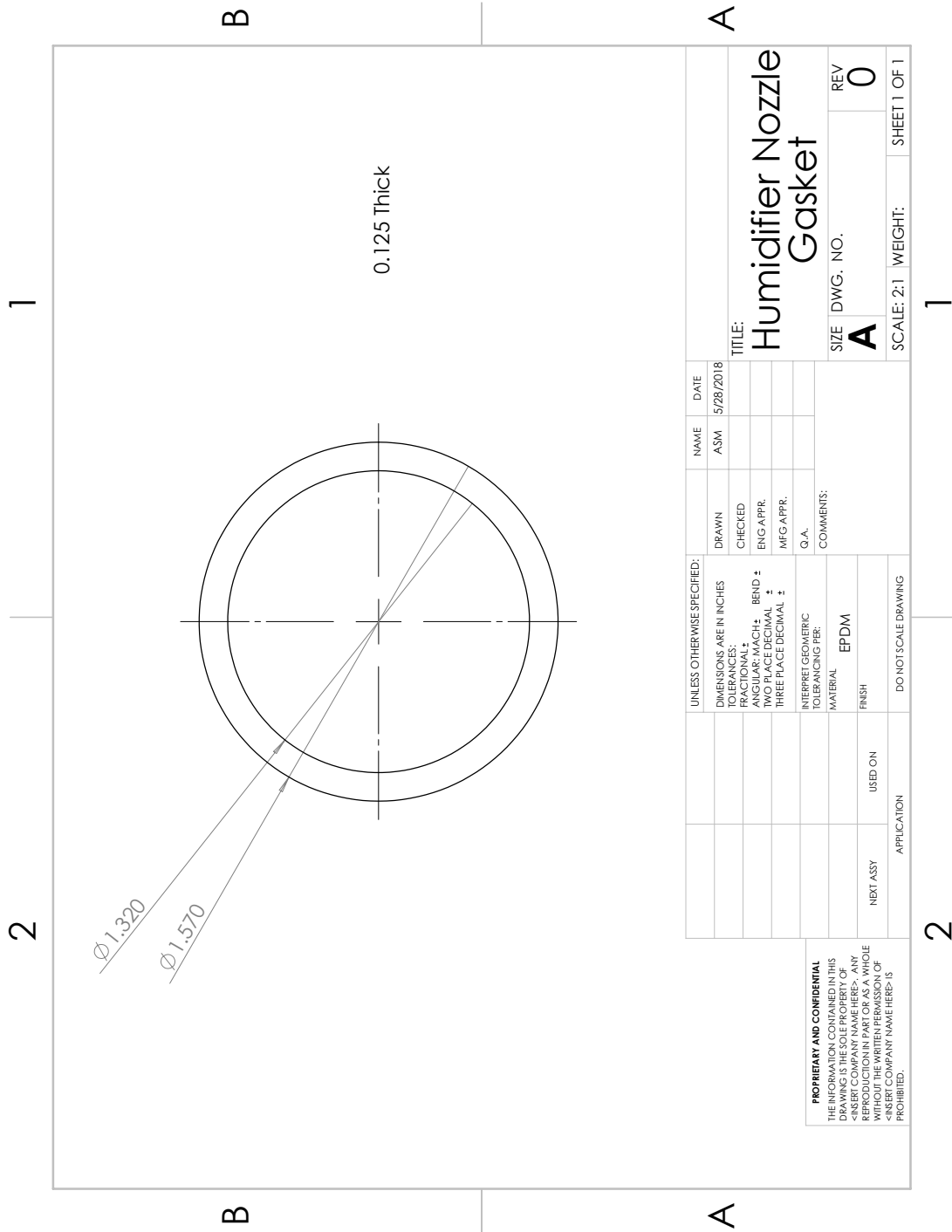
UNLESS OTHERWISE SPECIFIED:		NAME	DATE
DIMENSIONS ARE IN INCHES		ASM	5/28/2018
TOLERANCES:			
FRACTIONAL ±		DRAWN	CHECKED
ANGULAR: MACH ± BEND ±		ENG APPR.	
TWO PLACE DECIMAL ±		MFG APPR.	
THREE PLACE DECIMAL ±			
INTERPRET GEOMETRIC TOLERANCING PER:			
MATERIAL			
FINISH			
NEXT ASSY			
USED ON			
APPLICATION			
DO NOT SCALE DRAWING			

TITLE: **Sensor Probe Gasket**

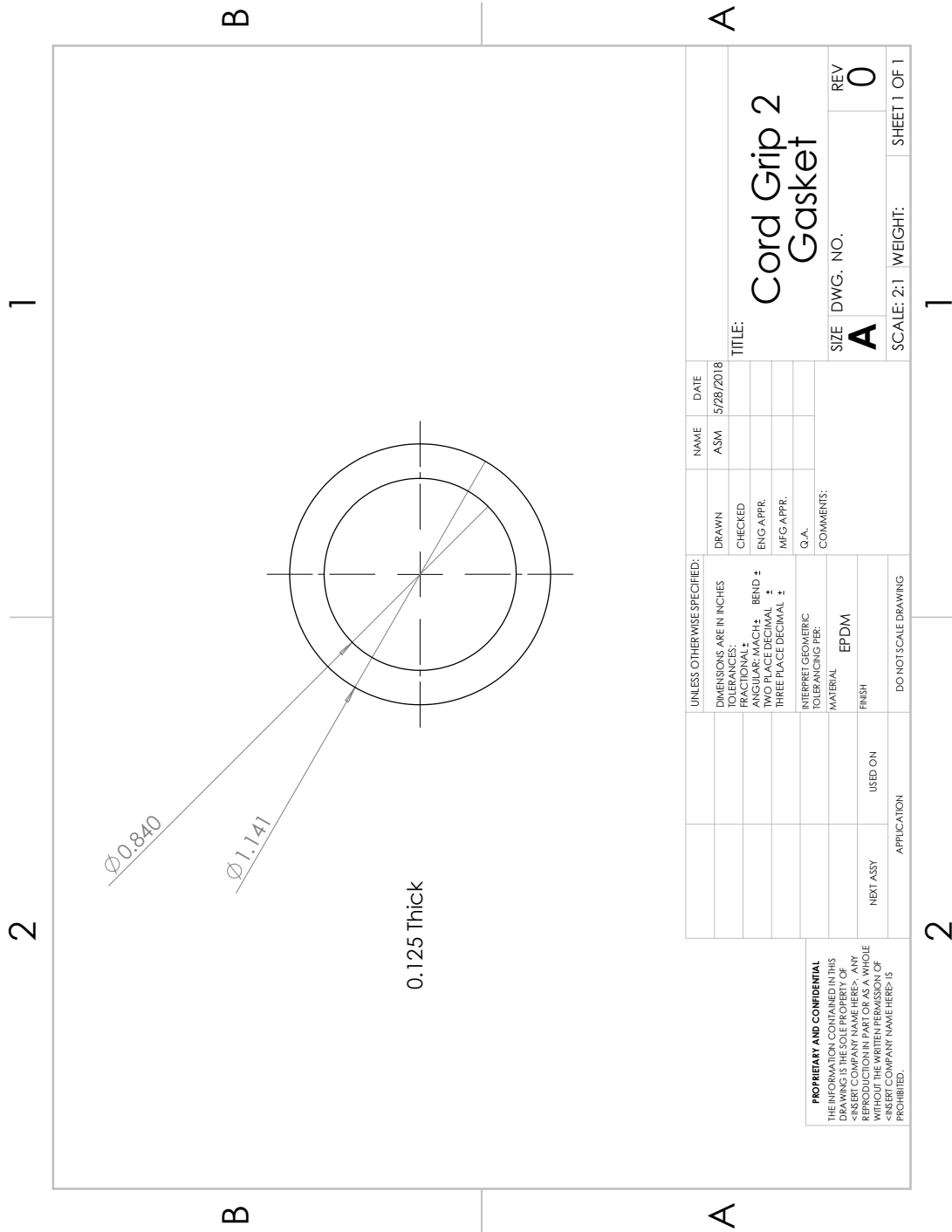
SIZE DWG. NO. **A** REV **0**

SCALE: 2:1 WEIGHT: SHEET 1 OF 1

PROPRIETARY AND CONFIDENTIAL
 THE INFORMATION CONTAINED IN THIS DRAWING IS THE SOLE PROPERTY OF <INSERT COMPANY NAME HERE>. ANY REPRODUCTION IN PART OR AS A WHOLE WITHOUT THE WRITTEN PERMISSION OF <INSERT COMPANY NAME HERE> IS PROHIBITED.

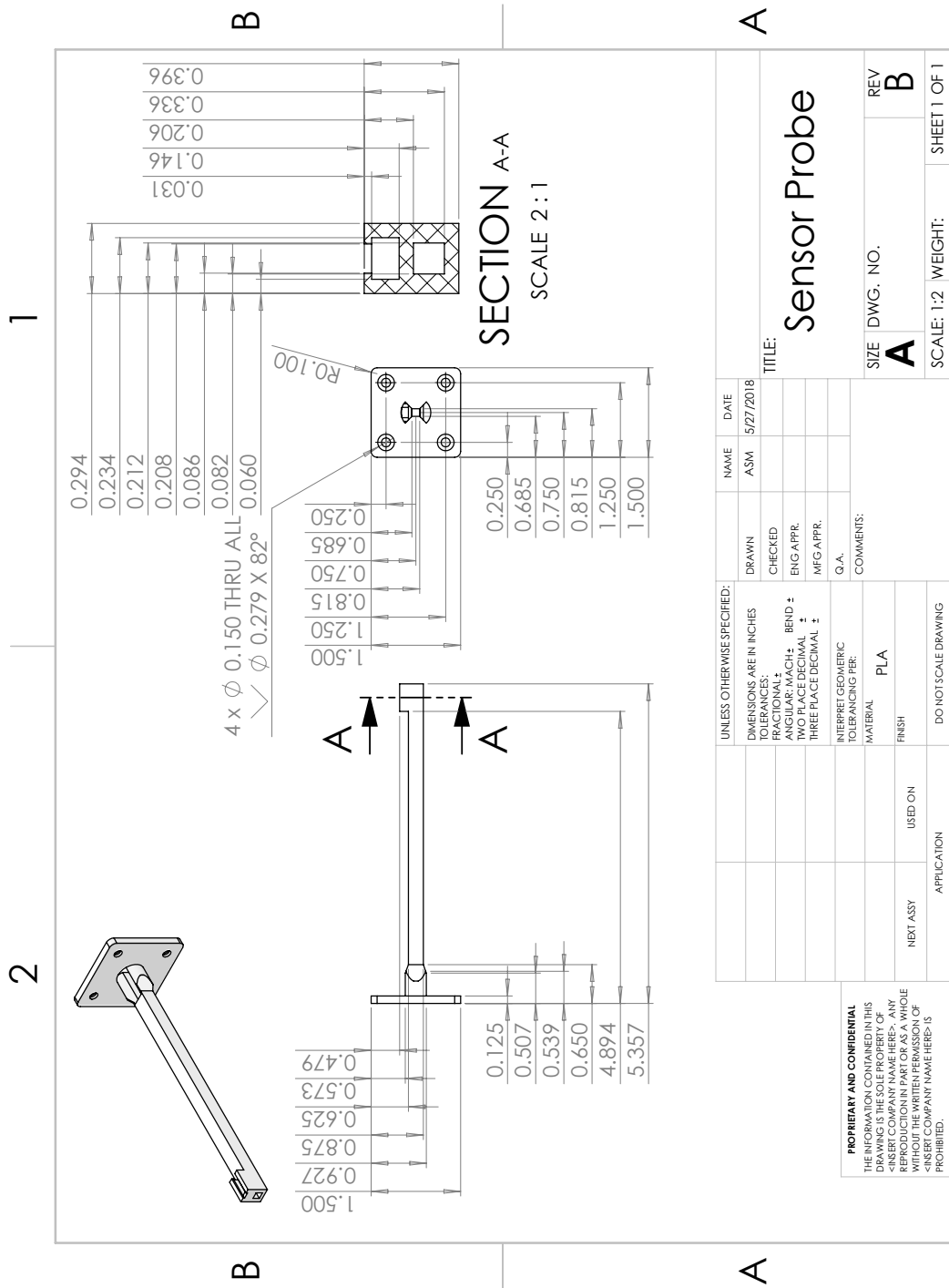


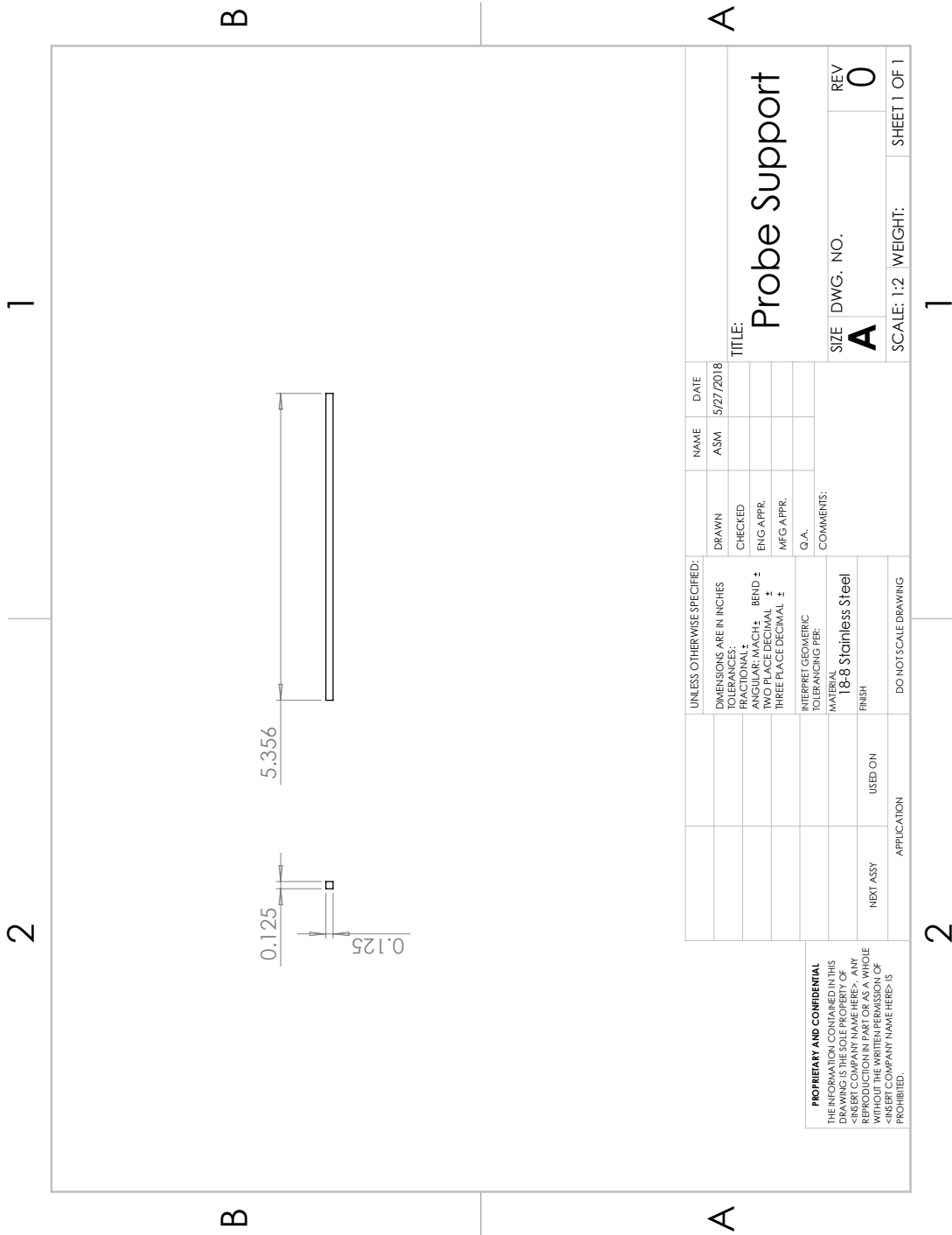
PROPRIETARY AND CONFIDENTIAL THE INFORMATION CONTAINED IN THIS DRAWING IS THE SOLE PROPERTY OF <INSERT COMPANY NAME HERE>. ANY REPRODUCTION IN PART OR AS A WHOLE WITHOUT THE WRITTEN PERMISSION OF <INSERT COMPANY NAME HERE> IS PROHIBITED.		UNLESS OTHERWISE SPECIFIED: DIMENSIONS ARE IN INCHES TOLERANCES: FRACTIONAL ± ANGULAR: MACH ± BEND ± TWO PLACE DECIMAL ± THREE PLACE DECIMAL ±		DRAWN	CHECKED	NAME	DATE
NEXT ASSY	USED ON	INTERPRET GEOMETRIC TOLERANCING PER:	ENG APPR.	ASM	5/28/2018	TITLE: Humidifier Nozzle Gasket	
APPLICATION	FINISH	MATERIAL	MFG APPR.	COMMENTS:		SIZE	DWG. NO.
	EPDM					A	0
						SCALE: 2:1	WEIGHT:
						SHEET 1 OF 1	



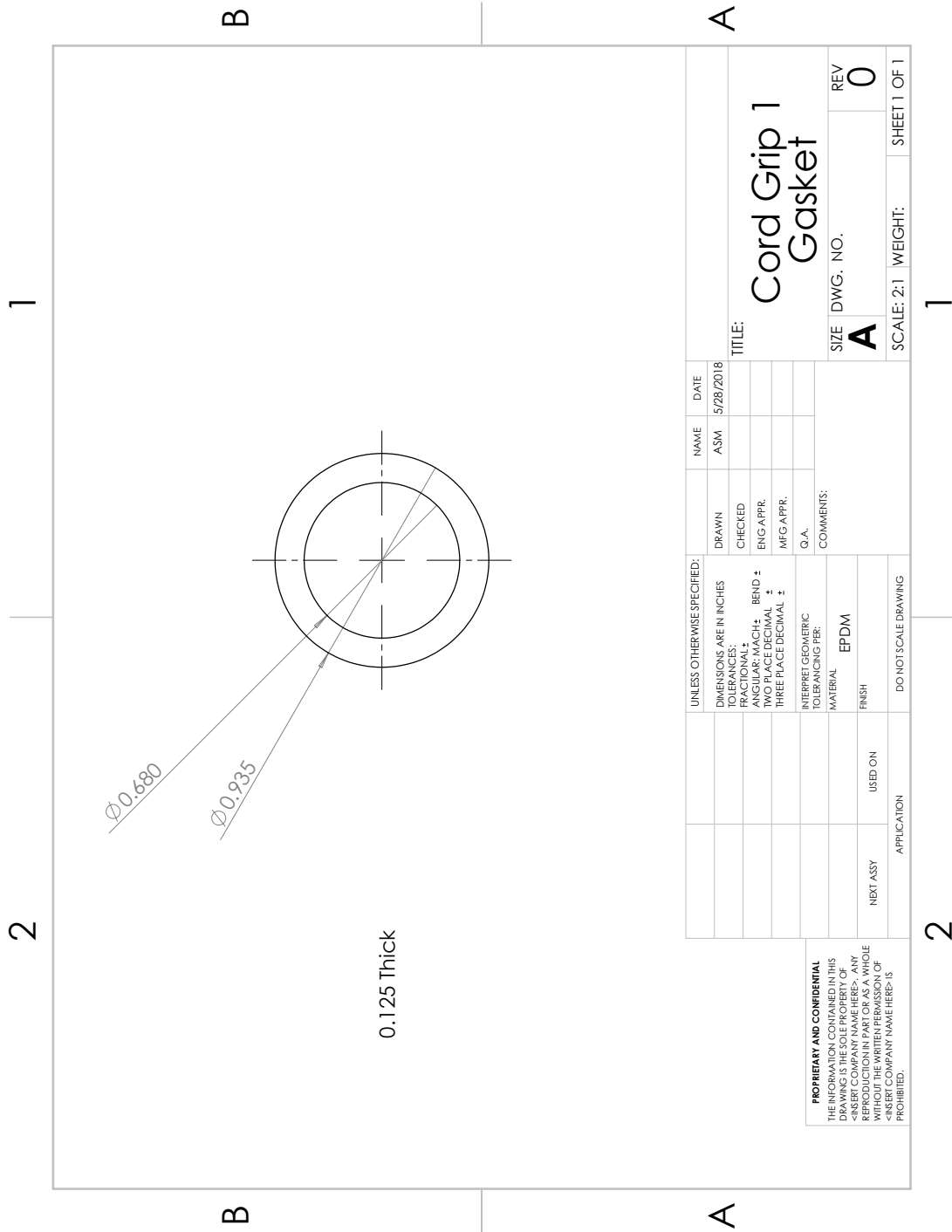
<p>PROPRIETARY AND CONFIDENTIAL THE INFORMATION CONTAINED IN THIS DRAWING IS THE SOLE PROPERTY OF <INSERT COMPANY NAME HERE>. ANY REPRODUCTION IN PART OR AS A WHOLE WITHOUT THE WRITTEN PERMISSION OF <INSERT COMPANY NAME HERE> IS PROHIBITED.</p>		<p>UNLESS OTHERWISE SPECIFIED: DIMENSIONS ARE IN INCHES TOLERANCES: FRACTIONAL ± ANGULAR: MACH ± BEND ± TWO PLACE DECIMAL ± THREE PLACE DECIMAL ±</p>	<p>DRAWN CHECKED ENG APPR. MFG APPR. Q.A. COMMENTS:</p>	<p>NAME ASM</p>	<p>DATE 5/28/2018</p>
<p>NEXT ASSY</p>	<p>USED ON</p>	<p>MATERIAL EPDM</p>	<p>FINISH</p>	<p>SCALE: 2:1</p>	<p>WEIGHT:</p>
<p>APPLICATION</p>	<p>DO NOT SCALE DRAWING</p>	<p>SIZE A</p>	<p>DWG. NO.</p>	<p>REV 0</p>	<p>SHEET 1 OF 1</p>

**Cord Grip 2
Gasket**





<p>PROPRIETARY AND CONFIDENTIAL THE INFORMATION CONTAINED IN THIS DRAWING IS THE SOLE PROPERTY OF <INSERT COMPANY NAME HERE>. ANY REPRODUCTION IN PART OR AS A WHOLE WITHOUT THE WRITTEN PERMISSION OF <INSERT COMPANY NAME HERE> IS PROHIBITED.</p>		<p>UNLESS OTHERWISE SPECIFIED: DIMENSIONS ARE IN INCHES TOLERANCES: FRACTIONAL ± ANGULAR: MACH ± BEND ± TWO PLACE DECIMAL ± THREE PLACE DECIMAL ±</p>		<p>DRAWN</p>	<p>NAME</p>	<p>DATE</p>
<p>NEXT ASSY</p>	<p>USED ON</p>	<p>INTERPRET GEOMETRIC TOLERANCING PER: MATERIAL: FINISH</p>	<p>CHECKED</p>	<p>ASM</p>	<p>5/27/2018</p>	
<p>APPLICATION</p>		<p>18-8 Stainless Steel</p>	<p>ENG APPR.</p>	<p>TITLE: Probe Support</p>		
<p>DO NOT SCALE DRAWING</p>		<p>COMMENTS:</p>	<p>MFG APPR.</p>	<p>SIZE</p>	<p>REV</p>	
			<p>Q.A.</p>	<p>A</p>	<p>0</p>	
				<p>SCALE: 1:2</p>	<p>WEIGHT:</p>	
				<p>SHEET 1 OF 1</p>	<p>SHEET 1 OF 1</p>	



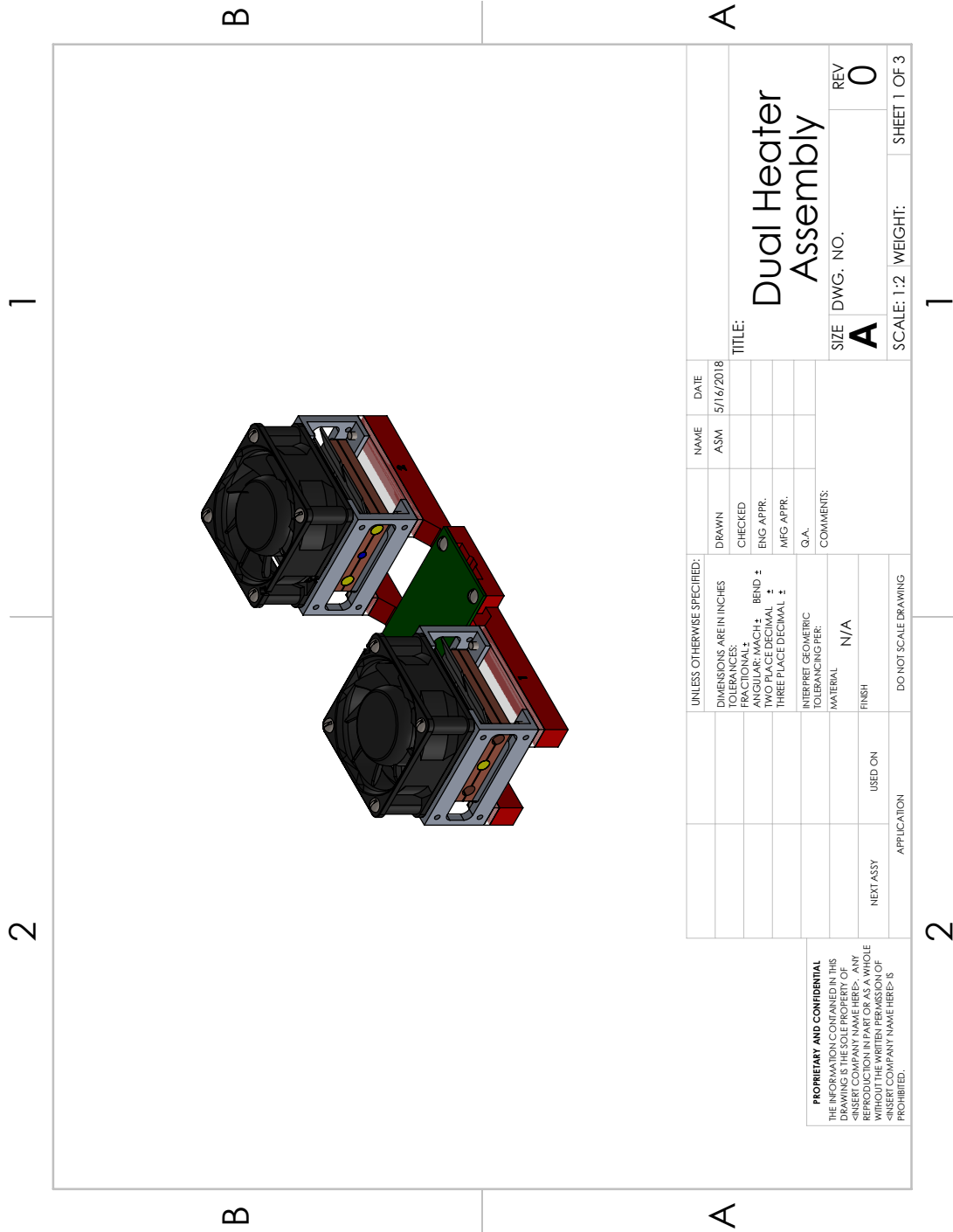
UNLESS OTHERWISE SPECIFIED:		NAME	DATE
DIMENSIONS ARE IN INCHES		ASM	5/28/2018
TOLERANCES:		DRAWN	CHECKED
FRACTIONAL ±		ENG APPR.	MFG APPR.
ANGULAR: MACH ± BEND ±		Q.A.	
TWO PLACE DECIMAL ±		COMMENTS:	
THREE PLACE DECIMAL ±		MATERIAL	
INTERPRET GEOMETRIC TOLERANCING PER:		FINISH	
MATERIAL		EPDM	
FINISH		USED ON	
NEXT ASSY		APPLICATION	
DO NOT SCALE DRAWING		SCALE: 2:1	
DO NOT SCALE DRAWING		WEIGHT:	
DO NOT SCALE DRAWING		SHEET 1 OF 1	

PROPRIETARY AND CONFIDENTIAL
 THE INFORMATION CONTAINED IN THIS DRAWING IS THE SOLE PROPERTY OF <INSERT COMPANY NAME HERE>. ANY REPRODUCTION IN PART OR AS A WHOLE WITHOUT THE WRITTEN PERMISSION OF <INSERT COMPANY NAME HERE> IS PROHIBITED.

Cord Grip 1 Gasket

SIZE DWG. NO. **A** REV **0**

B.3 Heater Assembly



UNLESS OTHERWISE SPECIFIED:		NAME	DATE
DIMENSIONS ARE IN INCHES		ASM	5/16/2018
TOLERANCES:			
FRACTIONAL ±			
ANGULAR: MACH ± BEND ±			
TWO PLACE DECIMAL ±			
THREE PLACE DECIMAL ±			
INTERPRET GEOMETRIC TOLERANCING PER:			
MATERIAL			
FINISH			
NEXT ASSY			
USED ON			
APPLICATION			
DO NOT SCALE DRAWING			

DRAWN		TITLE:	
CHECKED		Dual Heater Assembly	
ENG APPR.		SIZE	DWG. NO.
MFG APPR.		A	0
Q.A.		SCALE: 1:2	WEIGHT:
COMMENTS:		SHEET 1 OF 3	

<p>PROPRIETARY AND CONFIDENTIAL</p> <p>THE INFORMATION CONTAINED IN THIS DRAWING IS THE SOLE PROPERTY OF [INSERT COMPANY NAME HERE]. ANY REPRODUCTION IN PART OR AS A WHOLE WITHOUT THE WRITTEN PERMISSION OF [INSERT COMPANY NAME HERE] IS PROHIBITED.</p>	
--	--

ITEM NO.	PART NUMBER	DESCRIPTION	QTY.
2	Proto PCB - Rev 0		1
3	Heater Mount - Rev 0		1
4	McMaster-Carr 91781A151	SL-FHMS 6-32 0.75x0.75-N	8
5	CopperBlock_Bottom - Rev B		2
6	CopperBlock_Top - Rev B		2
7	Guard Bracket - Rev 0		4
8	Heater Base - Rev 0		2
9	McMaster-Carr 8822T13	Heatsink	2
10	Cartridge Heater	40W ceramic cartridge heater	6
11	McMaster-Carr 94335A110	6-32 1/4 in. ceramic standoffs	8
12	McMaster-Carr 91781A146	SL-FHMS 6-32 0.375x0.375-N	4
13	McMaster-Carr 91781A145	SL-FHMS 6-32 0.3125x0.3125-N	8
14	Adafruit 3290	RTD Sensor	2
15	Mouser 978-9G0624P4S001 Sanyo Denki 9G0624P4S001	60 mm PWM DC fan	2
16	McMaster-Carr 91781A155	SL-RHMS 6-32 1.25x1-N	8

2 1

2

B

B

A

A

PROPRIETARY AND CONFIDENTIAL
 THE INFORMATION CONTAINED IN THIS DRAWING IS THE SOLE PROPERTY OF <INSERT COMPANY NAME HERE>. ANY REPRODUCTION IN PART OR AS A WHOLE WITHOUT THE WRITTEN PERMISSION OF <INSERT COMPANY NAME HERE> IS PROHIBITED.

UNLESS OTHERWISE SPECIFIED:		NAME	DATE
DIMENSIONS ARE IN INCHES	DRAWN	ASM	5/16/2018
TOLERANCES:	CHECKED		
FRACTIONAL ±	ENG APPR.		
ANGULAR: MACH ±	MFG APPR.		
BEND ±	Q.A.		
TWO PLACE DECIMAL ±	COMMENTS:		
THREE PLACE DECIMAL ±			
INTERPRET GEOMETRIC TOLERANCING PER:			
MATERIAL			
FINISH			
NEXT ASSY	USED ON		
APPLICATION	DO NOT SCALE DRAWING		

TITLE: **Dual Heater Assembly**

SIZE DWG. NO. **A** REV **0**

SCALE: 1:2 WEIGHT: SHEET 2 OF 3

2 1

2

2		1		1	
ITEM NO.	PART NUMBER	DESCRIPTION	QTY.		
17	McMaster-Carr 91781A 144	SL-FHMS 6-32 0.25x0.25-N	8		
18	McMaster-Carr 91783A 146	SL-RHMS 6-32 0.375x0.375-N	4		

B

B

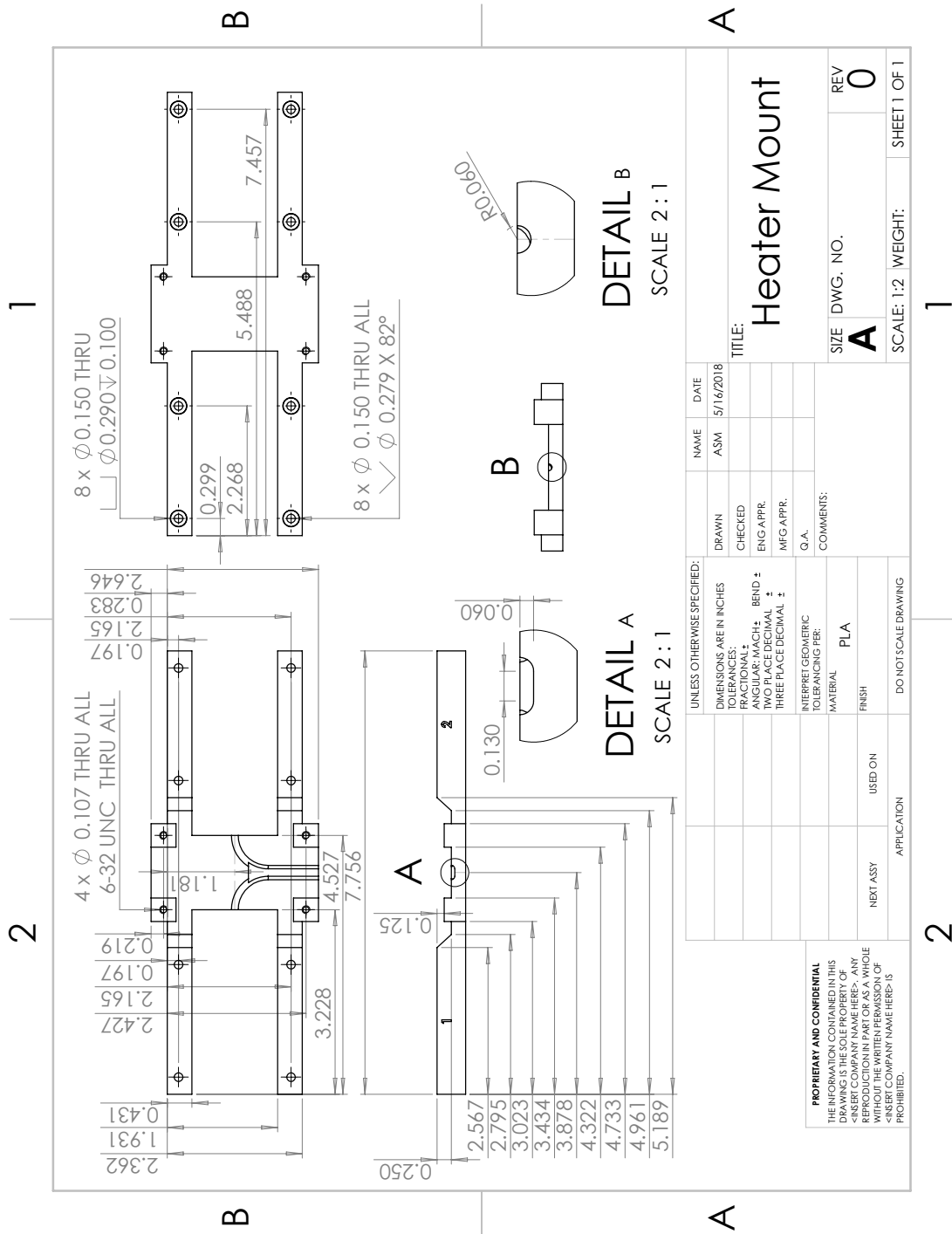
<p>PROPRIETARY AND CONFIDENTIAL THE INFORMATION CONTAINED IN THIS DRAWING IS THE SOLE PROPERTY OF <INSERT COMPANY NAME HERE>. ANY REPRODUCTION IN PART OR AS A WHOLE WITHOUT THE WRITTEN PERMISSION OF <INSERT COMPANY NAME HERE> IS PROHIBITED.</p>		UNLESS OTHERWISE SPECIFIED:		NAME DATE	
		DIMENSIONS ARE IN INCHES TOLERANCES: FRACTIONAL ± ANGULAR: MACH ± BEND ± TWO PLACE DECIMAL ± THREE PLACE DECIMAL ±		DRAWN CHECKED ENG APPR. MFG APPR. Q.A. COMMENTS:	
NEXT ASSY USED ON		MATERIAL N/A		TITLE: Dual Heater Assembly	
APPLICATION		FINISH		SIZE DWG. NO. REV	
		DO NOT SCALE DRAWING		A A 0	
				SCALE: 1:2 WEIGHT: SHEET 3 OF 3	

A

A

1

1

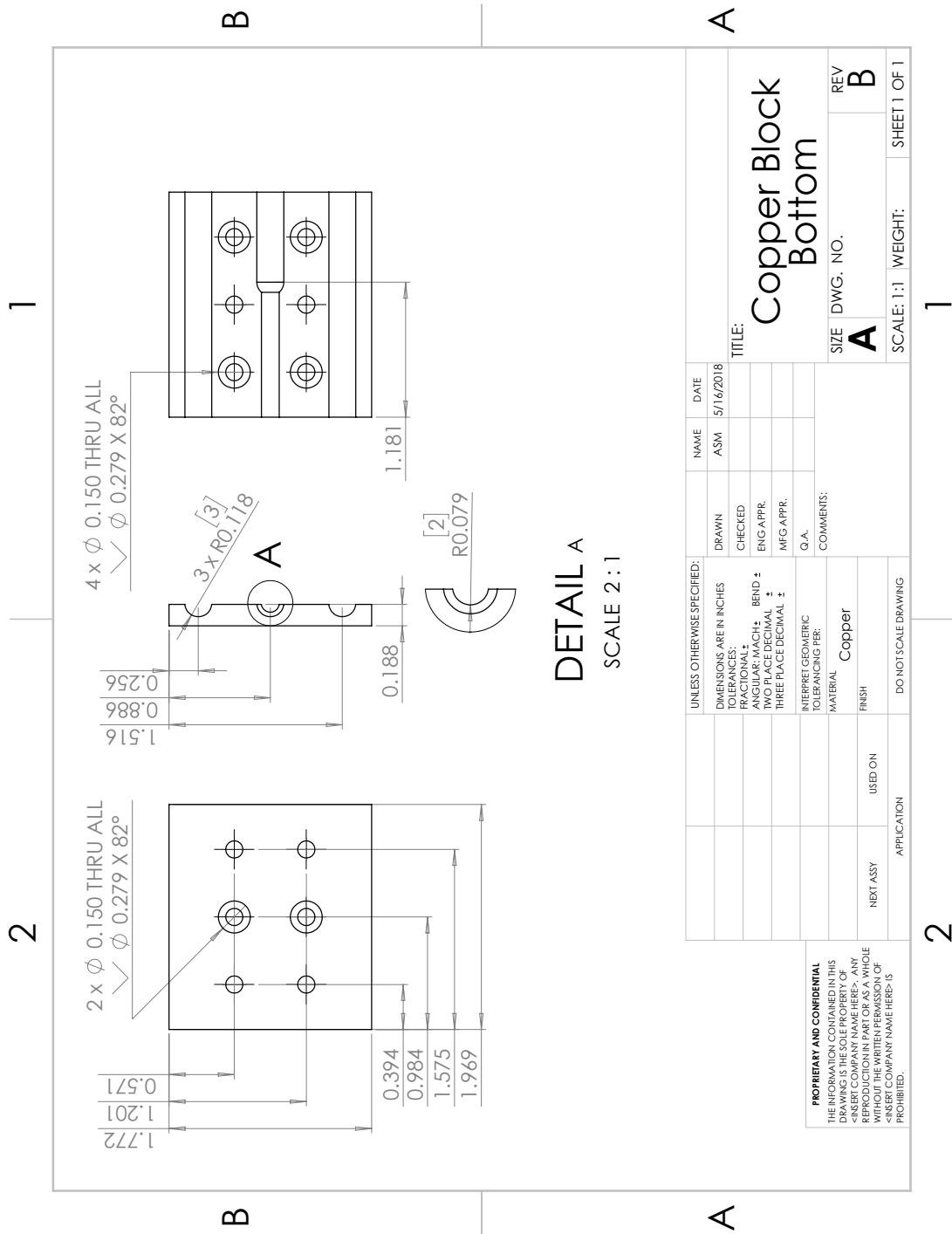


UNLESS OTHERWISE SPECIFIED:		NAME	DATE
DIMENSIONS ARE IN INCHES		ASM	5/16/2018
TOLERANCES:			
FRACTIONAL \pm		DRAWN	CHECKED
ANGULAR: MACH \pm	BEND \pm	ENG APPR.	MFG APPR.
TWO PLACE DECIMAL \pm			
THREE PLACE DECIMAL \pm			
INTERPRET GEOMETRIC TOLERANCING PER:			
MATERIAL	PLA		
FINISH			
USED ON			
APPLICATION			
DO NOT SCALE DRAWING			

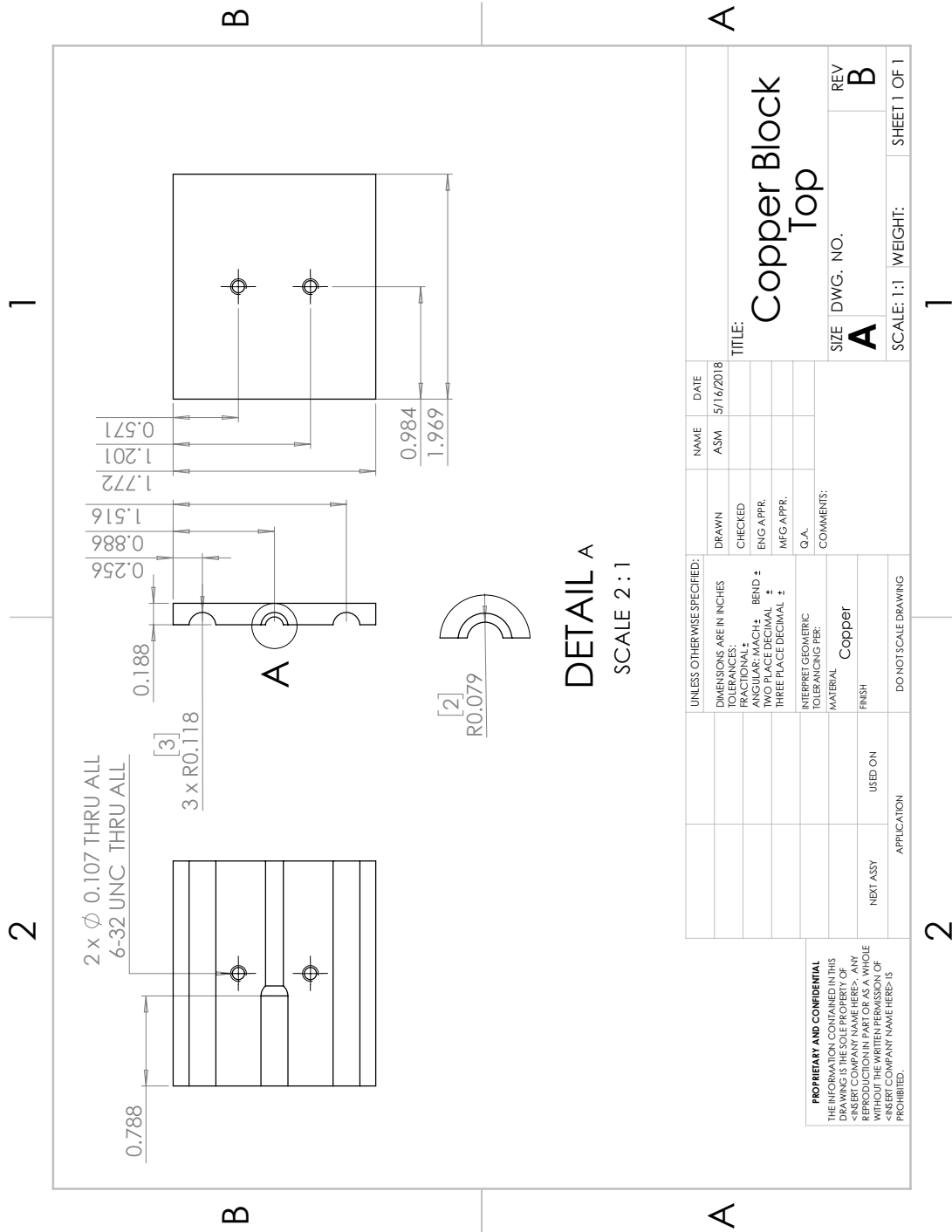
Heater Mount

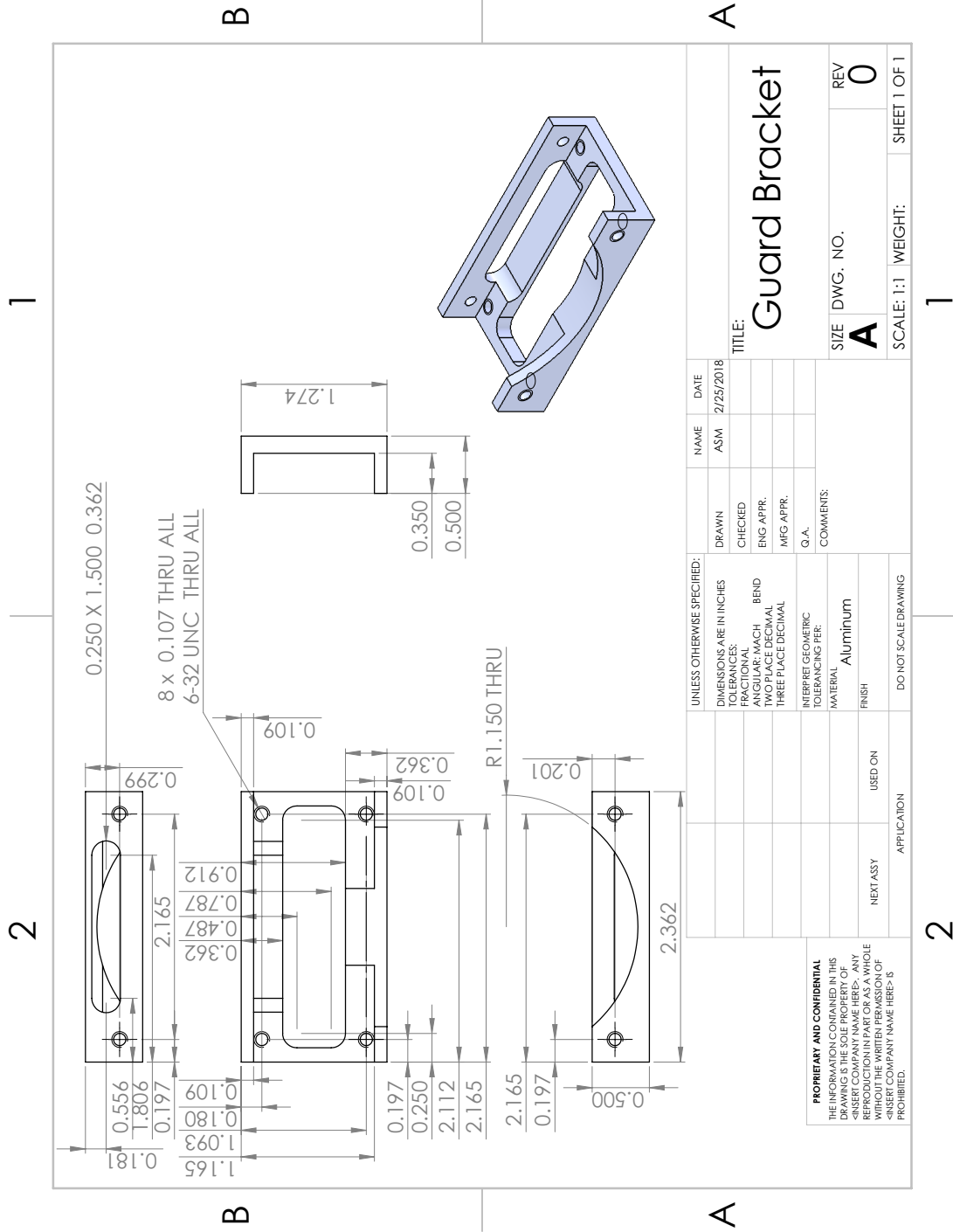
SIZE	DWG. NO.	REV
A		0
SCALE: 1:2	WEIGHT:	SHEET 1 OF 1

PROPRIETARY AND CONFIDENTIAL
 THE INFORMATION CONTAINED IN THIS DRAWING IS THE SOLE PROPERTY OF <INSERT COMPANY NAME HERE>. ANY REPRODUCTION IN PART OR AS A WHOLE WITHOUT THE WRITTEN PERMISSION OF <INSERT COMPANY NAME HERE> IS PROHIBITED.



UNLESS OTHERWISE SPECIFIED:		NAME	DATE	
DIMENSIONS ARE IN INCHES		ASM	5/16/2018	
TOLERANCES:		DRAWN	CHECKED	
FRACTIONAL ±		ENG APPR.	MFG APPR.	
ANGULAR: MACH ± BEND ±		G.A.		
TWO PLACE DECIMAL ±		COMMENTS:		
THREE PLACE DECIMAL ±		MATERIAL Copper		
INTERPRET GEOMETRIC TOLERANCING PER:		FINISH		
NEXT ASSY		USED ON		
APPLICATION		DO NOT SCALE DRAWING		
<p>PROPRIETARY AND CONFIDENTIAL</p> <p>THE INFORMATION CONTAINED IN THIS DRAWING IS THE SOLE PROPERTY OF <INSERT COMPANY NAME HERE>. ANY REPRODUCTION IN PART OR AS A WHOLE WITHOUT THE WRITTEN PERMISSION OF <INSERT COMPANY NAME HERE> IS PROHIBITED.</p>		SIZE	DWG. NO.	REV
		A		B
		SCALE: 1:1	WEIGHT:	SHEET 1 OF 1



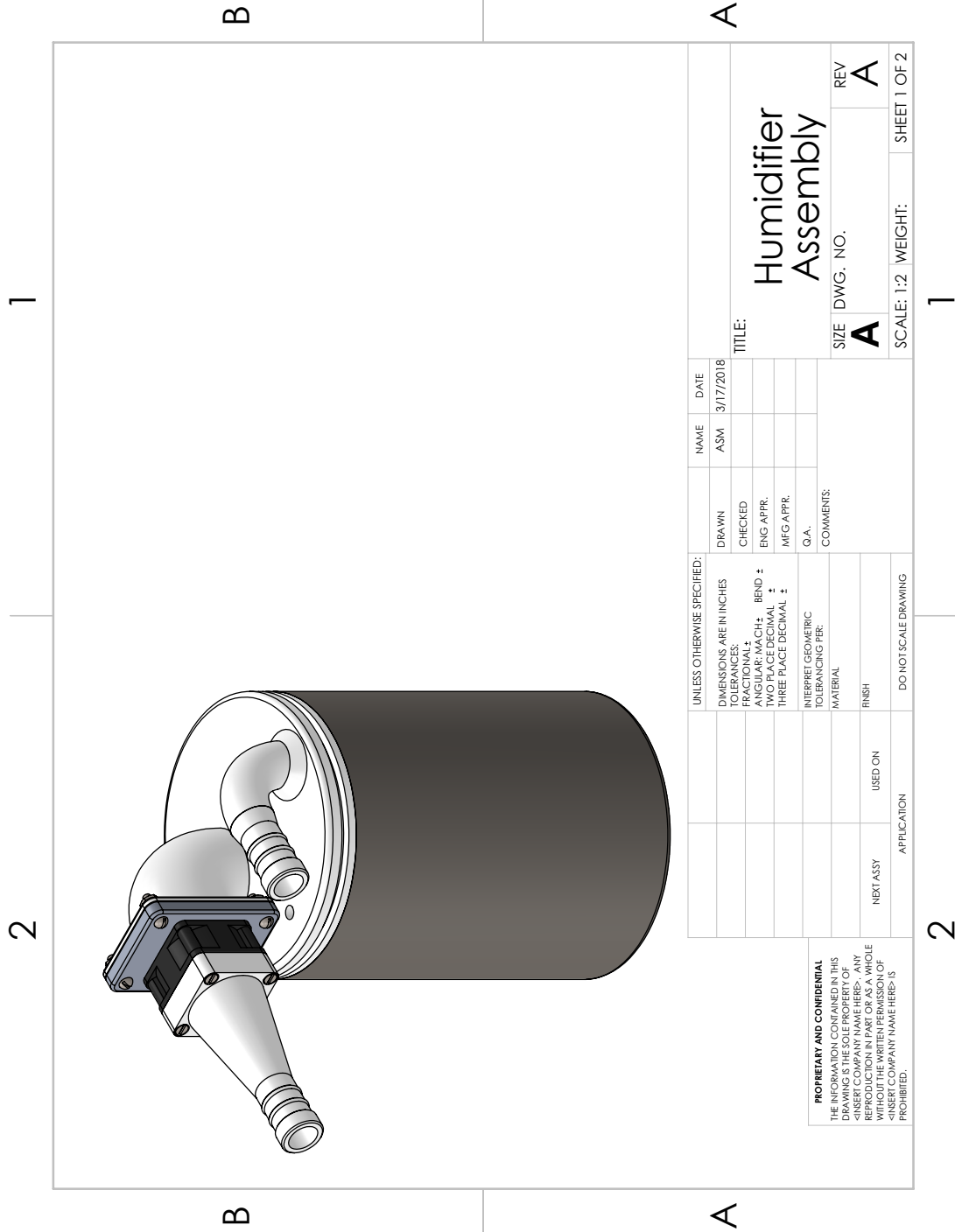


UNLESS OTHERWISE SPECIFIED:		NAME	DATE
DIMENSIONS ARE IN INCHES	DRAWN	ASM	2/25/2018
TOLERANCES:	CHECKED		
FRACTIONAL	ENG. APPR.		
ANGULAR: MACH	MFG APPR.		
BEND	G.A.		
TWO PLACE DECIMAL	COMMENTS:		
THREE PLACE DECIMAL			
INTERPRET GEOMETRIC TOLERANCING PER:			
MATERIAL: Aluminum			
FINISH:			
DO NOT SCALE DRAWING			

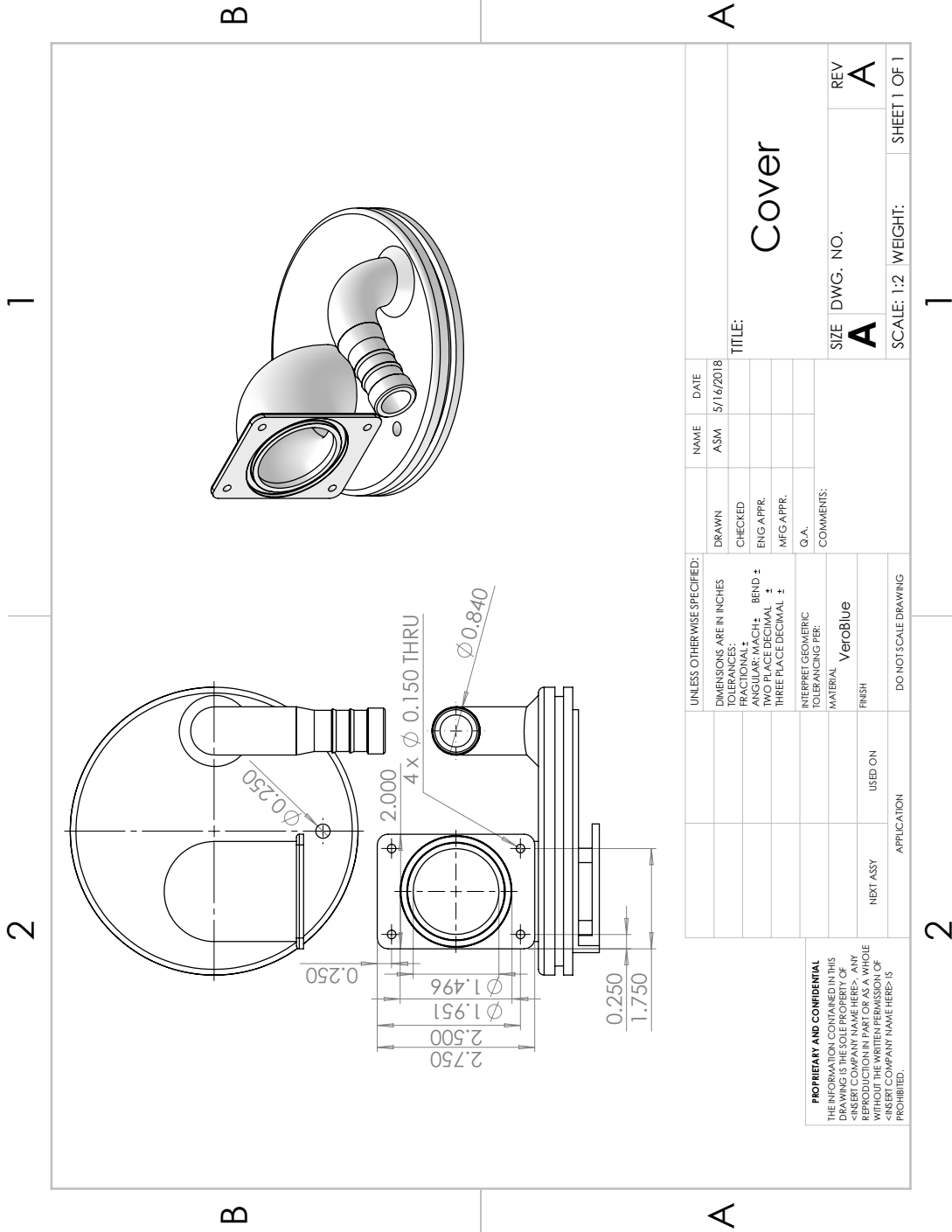
PROPRIETARY AND CONFIDENTIAL
 THE INFORMATION CONTAINED IN THIS DRAWING IS THE SOLE PROPERTY OF <INSERT COMPANY NAME HERE>. ANY REPRODUCTION IN PART OR AS A WHOLE WITHOUT THE WRITTEN PERMISSION OF <INSERT COMPANY NAME HERE> IS PROHIBITED.

TITLE: **Guard Bracket**
 SIZE: **A** DWG. NO.: **0** REV: **0**
 SCALE: 1:1 WEIGHT: SHEET 1 OF 1

B.4 Humidifier

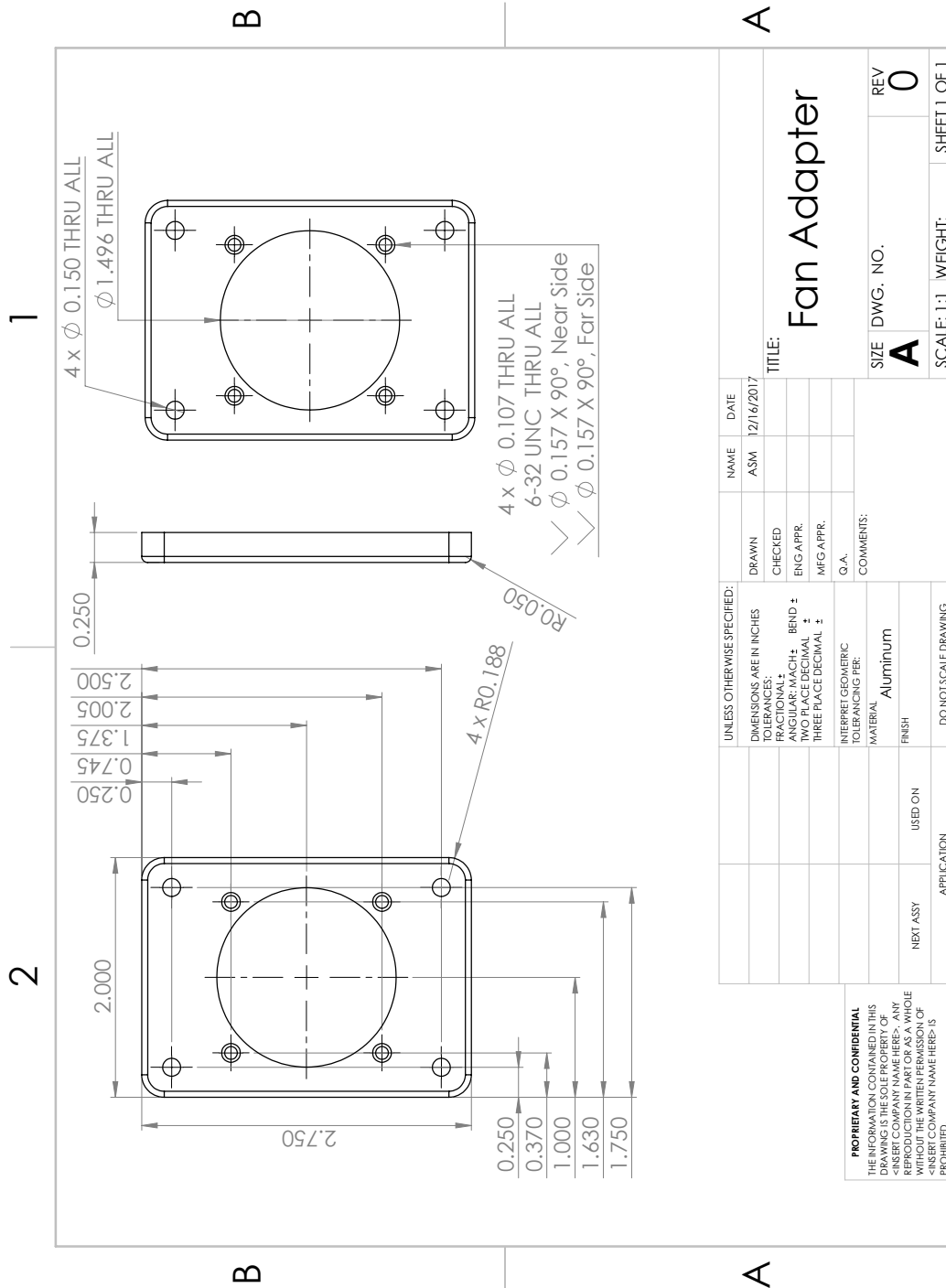


<p>PROPRIETARY AND CONFIDENTIAL THE INFORMATION CONTAINED IN THIS DRAWING IS THE SOLE PROPERTY OF <INSERT COMPANY NAME HERE>. ANY REPRODUCTION IN PART OR AS A WHOLE WITHOUT THE WRITTEN PERMISSION OF <INSERT COMPANY NAME HERE> IS PROHIBITED.</p>		<p>UNLESS OTHERWISE SPECIFIED: DIMENSIONS ARE IN INCHES TOLERANCES: FRACTIONAL ± ANGULAR: MACH ± BEND ± TWO PLACE DECIMAL ± THREE PLACE DECIMAL ±</p>		<p>DRAWN</p>	<p>NAME ASM</p>	<p>DATE 3/17/2018</p>
		<p>INTERPRET GEOMETRIC TOLERANCING PER: MATERIAL FINISH</p>	<p>CHECKED</p>	<p>ENG APPR.</p>	<p>MFG APPR.</p>	<p>Q.A.</p>
<p>NEXT ASSY</p>	<p>USED ON</p>	<p>DO NOT SCALE DRAWING</p>	<p>TITLE: Humidifier Assembly</p>			
<p>APPLICATION</p>	<p>SCALE: 1:2</p>	<p>WEIGHT:</p>	<p>SIZE A</p>	<p>DWG. NO. A</p>	<p>REV A</p>	<p>SHEET 1 OF 2</p>



PROPRIETARY AND CONFIDENTIAL
 THE INFORMATION CONTAINED IN THIS
 DRAWING IS THE SOLE PROPERTY OF
 <INSERT COMPANY NAME HERE>. ANY
 REPRODUCTION IN PART OR AS A WHOLE
 WITHOUT THE WRITTEN PERMISSION OF
 <INSERT COMPANY NAME HERE> IS
 PROHIBITED.

UNLESS OTHERWISE SPECIFIED:	DRAWN	NAME	DATE	TITLE: Cover	SIZE A	DWG. NO. A	REV A
DIMENSIONS ARE IN INCHES	CHECKED	ASM	5/16/2018				
TOLERANCES:	ENG APPR.						
FRACTIONAL ±	MFG APPR.						
ANGULAR: MACH ±	Q.A.						
BEND ±	COMMENTS:						
TWO PLACE DECIMAL ±							
THREE PLACE DECIMAL ±							
INTERPRET GEOMETRIC TOLERANCING PER:							
MATERIAL:							
Veroblu							
FINISH:							
USED ON:							
NEXT ASSY:							
APPLICATION:							
DO NOT SCALE DRAWING							



APPENDIX

Matlab Scripts

C.1 Heater Model Function

```
1 function [t,T]=Heater(n,Ta,tmax)
2 % Theoretical model for a single heater
3
4 % INPUTS
5 % n - number of cartridge heaters in heater block
6 % Ta - ambient temperature in Centigrade
7 % tmax - end time of simulation in seconds
8 % OUTPUTS
9 % t - time in seconds
10 % T - heater temperature in Centigrade
11
12 %% Heat loss due to IRL540 electric power dissipation
13
14 Rds=0.077; % Rds of IRL540 in Ohms
15 Rh=14.4; % Electric resistance of cartridge heater in Ohms
16 Rs=1/(n/Rh);
17 Re=Rds+Rs;
18 i=24/Re;
19 q=Rs*i^2;
20
21 %% State space for a single heater
22 t=linspace(0,tmax,tmax);
23 R=1.105; % K/W
24 C=84.77; % J/K
25 A=-1/(R*C);
26 B=[1/C 1/(R*C)];
```

```
27 C=1;
28 D=0;
29
30 %% Simulation
31 u = [q*ones(length(t),1),Ta*ones(length(t),1)];
32 sys=ss(A,B,C,D);
33 [T,t] = lsim(sys,u,t);
34 T=T';
35 t=t';
36 end
```

C.2 Enclosure Model Function

```
1 function [t,T]=Encl4(n,Ta,tmax)
2 % Theoretical model for enclosure assembly minus humidifier
3
4 % INPUTS
5 % n - number of cartridge heaters in heater block
6 % Ta - ambient temperature in Centigrade
7 % tmax - end time of simulation in seconds
8 % OUTPUTS
9 % t - time in seconds
10 % T - temperature in Centigrade
11
12 %% Heat loss due to IRL540 electric power dissipation
13
14 Rds=0.077; % Rds of IRL540 in Ohms
15 Rh=14.4; % Electric resistance of cartridge heater in Ohms
16 Rs=Rh/n;
17 Re=Rds+Rs;
18 i=24/Re;
19 q=Rs*i^2;
20
21 %% State space
22 t=linspace(0,tmax,tmax);
23 % Thermal Resistances (K/W)
24 R1=0.5578;
25 R2=0.0432;
26 R3=0.1677;
27 R4=0.1776;
28 % Thermal Capacitances (J/K)
29 C1=169.5400;
```

```

30 C2=12.3;
31 C3=1900;
32 C4=3378.4;
33 A=[-1/(R1*C1) 1/(C1*R1) 0 0;1/(C2*R1) -1/(C2*R1)-1/(C2*R2) ...
      1/(C2*R2) 0;0 1/(C3*R2) -1/(C3*R2)-1/(C3*R3) 1/(C3*R3);0 0 ...
      1/(C4*R3) -1/(C4*R3)-1/(C4*R4)];
34 B=[1/C1 0 0 0;0 0 0 0;0 0 0 0;0 0 0 1/(R4*C4)];
35 C=[1 0 0 0;0 1 0 0;0 0 1 0;0 0 0 1];
36 D=0;
37
38 %% Simulation
39 u = [q*ones(length(t),1), zeros(length(t),1), zeros(length(t),1), Ta];
40 sys=ss(A,B,C,D);
41 [T,t] = lsim(sys,u,t);
42 T=T';
43 t=t';
44 end

```

C.3 Enclosure Model Function With Humidifier Attached

```
1 function [t,T]=Enclh4(n,Ta,tmax)
2 % Theoretical model for enclosure assembly with humidifier ...
   considered
3
4 % INPUTS
5 % n - number of cartridge heaters in heater block
6 % Ta - ambient temperature in Centigrade
7 % tmax - end time of simulation in seconds
8 % OUTPUTS
9 % t - time in seconds
10 % T - temperature in Centigrade
11
12 %% Heat loss due to IRL540 electric power dissipation
13
14 Rds=0.077; % Rds of IRL540 in Ohms
15 Rh=14.4; % Electric resistance of cartridge heater in Ohms
16 Rs=Rh/n;
17 Re=Rds+Rs;
18 i=24/Re;
19 q=Rs*i^2;
20
21 %% State space
22 t=linspace(0,tmax,tmax);
23 % Thermal Resistances (K/W)
24 R1=0.56;
25 R2=0.0379;
26 R3=0.162;
27 R4=0.123;
28 % Thermal Capacitances (J/K)
```

```

29 C1=169.5400;
30 C2=12.3;
31 C3=2200;
32 C4=1000;
33 A=[-1/(R1*C1) 1/(C1*R1) 0 0;1/(C2*R1) -1/(C2*R1)-1/(C2*R2) ...
      1/(C2*R2) 0;0 1/(C3*R2) -1/(C3*R2)-1/(C3*R3) 1/(C3*R3);0 0 ...
      1/(C4*R3) -1/(C4*R3)-1/(C4*R4)];
34 B=[1/C1 0 0 0;0 0 0 0;0 0 0 0;0 1/(C4*R4) 0 0];
35 C=eye(4);
36 D=0;
37
38 %% Simulation
39 [row,column]=size(Ta);
40 if (row>1) && (column==1)
41     u = [q*ones(length(t),1),Ta,zeros(length(t),1),...
42         zeros(length(t),1)];
43 elseif (row==1) && (column==1)
44     u = [q*ones(length(t),1),Ta*ones(length(t),1),...
45         zeros(length(t),1),zeros(length(t),1)];
46 else
47     error('Incorrect input array dimension for input Ta')
48 end
49 sys=ss(A,B,C,D);
50 [T,t] = lsim(sys,u,t);
51 T=T';
52 t=t';
53 end

```

C.4 Humidification Model

```
1 function [Phi,t]=HumidModel160 (mdot,phia,phio,Ta,T,tmax)
2 % INPUTS
3 % mdot - mass flow rate of water vapour (kg/s)
4 % phia - Ambient relative humidity (%)
5 % phio - Relative humidty initial condition (%)
6 % Ta - Ambient temperature (Centigrade)
7 % T - Air temperature (Centigrade)
8 % tmax - Maximum simulation time (s)
9 % OUTPUTS
10 % P1 - vapor pressure inside enclosure (Pa)
11 % t - time (s)
12 % CALCULATION
13 t=linspace(0,tmax,tmax);
14 Psa=SVP (Ta);
15 Pa=(phia/100).*Psa;
16 P1o=SVP (T(1))* (phio/100);
17 %% State space
18 R1=1.3821e+08;
19 C1=2.8941e-06;
20 A=-1/(R1*C1);
21 B=[1/C1 1/(R1*C1)];
22 C=1;
23 D=0;
24 tsim=t;
25 %% Simulation
26 if length(mdot)==1
27 u = [mdot*ones (tmax,1),Pa];
28 else
29     u=[mdot,Pa];
```

```

30 end
31     sys=ss(A,B,C,D);
32 [Pld,t] = lsim(sys,u,tsim);
33 [Pli,t]=initial(sys,Plo,tsim);
34 P1=Pld+Pli;
35 P1=P1';
36 Ps=SVP(T)';
37 Phi=100*P1./Ps;
38 t=t';
39     function [Ps]=SVP(T)
40         % Calculates saturation vapour pressure at dry bulb ...
41         % temperature T
42         % in Centigrade. Output is in Pascals.
43         % Coefficients for Hyland-Wexler approximation
44         a=[6.11213476 0.444007856 0.143064234e-1 0.264461437e-3 ...
45             0.305903558e-5 0.196237241e-7 0.892344772e-10 ...
46             -0.373208410e-12 0.209339997e-15]';
47         % Hyland Wexler approximation
48         Ps=100.*(a(1).*T.^(0)+a(2).*T.^(1)+a(3).*T.^(2)...
49             +a(4).*T.^(3)+a(5).*T.^(4)+a(6).*T.^(5)...
50             +a(7).*T.^(6)+a(8).*T.^(7)+a(9).*T.^(8));
51     end
52 end

```

APPENDIX

Manufacturer Datasheets

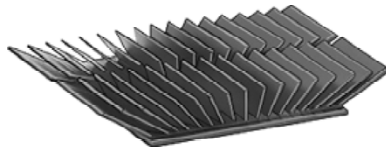
D.1 Heat Sink

 **McMASTER-CARR** OVER 555,000 PRODUCTS
(609) 259-8900
(609) 259-3575 (fax)
nj.sales@mcmaster.com

Flat-Surface Heat Sink

High-Efficiency Fin Style, 1-3/4" Long x 2-5/8" Wide x 5/16" High

In stock
\$11.88 Each
8822T13



Overall Size	
Length	1 3/4"
Width	2 5/8"
Height	5/16"
Number of Pins/Fins 34 Fins	
Additional Specifications	High-Efficiency Fin Style

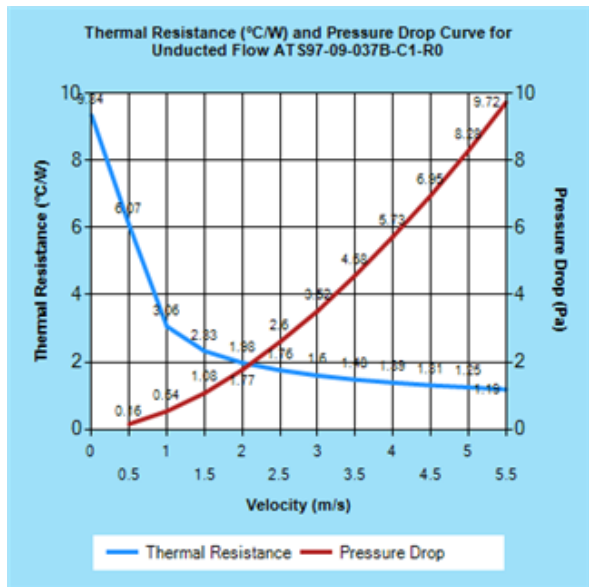
Cool flat metal surfaces as well as electrical panels and components by dissipating heat. Heat sinks are made of black-anodized aluminum. Thermal mounting tape is included.

High-efficiency fin-style heat sinks have more surface area to dissipate heat more efficiently.

Heat Sink Details	
Heat Sink Type = maxiFLOW	
Material = Aluminum	
TIM Type ($^{\circ}\text{C}\cdot\text{in}^2/\text{W}$) = No Tape $R_{\text{TIM}} = 0$	
Mass(gr) = 15.88	Volumn(mm^3) = 5882.4
Dimensions(mm) :	
Length = 50	Width = 45 Height = 8.20
System:	
Coolant = Air	Device Power (W) = 10



Thermal Resistance ($^{\circ}\text{C}/\text{W}$) and Pressure Drop Unducted > ATS97-09-037B-C1-R0		
Velocity (m/s)	R_{c_a} ($^{\circ}\text{C}/\text{W}$)	DP (Pa)
0	9.34	0
0.5	6.07	0.16
1	3.06	0.54
1.5	2.33	1.08
2	1.98	1.77
2.5	1.76	2.6
3	1.6	3.52
3.5	1.48	4.58
4	1.39	5.73
4.5	1.31	6.95
5	1.25	8.28
5.5	1.19	9.72



D.2 Heater Fan

DC Fan

60mm sq.

San Ace 60



General Specifications

- Material Frame: Plastics (Flammability: UL94V-0),
Impeller: Plastics (Flammability: UL94V-0)
- Expected Life Refer to specifications (L10:Survival rate:90% at 60°C ,
rated voltage, and continuously run in a free air state)
- Lead Wire ⊕red ⊖black (Sensor) yellow (Control) brown
- Storage Temperature -30°C to +70°C (Non-condensing)

60×60×25mm (Mass : 90g) **9G type**

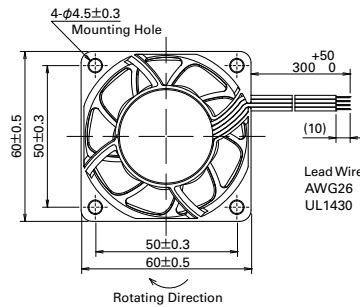
Specifications The following nos. **have PWM controls, pulse sensors, and ribs**. For ribless, append "1" to the model no.

Model No.	Rated Voltage [V]	Operating Voltage Range [V]	PWM duty cycle [%]	Rated Current [A]	Rated Input [W]	Rated Speed [min ⁻¹]	Max. Airflow [m ³ /min] [CFM]	Max. Static Pressure [Pa] [inchH ₂ O]	SPL [dB(A)]	Operating Temperature Range [°C]	Expected Life [h]
9G0612P4S001	12	10.2 to 13.8	100	0.67	8.04	11,000	1.4 49.4	300 1.20	53	-20 to +70	40,000/60°C (70,000/40°C)
			0	0.07	0.84	3,300	0.42 14.8	27 0.11	19		
9G0612P4H001	12	10.2 to 13.8	100	0.50	6.00	9,500	1.21 42.7	224 0.90	49		
			0	0.06	0.72	2,850	0.36 12.7	20.2 0.08	18		
9G0624P4S001	24	20.4 to 27.6	100	0.34	8.16	11,000	1.4 49.4	300 1.20	53		
			0	0.04	0.96	3,300	0.42 14.8	27 0.11	19		
9G0624P4H001	24	20.4 to 27.6	100	0.25	6.00	9,500	1.21 42.7	224 0.90	49		
			0	0.04	0.96	2,850	0.36 12.7	20.2 0.08	18		
9G0648P4S001	48	36 to 72	100	0.18	8.64	11,000	1.4 49.4	305 1.22	53		
			0	0.02	0.96	3,300	0.42 14.8	27.4 0.11	19		

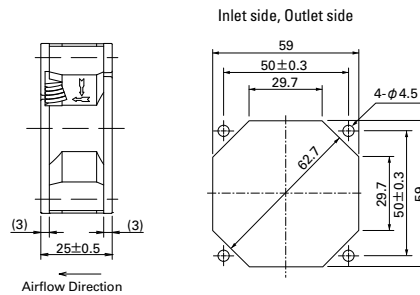
*PWM Frequency : 25KHz

Other sensor specifications are available as options. Please refer to the index (pp. 501 to 502).

Dimensions (unit: mm) (With ribs)



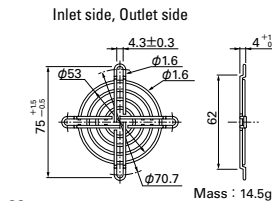
Reference Dimensions of Mounting Holes and Vent Opening (unit: mm)



Options (unit: mm)

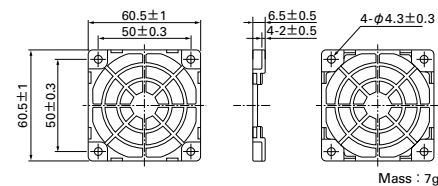
Finger Guards

Model : 109-139E Surface treatment : Nickel-chrome plating (silver) Color : 109-139H : Carbon electropainting (black)



Resin Finger Guards

Model : 109-1003G

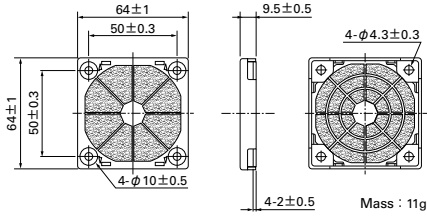


69

Options (unit: mm)

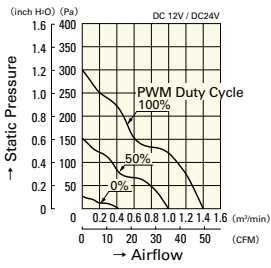
Resin Filter Kits

Model : 109-1003F13 (13PPI), 109-1003F20 (20PPI)
 : 109-1003F30 (30PPI), 109-1003F40 (40PPI)

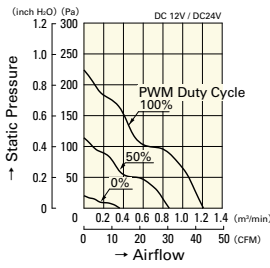


Airflow - Static Pressure Characteristics

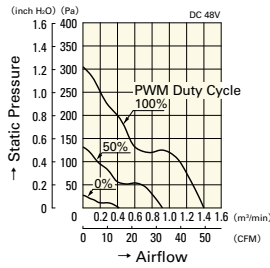
PWM Duty Cycle



9G0612P4S001
9G0624P4S001

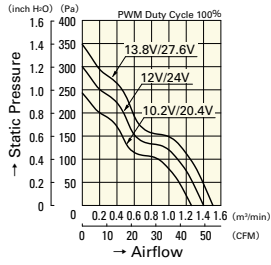


9G0612P4H001
9G0624P4H001

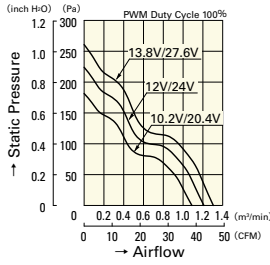


9G0648P4S001

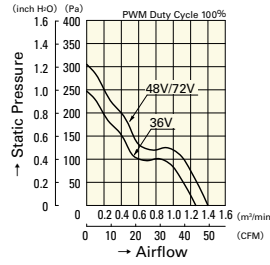
Operating Voltage Range



9G0612P4S001
9G0624P4S001

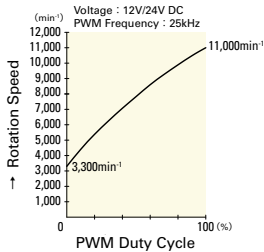


9G0612P4H001
9G0624P4H001

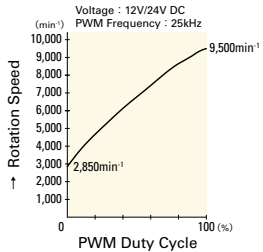


9G0648P4S001

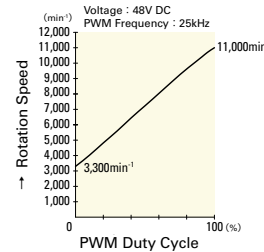
PWM Duty - Speed Characteristics Example



9G0612P4S001
9G0624P4S001



9G0612P4H001
9G0624P4H001



9G0648P4S001

BIBLIOGRAPHY

- “arduino-pwm-frequency-library.” [Online]. Available: <https://code.google.com/archive/p/arduino-pwm-frequency-library/downloads>
- Abraham, J. P. and Sparrow, E. M., “A simple model and validating experiments for predicting the heat transfer to a load situated in an electrically heated oven,” *Journal of Food Engineering*, vol. 62, no. 4, pp. 409–415, 2004. [Online]. Available: [https://doi.org/10.1016/S0260-8774\(03\)00265-6](https://doi.org/10.1016/S0260-8774(03)00265-6)
- Adafruit. “Platinum RTD Sensor - PT100 - 3 Wire 1 meter long.” [Online]. Available: <https://www.adafruit.com/product/3290>
- Amazon. “AGPtEK aluminum mist maker fog maker for water fountain pond rockery fishtank vase birdbath.” [Online]. Available: https://smile.amazon.com/Aluminum-Fountain-Rockery-Fishtank-Birdbath/dp/B00PAK245E/ref=sr_1_23.sspa?ie=UTF8&qid=1528913523&sr=8-23-spons&keywords=ultrasonic+humidifier+head&psc=1
- Amazon. “Arctic MX-4 - thermal compound paste, carbon based high performance, heatsink paste, thermal compound cpu for all coolers, thermal interface material - 4 grams.” [Online]. Available: https://smile.amazon.com/ARCTIC-MX-4-Compound-Performance-Interface/dp/B0045JCFLY/ref=sr_1_1.sspa?ie=UTF8&qid=1529001107&sr=8-1-spons&keywords=mx-4+thermal+compound&psc=1
- Amazon. “Balitensen 24v 40w ceramic cartridge heater 620 for 3d printer rewrap prusa mendel pack of 5.” [Online]. Available: https://www.amazon.com/BALITENSEN-Ceramic-Cartridge-Heater-Printer/dp/B078SQ4BPR/ref=sr_1_2.sspa?ie=UTF8&qid=1526408204&sr=8-2-spons&keywords=3d+printer+heater+24v&psc=1
- Arduino. “Arduino UNO Rev3.” [Online]. Available: https://www.arduino.cc/en/uploads/Main/Arduino_Uno_Rev3-schematic.pdf
- Auburn University College of Engineering. “Radiation exchange between surfaces.” [Online]. Available: <http://www.eng.auburn.edu/~dmckwski/mech7210/radexchange.pdf>
- Britannica. “Thermal conduction.” [Online]. Available: <https://www.britannica.com/science/thermal-conduction>
- Burlon, F., Tiberi, E., Micheli, D., Furlanetto, R., and Simonato, M., “Transient model of a professional oven,” *Energy Procedia*, vol. 126, pp. 2–9, 2017. [Online]. Available: <https://doi.org/10.1016/j.egypro.2017.08.045>

- Cabra, V. and Sams, M., “Do’s and don’ts of cryo-electron microscopy: A primer on sample preparation and high quality data collection for macromolecular 3D reconstruction,” *Journal of Visualized Experiments*, vol. 95, Jan. 2015. [Online]. Available: <http://www.jove.com/video/52311>
- Croote, D., Godfrin, M. P., Bose, A., Tripathi, A., and Lee, J., “A platform for retaining native morphology at sub-second time scales in cryogenic transmission electron microscopy,” *Review of Scientific Instruments*, vol. 84, 2013. [Online]. Available: <http://dx.doi.org/10.1063/1.4804648>
- Dartmouth College. “System analogies.” [Online]. Available: https://www.dartmouth.edu/~sullivan/22files/System_analogy_all.pdf
- Delta Electronics. “PMT panel mount power supply.” 2018. [Online]. Available: <http://www.deltapsu.com/products/download/Datasheet/PMT-24V350W1AK>
- Dostál, J. and Ferkl, L., “Model predictive control of climatic chamber with on-off actuators,” *IFAC Proceedings Volumes*, vol. 47, no. 3, pp. 4423–4428, 2014. [Online]. Available: <https://doi.org/10.3182/20140824-6-ZA-1003.01571>
- Elmhurst College. “Denaturing of proteins.” 2003. [Online]. Available: <http://chemistry.elmhurst.edu/vchembook/568denaturation.html>
- EM Resolutions. “Carbon film on copper 400 mesh.” [Online]. Available: https://emresolutions.com/wp-content/uploads/2015/12/Carbon_on_square_grid-57.png
- The Engineering Toolbox. “Density of dry air and water vapor - moist or humid air.” [Online]. Available: https://www.engineeringtoolbox.com/density-air-d_680.html
- The Engineering Toolbox. “Specific heats for metals.” [Online]. Available: https://www.engineeringtoolbox.com/specific-heat-metals-d_152.html
- The Engineering Toolbox. “Thermal conductivity of common metals and gases.” [Online]. Available: https://www.engineeringtoolbox.com/thermal-conductivity-d_429.html
- Engineering ToolBox. “Relative humidity in air.” 2004. [Online]. Available: https://www.engineeringtoolbox.com/relative-humidity-air-d_687.html
- Engineers Edge. “Convective heat transfer coefficient.” [Online]. Available: https://www.engineersedge.com/thermodynamics/convective_heat_transfer.htm
- Flatau, P. J., Walko, R. L., and Cotton, W. R., “Polynomial fits to saturation vapor pressure,” *Journal of Applied Meteorology*, vol. 31, no. 12, pp. 1507–1513, 1992. [Online]. Available: [https://doi.org/10.1175/1520-0450\(1992\)031%3C1507:PFTSVP%3E2.0.CO;2](https://doi.org/10.1175/1520-0450(1992)031%3C1507:PFTSVP%3E2.0.CO;2)

- Goldie, K. N., Abeyrathne, P., Kebbel, F., Chami, M., ringler, P., and Stahlberg, H. ResearchGate. “Cryo-electron microscopy of membrane proteins.” Jan. 2014. [Online]. Available: https://www.researchgate.net/The-plunge-freezing-device-FEI-Vitrobot-fitted-with-a-humidity-and-temperature_fig1_259395292
- Grassucci, R. A., Taylor, D. J., and Frank, J., “Preparation of macromolecular complexes for cryo-electron microscopy,” *Nature Protocols*, vol. 2, no. 12, pp. 3239–3246, 2007. [Online]. Available: <https://doi.org/10.1016/j.ymeth.2016.02.017>
- Hanania, J., Jenden, J., Kosasih, S., Stenhouse, K., Toor, J., and Donev, J. Energy Education. “Heat transfer mechanisms.” [Online]. Available: http://energyeducation.ca/encyclopedia/Heat_transfer_mechanisms
- Hanania, J., Jenden, J., Kosasih, S., Stenhouse, K., Toor, J., and Donev, J. The Engineering Toolbox. “Conductive heat transfer.” 2003. [Online]. Available: https://www.engineeringtoolbox.com/conductive-heat-transfer-d_428.html
- Holmes. “How does an ultrasonic humidifier work?” [Online]. Available: <http://www.holmesproducts.com/blog/archive/2014/october/how-does-an-ultrasonic-humidifier-work%3F.html>
- Honeywell. “Hih-4010/4020/4021 series.” 2007. [Online]. Available: <https://sensing.honeywell.com/honeywell-sensing-hih4010-4020-4021-series-product-sheets-009020-1-en.pdf>
- Jindal, V. K., Kalus, J., Pilsl, H., Hoffmann, H., and Linder, P., “Dynamic small-angle neutron scattering study of rodlike micelles in a surfactant solution,” *The Journal of Physical Chemistry*, vol. 94, no. 7, 1990. [Online]. Available: <https://doi.org/10.1021/j100370a070>
- Lasance, C. J. M. Electronics Cooling. “Thermal capacitance.” 2003. [Online]. Available: <https://www.electronics-cooling.com/2003/05/thermal-capacitance/#>
- Luma Comfort. “See how an evaporative humidifier works.” [Online]. Available: <http://www.lumacomfort.com/article/how-evaporative-humidifier-works.htm>
- Lumen Learning. “Humidity, evaporation, and boiling.” [Online]. Available: <https://courses.lumenlearning.com/physics/chapter/13-6-humidity-evaporation-and-boiling/>
- Measurement Computing. “Usb-1208fs-plus/ls/1408fs-plus series.” [Online]. Available: <https://www.mccdaq.com/usb-data-acquisition/USB-1208FS-LS-1408FS-Series.aspx>

- Miami University. “What is resolution?” Nov. 2013. [Online]. Available: <https://www.cas.miamioh.edu/mbiws/microscopes/resolution.html>
- Mifflin, M. The Spruce. “Ultrasonic vs evaporative portable humidifiers.” [Online]. Available: <https://www.thespruce.com/humidifiers-ultrasonic-vs-evaporative-humidifiers-1908160>
- Mistry, H., Ganapathi-subbu, Dey, S., Bishnoi, P., and Castillo, J. L., “Modeling of transient natural convection heat transfer in electric ovens,” *Applied Thermal Engineering*, vol. 26, no. 17-18, pp. 2448–2456, 2006. [Online]. Available: <https://doi.org/10.1016/j.applthermaleng.2006.02.007>
- Monoprice. “Maker select 3d printer v2.” [Online]. Available: https://www.monoprice.com/product?p_id=13860
- Moran, M. J., Shapiro, H. N., Boettner, D. D., and Bailey, M. B., *Fundamentals of Engineering Thermodynamics*. Wiley, 2014, pp. 753–784.
- National Physical Laboratory. “Why is humidity important?” [Online]. Available: <http://www.npl.co.uk/publications/good-practice-online-modules/humidity/humidity-basics/why-is-humidity-important/>
- Phidgets Inc. “Miniature linear motion series L12.” 2016. [Online]. Available: https://www.phidgets.com/productfiles/3540/3540_0/Documentation/3540_0_Datasheet.pdf
- Ramirez-Laboreo, E., Sagues, C., and Llorente, S., “Dynamic heat and mass transfer model of an electric oven for energy analysis,” *Applied Thermal Engineering*, vol. 93, pp. 683–691, 2016. [Online]. Available: <https://doi.org/10.1016/j.applthermaleng.2015.10.040>
- Robertson, A. F. and Gross, D., “An electrical-analog method for transient heat-flow analysis,” *Journal of Research of the National Bureau of Standards*, vol. 61, no. 2, pp. 105–115, 1958. [Online]. Available: <http://dx.doi.org/10.6028/jres.061.016>
- Rotronic. “Incubators and humidity.” June 2015. [Online]. Available: <https://www.rotronic.com/en-us/rotronic-cases-read?id=361/>
- Science Learning Hub. “Types of electron microscope.” Feb. 2012. [Online]. Available: <https://www.sciencelearn.org.nz/resources/502-types-of-electron-microscope>
- Tapia, S. and del Río, J. A. Universidad Nacional Autónoma de México. “One temperature model for effective ovens.” 2011. [Online]. Available: <https://arxiv.org/pdf/1109.0664.pdf>

- Teodosiu, C., Ilie, V., and Teodosiu, R., “Modeling of water vapor sources in enclosures,” *International Journal of Structural and Civil Engineering Research*, vol. 4, no. 2, pp. 212–217, 2015. [Online]. Available: <http://www.ijscer.com/uploadfile/2015/0922/20150922014808395.pdf>
- Texas Instruments. “Lm35 precision centigrade temperature sensors.” 2017. [Online]. Available: <http://www.ti.com/lit/ds/symlink/lm35.pdf>
- ThermoFisher Scientific. “Vitrobot for life sciences.” [Online]. Available: <https://www.fei.com/Vitrobot/>
- Thompson, R. F., Walker, M., Siebert, C. A., Muench, S. P., and Ranson, N. A., “An introduction to sample preparation and imaging by cryo-electron microscopy for structural biology,” vol. 100, pp. 3–15, Feb. 2016. [Online]. Available: <https://doi.org/10.1016/j.jymeth.2016.02.017>
- University of Washington. “What is cryo-EM?” [Online]. Available: <https://faculty.washington.edu/lw32/images/fig1.png>
- Unklesbay, K., Boza-Chacon, A., and Unklesbay, N., “Air temperature transfer function of a convection oven,” *Food Control*, vol. 8, no. 1, pp. 39–43, 1997. [Online]. Available: [https://doi.org/10.1016/S0956-7135\(96\)00045-X](https://doi.org/10.1016/S0956-7135(96)00045-X)
- Vaisala. “HUMICAP humidity and temperature probe HMP110.” 2018. [Online]. Available: https://www.vaisala.com/sites/default/files/documents/HMP110-Datasheet-B210852EN_1.pdf
- Vishay. “Power MOSFET.” [Online]. Available: <https://www.vishay.com/docs/91300/91300.pdf>
- W. Palm III, *System Dynamics*. McGraw-Hill, 2013, pp. 402–430.
- White, F., *Heat and Mass Transfer*. Addison-Wesley Publishing Company, 1988, pp. 119–170.
- White, F., *Heat and Mass Transfer*. Addison-Wesley Publishing Company, 1988, pp. 270–271.
- White, F., *Heat and Mass Transfer*. Addison-Wesley Publishing Company, 1988, p. 272.
- White, F., *Heat and Mass Transfer*. Addison-Wesley Publishing Company, 1988, pp. 285–417.
- White, F., *Heat and Mass Transfer*. Addison-Wesley Publishing Company, 1988, pp. 17–18.
- White, F., *Heat and Mass Transfer*. Addison-Wesley Publishing Company, 1988, p. 363.

- White, F., *Heat and Mass Transfer*. Addison-Wesley Publishing Company, 1988, pp. 48–99.
- White, F., *Viscous Fluid Flow*. McGraw-Hill, 2005, pp. 183–205.
- White, F., *Fluid Mechanics*. McGraw-Hill, 2015, pp. 225–246.
- Wikipedia. “COMSOL Multiphysics.” [Online]. Available: https://en.wikipedia.org/wiki/COMSOL_Multiphysics
- Wikipedia. “OpenFOAM.” [Online]. Available: <https://en.wikipedia.org/wiki/OpenFOAM>
- Zhang, Z. and Pate, M. B., *A Methodology for Implementing a Psychrometric Chart in a Computer Graphics System*. ASHARE Transactions, 1988, vol. 94.